Outburst Floods☆

Jim E O'Connor[a], John J Clague[b], Joseph S Walder[c], Vernon Manville[d], and Robin A Beebee[e], [a]U.S. Geological Survey, Portland, OR, United States; [b]Simon Fraser University, Burnaby, BC, Canada; [c]U.S. Geological Survey, Vancouver, WA, United States; [d]University of Leeds, Leeds, United Kingdom; [e]U.S. Geological Survey, Anchorage, AK, United States

© 2020 Elsevier Inc. All rights reserved.

1	**Introduction**	**1**
2	**Flood sources**	**2**
2.1	Floods from breached valley blockages	3
2.1.1	Ice dams	3
2.1.2	Landslide dams	5
2.1.3	Volcanogenic dams	8
2.1.4	Constructed dams	9
2.1.5	Other types of valley blockages	9
2.2	Floods from breached basins	11
2.2.1	Basins marginal to ice sheets	11
2.2.2	Moraine-rimmed basins	11
2.2.3	Tectonic basins	13
2.2.4	Volcanic basins	16
2.2.5	Meteorite craters	17
2.3	Floods from release of subglacial and subterranean storage	18
2.3.1	Subglacial and englacial impoundments	18
2.3.2	Groundwater	19
2.4	Floods from unusual sources	19
3	**Outburst flood magnitude and behavior**	**20**
3.1	Triggers and breach processes	21
3.2	Peak discharge	23
3.3	Downstream flood behavior	26
4	**Signs left behind – Erosional and depositional features**	**29**
4.1	Erosional features and processes	31
4.2	Depositional features and processes	32
4.3	Outburst floods and landscape evolution	32
5	**Summary**	**34**
Acknowledgments		**42**
References		**42**

1 Introduction

Aluviones, jökulhlaups, chhugyümha, débâcles, bishyari, GLOFs (glacial lake outburst floods), pond-letting and *lake and bog bursts* all refer to the universal phenomena of outburst floods. Breaches of naturally impounded waterbodies have caused most of the largest and most lethal floods known (Table 1; Costa and Schuster, 1988; Cenderelli, 2000; Clague and Evans, 2000; O'Connor et al., 2002; O'Connor and Costa, 2004; Carey, 2005; Carrivick and Tweed, 2016; Liu et al., 2019), giving rise to special vocabulary in cultures worldwide. Similarly, floods from breached constructed dams have caused significant human disasters (Outland, 1963; McCullough, 1968; Coleman, 2019), as well as geomorphic consequences (Scott and Gravlee, 1968; Rydlund, 2006; Major et al., 2012).

Outburst floods on Earth have had discharges up to 10^8 m^3 s^{-1}, exceeding those of the largest known meteorological floods by a factor of 100 (Table 1; Fig. 1; O'Connor et al., 2002). Even larger outburst floods on Mars likely had peak discharges exceeding 10^9 m^3 s^{-1} (Komatsu and Baker, 1997; Dohm et al., 2000; Coleman and Baker, 2009; Baker et al., 2015). Because outburst floods—even ones as small as 10^1 m^3 s^{-1}—typically inundate landscapes unadjusted to such flows, they almost always have profound and long-lasting geomorphic effects. Additionally, rapid releases of immense volumes of freshwater to oceans during large outburst floods in the past have affected ocean circulation and climate at broad scales (Teller et al., 2002; Murton et al., 2010; Praetorius et al., 2020). Consideration of outburst floods thereby provides perspective on a fundamental aspect of global systems and one of important physical and human consequences.

The study of outburst floods has deep roots in geology and geomorphology, touching on core concepts and controversies framing our science (Baker, 2009, 2020; Baker et al., 2015). Ranging from Lyell's (1830) discussion on the role of "obstructions" and "lake bursts" in forming river valleys, to the great Channeled Scabland debate of the 1920s and 1930s (e.g., Bretz, 1923a,b), and

☆Change History: September 2020. JE O'Connor, JJ Clague, JS Walder, V Manville, and RA Beebee updated all sections and several figures. No change in authorship and all participated in the update. Figures 1, 3, 14, 15, and 16 are new.

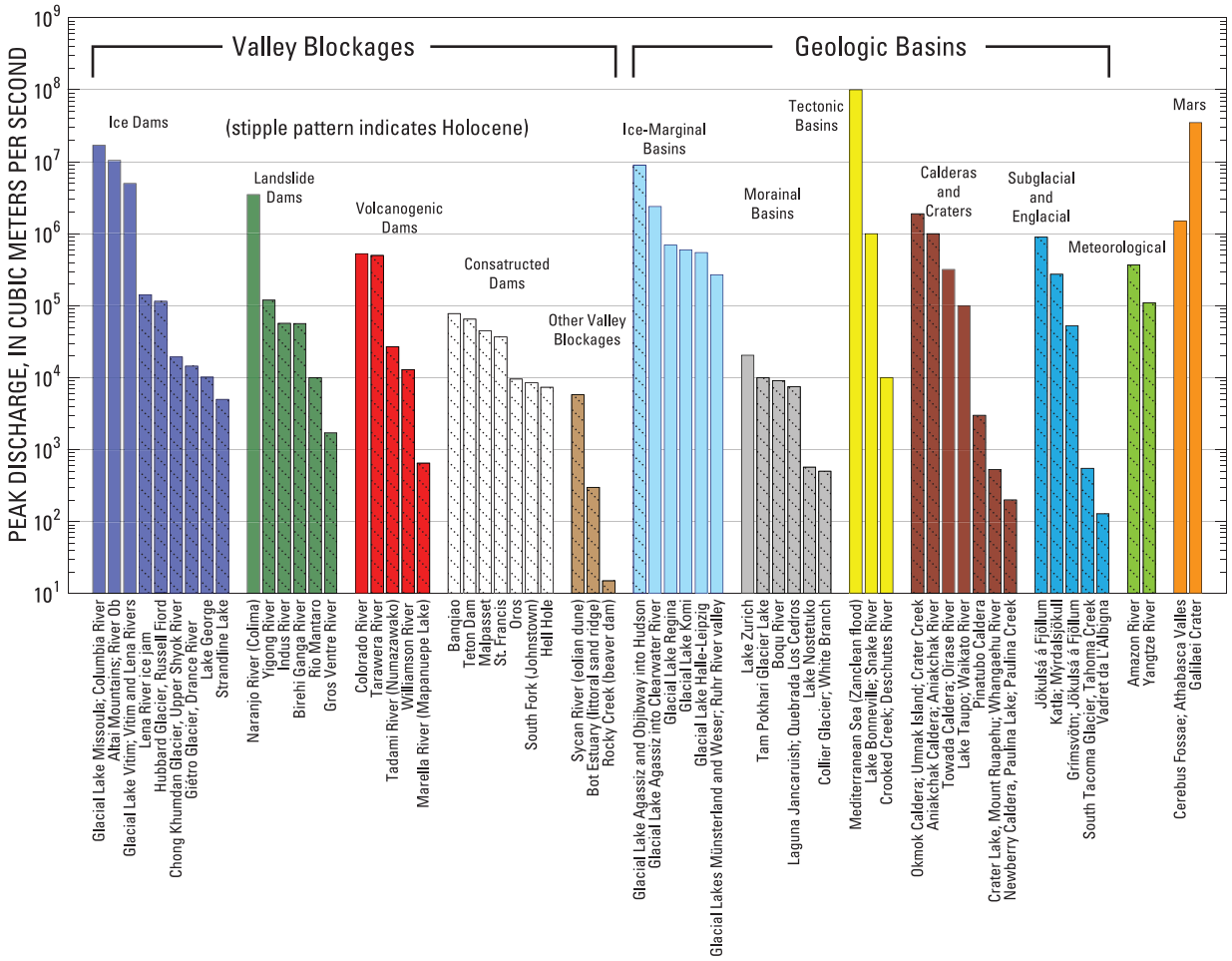

Fig. 1 Selected Cenozoic outburst floods on Earth arrayed by geologic setting. Stipple pattern indicates Holocene floods. Also shown are largest meteorological floods and selected outburst floods on Mars. Data from Table 1 and O'Connor et al. (2002).

then later 20th-century examinations of the role of water in sculpting the surface of Mars (e.g., Baker and Milton, 1974), the field of fluvial geomorphology has been in part shaped by growing understanding of the role of outburst floods. This understanding is founded on the many related fields of engineering, geography, geology, glaciology and planetary science that have come to view outburst floods as an integral and sometimes cataclysmic component of the natural and constructed universe. Growing interest in outburst floods has produced an unfathomable literature of recent years—a cursory Google Scholar search on "outburst floods" returned about 6300 publications for the decade between 2011—the time of the initial writing of this review—and 2020, when this update was written, far exceeding the 3870 results of all time up to 2011.

This review is in part derived from several review articles, including Costa (1988), Costa and Schuster (1988), Clague and Evans (1994, 2000), Walder and Costa (1996), Walder and O'Connor (1997), Tweed and Russell (1999), Roberts (2005), Korup and Tweed (2007), O'Connor and Beebee (2009), Björnsson (2009), Manville (2010a, 2015), Carrivick and Tweed (2013, 2016), Fan et al. (2019), Liu et al. (2019), and Clague and O'Connor (2020). Unless otherwise noted, data depicted in the accompanying figures and plots are from the compilation of dam-failure measurements summarized in Table 1 of O'Connor and Beebee (2009). This contribution expands on many of these prior reviews—many of which focus on specific types of outburst floods—by synthesizing both specific and general conditions associated with the failure of natural and constructed dams and their geomorphic consequences. After general discussion of the environments leading to large water accumulations, we describe processes and factors controlling breaching and downstream flood characteristics, and how these attributes may relate to downstream flood features.

2 Flood sources

Several geological processes lead to impoundment of water bodies that can then rapidly drain to cause large floods (Fig. 1; summarized by Swanson et al., 1986; Costa, 1988; Costa and Schuster, 1988; Clague and Evans, 1994; O'Connor et al., 2002; Carrivick and Rushmer, 2006; Korup and Tweed, 2007; O'Connor and Beebee, 2009; Manville, 2015; Goudge et al., 2018; Clague

and O'Connor, 2020; among others). Three broad classes of impoundments produce outburst floods on Earth: (1) valley blockages; (2) natural closed basins filled with water; and (3) sub-surface water accumulations. These categories are not completely distinct: Some processes such as volcanism can impound water bodies of all three types, and some features, such as moraines, could be considered both a valley-blocking feature and a geologically formed basin. And constructed dams commonly take advantage of narrow outlets to geological basins to impound water. Nevertheless, this classification provides a framework for the following discussion of sources of outburst floods.

2.1 Floods from breached valley blockages

Valley blockage can result from purposeful damming by humans for societal aims of water storage, hydropower generation, flood control and recreation, and from uncontrolled geological processes, such as landslides, debris flows, lahars, lava flows, and lahars, and glaciation. Such blockages can form large and deep lakes with the potential for immense downstream floods. Blockage of valleys is the most common mechanism for producing large non-meteorological floods. Some of the largest floods of the Quaternary have resulted from failure of valley-blocking ice dams. Examples are the Pleistocene Missoula floods in the Pacific Northwest of North America and the Altai floods of Central Asia (Table 1 and Fig. 1). Ice dams and jams also have contributed to some of the largest known floods of more recent times, but most Holocene and historical large floods resulting from breached valley blockages are due to failure of either landslide dams or constructed dams. Rarer are breaches of lava-flow dams or other volcanically emplaced materials.

2.1.1 Ice dams

Outburst floods associated with glacier ice dams have produced the largest freshwater floods on Earth (Fig. 1; O'Connor and Costa, 2004), leaving profoundly affected landscapes in their wake (Bretz, 1923a,b; Herget, 2005; Baker, 2009; Herget et al., 2020). Historically, more than 1300 glacial outburst floods have caused ~12,500 fatalities (Carrivick and Tweed, 2016), documented by reports filling journals at an exponential rate (Emmer, 2018). Valley blockages associated with ice can result either from glacier advance, typically by ice advancing down a valley and blocking either a tributary or mainstem valley (Fig. 2) or from glacier retreat where confluent glaciers retreat and separate, forming open valley space between glaciers (Post and Mayo, 1971; Costa and Schuster, 1988; Tweed and Russell, 1999). They have been described and reviewed globally (Walder and Costa, 1996; Tweed and Russell, 1999; Korup and Tweed, 2007; Carrivick and Tweed, 2013, 2016) and regionally, including Alaska (Post and Mayo, 1971; Wilcox et al., 2014b), the Canadian Cordillera (Clague and Mathews, 1973; Clague and Evans, 1994, 2000), Scandinavia (Liestøl, 1956; Xu et al., 2014), Iceland (Roberts, 2005; Björnsson, 2009; Carrivick and Tweed, 2019); Greenland (Carrivick et al., 2017; Grinsted et al., 2017; Carrivick and Tweed, 2019); Europe (Haeberli, 1983; Eisbacher and Clague, 1984; Haeberli et al., 2001; Kääb et al., 2004, Emmer et al., 2015), Asia (Hewitt, 1968 1982, 2002; Ives, 1986; Ding and Liu, 1992; Richardson and Reynolds 2000; Xin et al.,

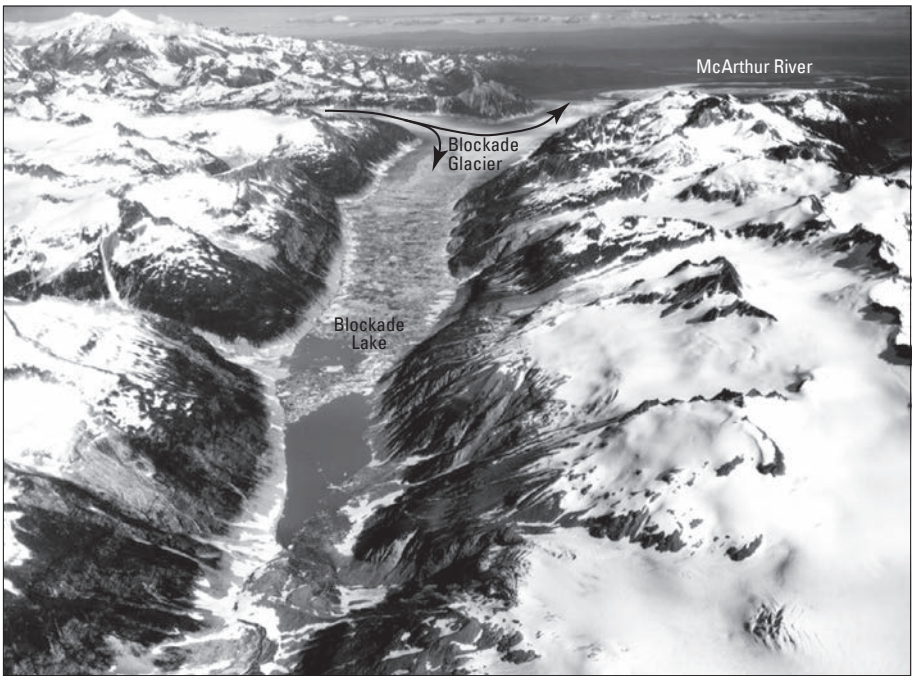

Fig. 2 View east of ice-dammed Blockade Lake in the process of refilling behind Blockade Glacier, Chigmit Mountains, Alaska; photograph by Austin Post ca. 1970. According to Post and Mayo (1971), this lake failed every several years causing floods on the McArthur River. More recent observations by U.S. Geological Survey geologists F. Wilson and P. Haeussler indicate that in July 2006 the lake nearly emptied by draining underneath Blockade Glacier.

2008; Hewitt and Liu, 2010; Bolch et al., 2011; Mergili and Schneider, 2011; Rounce et al., 2016; Margold et al., 2018; Zhang et al., 2019) and South America (Lliboutry et al., 1977; Dussaillant et al., 2010; Anacona et al., 2015a; Emmer et al., 2016a; Benito and Thornycraft, 2020).

Valley-blocking ice dams are now restricted to glacierized mountainous areas and polar regions but were more broadly distributed and larger during Pleistocene glaciations. The largest known outburst floods from breached ice dams were during the Pleistocene, when large alpine glaciers or tongues of ice from continental ice sheets blocked large drainage systems (Baker, 1983, 2009; Baker, 2020; Baker et al., 1993; Herget, 2005; Kehew et al., 2009; Kochel et al., 2009; Wiedmer et al., 2010; Margold and Jansson, 2011; Batbaatar and Gillespie, 2015; Komatsu et al., 2015; Hu et al., 2018; Bohorquez et al., 2019a; Yanchilina et al., 2019; Herget et al., 2020; O'Connor et al., 2020). But the relatively small ice dams of the Holocene have also produced outburst floods, commonly known by the Icelandic word 'jökulhlaup'. More than 100 outburst floods from ice-dammed lakes, excluding subglacial water bodies, with peak discharges ranging up to 10^5 m^3 s^{-1}, have occurred since 1800 CE (Walder and Costa, 1996). Hewitt (1982) alone documented evidence of at least 35 jökulhlaups since AD 1835 in the Karakoram Himalaya, but with apparently decreasing frequency as glaciers have retreated since the culmination of the Little Ice Age in the early 20th century.

As reviewed in more detail by Walder and Costa (1996), Tweed and Russell (1999), Roberts (2005), and Clague and O'Connor (2020), the interactions among the flowing valley-blocking ice, surrounding landscape, and impounded water are complex, leading to a variety of stable and unstable scenarios as well as diverse ice-dam failure mechanisms. Most ice dams impounding substantial water volumes ultimately fail (Carrivick and Tweed, 2016). In some situations, a "jökulhlaup cycle" (Evans and Clague, 1994) can develop, with repeated blockage, outburst flood, and then re-blockage owing to interactions among the deforming ice and impounded water. Such cycles are exemplified by nearly regular outburst floods from some glaciers for several years or decades. Such releases may be approximately annual or at shorter or longer periods depending on interactions between the blocking glacier and filling of the impounded valley (Hulsing, 1981; Mathews and Clague, 1993; Depetris and Pasquini, 2000; Walder et al., 2006; Kropáček et al., 2015). These cycles change with overall glacier condition; receding and thinning glaciers typically result in more frequent but smaller outburst floods, while the converse results from glacier thickening (Evans and Clague, 1994; Clague and Evans, 1997). Because of overall glacier retreat and thinning, the frequency of floods from ice-dammed lakes has apparently diminished over the past 50 years (Carrivick and Tweed, 2016).

A tremendous example of the jökulhlaup cycle is the dozens of late Pleistocene Missoula floods (Waitt, 1980, 1985) that at intervals of years to decades (Atwater, 1986) helped carve the Channeled Scabland of the northwestern United States with discharges up to 20×10^6 m^3 s^{-1} (Fig. 3; O'Connor and Baker, 1992; O'Connor et al., 2020). This episode of flooding resulted from repeated blockage of the Clark Fork River valley, western Montana, by the Purcell Trench lobe of the Cordilleran Ice Sheet, impounding glacial Lake Missoula, which at its maximum held 2.5×10^{12} m^3 of water.

Fig. 3 Nearly 40 beds of Missoula flood slackwater deposits exposed in 30-m-deep Burlingame Canyon within the Channeled Scablands of western United States. This section inspired the hypothesis by Waitt (1980) that glacial Lake Missoula released dozens of humongous jökulhlaups during the late Pleistocene. Photograph by Bruce Bjornstad.

Water impounded by valley-blocking ice dams can escape by overtopping or by passing through subglacial or englacial tunnels and cavities. Commonly, ice-dammed lakes drain via subglacial tunnels, typically described as being initiated by local flotation of the ice, although the physics are more complex (Fowler, 1999; Ng and Björnsson, 2003; Flowers et al., 2004; Ng and Liu, 2009). Outlets enlarge by both thermal and mechanical erosion but can narrow or close during and after the flood by cryostatic pressure and ice deformation, especially for subglacial releases under thick glaciers (Liestøl, 1956; Nye, 1976; Clarke, 1982; Roberts, 2005; Björnsson, 2010). Large peak discharges from subaerial lakes that emptied by subglacial or englacial tunnels include the floods from Vatnsdalslón, Iceland, 1898; Granænalón, Iceland, 1939; and Strandline Lake, Alaska, 1984; all of which had peak discharges of $3–5 \times 10^3$ m^3 s^{-1} (Thórarinsson, 1939; Sturm et al., 1987).

The largest and historically most lethal glacier outburst floods are the "sudden break" outbursts (Haeberli, 1983), denoted by Walder and Costa (1996) as "non-tunnel lake-drainage." These typically involve more rapid mechanical failure of the ice dam, including collapse of tunnels. Failure commonly occurs by overtopping and breach erosion along the junction between ice and a valley wall. In some instances outburst floods start as tunneling events, but roof collapse leads to open breaches (Walder and Costa, 1996). Historical examples of these types of floods include the 1986 Hubbard Glacier rupture, with a peak flow of 1.05×10^5 m^3 s^{-1} (Mayo, 1989). Walder and Costa's (1996) compilation notes several other non-tunnel outbursts from ice dams with peak discharges exceeding 10^4 m^3 s^{-1}.

Lakes impounded by tributary valley glaciers blocking large valleys appear especially susceptible to overtopping or ice-marginal breaches, as are lakes impounded by cold-based glaciers. In contrast, lakes impounded within tributary valleys by mainstem glaciers are more likely to escape, with lesser peak discharge for a given volume, by tunnels within or at the base of the glacier (Walder and Costa, 1996).

Ice avalanches also impound lakes. A notable example is the 1818 outburst from the foot of Giétro Glacier in the Dranz Valley, Switzerland (Ancey et al., 2019). Ice avalanches descending from the glacier front dammed the valley bottom to a depth of 80 m. During emergency drainage, implemented by tunneling through the ice dam, retrograde erosion initiated catastrophic failure, producing an outburst flood with a peak discharge of about 1.45×10^4 m^3 s^{-1} and resulting in about 40 fatalities. This is the largest glacial lake outburst flood of the last two centuries in Switzerland. Liu et al. (2019) also report three valley-blocking avalanches in Tibet in 1983, 1984, and 1985; the largest forming an impoundment 29 m high and producing an outburst flood of 8195 m^3 s^{-1}.

Another form of ice damming is ice jams in which seasonally formed river ice accumulates at constrictions or river bends, causing ponding upstream. Tremendous floods can result when these jams fail, commonly during spring break-up. Such was the case in April 1952 on the Missouri River, North Dakota, where the break-up of the seasonal ice accumulation resulted in an increase in discharge from 2.1×10^3 m^3 s^{-1} to 1.4×10^4 m^3 s^{-1} within 24 h (O'Connor and Costa, 2004). The U.S. Army Corps of Engineers Cold Regions Research & Engineering Laboratory maintains a database (White and Zufelt, 1994; White et al., 2006) that, as of 2020, listed more than 18,000 ice jams in 45 of the 50 U.S. states, dating back to 1780 for some states (https://icejam.sec.usace.army.mil/; accessed 04 April 2020).

Extreme ice-jam floods are most common in high-latitude, north-flowing continental river systems of northern Eurasia and North America, particularly the Lena, Yenisei, Ob, Yukon, and Mackenzie rivers. Large poleward flowing rivers are especially susceptible to large ice-jam floods because headwater reaches at lower latitudes may melt before downstream reaches, increasing the potential for large blockages. Some of the largest documented historical floods have resulted from ice jams on the Lena River in Russia, where ice accumulations several kilometers long can impound water to depths as great as 10 m, extensively inundating wide floodplains (Costard and Gautier, 2007). Several floods on the Lena River resulting from the combination of breached ice dams and heightened snowmelt runoff have exceeded 1×10^5 m^3 s^{-1} (Rodier and Roche, 1984; Costard and Gautier, 2007; http://rims.unh.edu/data.shtml [accessed 03 April 2020]).

2.1.2 Landslide dams

Breached landslide dams are the major source of historical outburst floods, known in the Himalaya by the Nepali word *bishyari* (Dixit, 2003). Many have been horrendously lethal. And some have possibly transformed cultures, such as Chinese Emperor Yu's great flood of ~4000 years ago marking the beginning of the Xia dynasty and onset of the Chinese Bronze Age, attributed to a breached landslide dam (Wu et al., 2016). Landslide dams (Fig. 4) are produced by a wide range of mass movements of rock, regolith, and sediment that block rivers or streams, typically by entering a valley from side slopes or tributary drainages. They are also the most studied type of natural dam, especially since Costa and Schuster's (1988) benchmark synthesis of natural dams and their inventory of landslide dams (Costa and Schuster, 1991). Recent summaries that expand or elaborate on classification systems, genesis, distribution, and geomorphic effects of landslide dams have been provided by Cenderelli (2000), Korup (2002), Shang et al. (2003), Hewitt (2006, 2009), Korup and Tweed (2007), Hewitt et al. (2008), Hermanns et al. (2011b); Evans et al. (2011), Peng and Zhang (2012), and Fan et al. (2020). The landslide-dam catalogs summarized by Fan et al. (2020) total more than 1800 entries, including 410 post-AD-1900 landslide dams with blockage volumes exceeding 10^6 m^3.

Landslide dams can have volumes exceeding 10^{10} m^3 and form lakes more than 1000 m deep (Hewitt, 1998, 2006; Korup, 2002). The largest recorded historical water flow on Earth was the 10 June 2000 breach of a 55-m-high landslide dam on the Yigong River, Tibet, which resulted in a peak flow of 1.2×10^5 m^3 s^{-1}. The largest existing dam of any kind in the world is the Usoi landslide dam in Tajikistan. This blockage formed in 1911 by a 2.2×10^9 m^3 rockslide into the Bartang River valley, damming it to a depth of >550 m and impounding a lake reported by Ischuk (2011) to be 55 km long and up to 500 m deep and containing 1.6×10^{10} m^3 of water. For comparison, the Usoi landslide dam is nearly twice the height of the world's tallest constructed dam, the 300-m-high Nurek rockfill dam, also in Tajikistan. Nevertheless, the Usoi landslide dam is only about half the height and one-tenth the volume

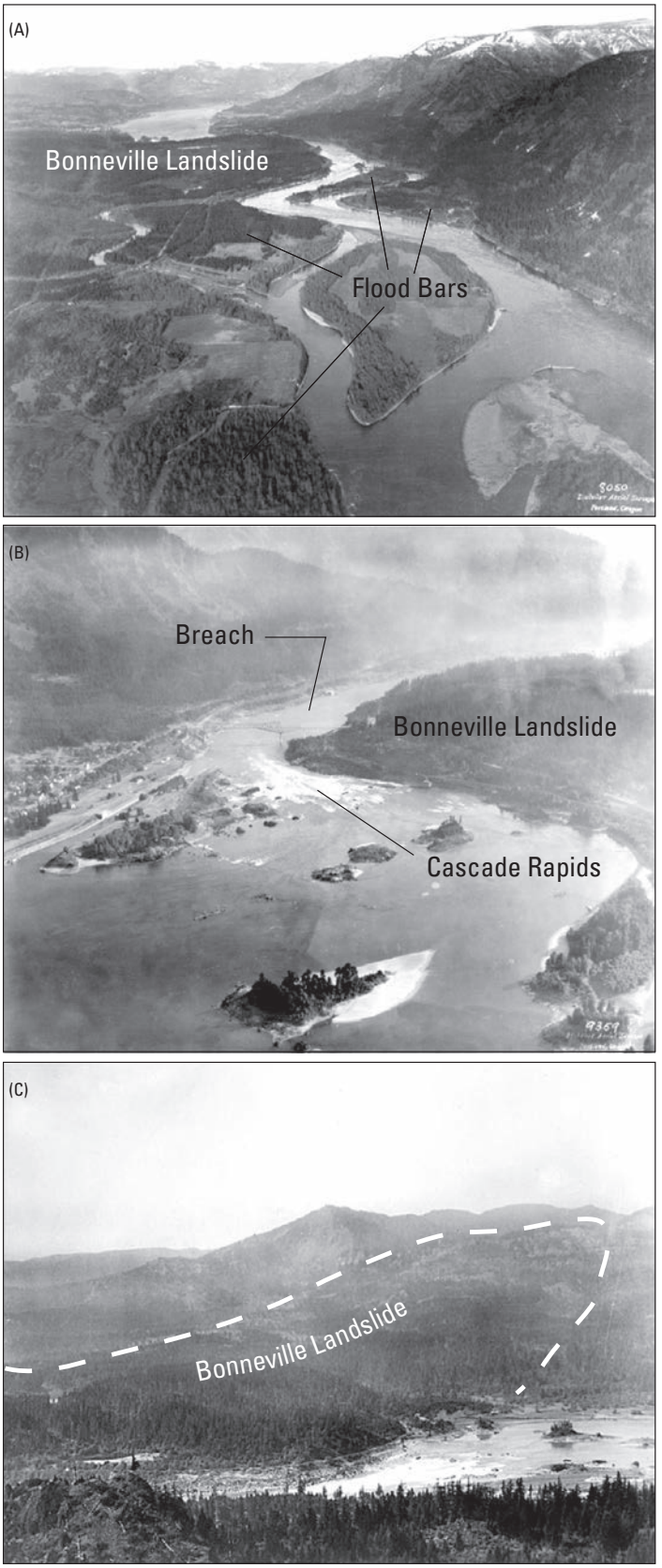

Fig. 4 Bonneville landslide dam, which blocked the Columbia River at the border between Oregon and Washington to a depth of more than 80 m about 1450 AD before breaching cataclysmically. Breaching occurred sometime before the Lewis and Clark exploration of the area in 1805 AD (O'Connor, 2004). (A) View upstream (east) toward the toe of the landslide, which completely filled the valley bottom. The impoundment breached at the southern distal end of the landslide, creating a new course of the Columbia River around the toe of the landslide. The breach was abrupt; floodwaters deposited bouldery flood bars in the valley bottom downstream. (B) View downstream (west) of the toe of landslide and the breach area. Cascade Rapids, where the Columbia River descends ~15 m over the bouldery debris, resulted from incomplete incision of the landslide dam. (C). View north-northwest across Cascade Rapids and the breach area toward main body of the landslide. Modified from O'Connor JE, Beebee RA (2009) Floods from natural rock-material dams. In: Burr, D.M., Carling, P.A., Baker, V.R. (eds.), Megaflooding on Earth and Mars. pp. 128–171. United Kingdom: Cambridge University Press. http://refhub.elsevier.com/S0012-8252(20)30223-3/rf9017. (A) Photograph taken on 11 April 1928; courtesy of U.S. Army Corps of Engineers. (B) Photograph taken on 9 September 1929; courtesy of U.S. Army Corp of Engineers. (C) Photograph is undated but was taken prior to 1932 when this reach was inundated by Bonneville Dam; courtesy of U.S. Army Corp of Engineers.

of Rondu-Mendi rock avalanche, which apparently blocked the Indus River in the Karakoram Himalaya of northern Pakistan sometime in the Pleistocene (Hewitt, 1998).

Fast-moving debris flows and landslides may form dams in seconds or minutes, whereas more sluggish landslides and earthflows may take several years to completely block a river, if at all. Landslide dams can remain stable and unbreached, can breach after long periods—130 years in the case of the Tegermach River blockage in Kirgizstan (Costa and Schuster, 1991)—or breach minutes after formation, as in the case of the Pollalie Creek debris flow, which blocked the East Fork Hood River, Oregon, for only about 12 min before failing (Gallino and Pierson, 1985). Some landslide dams, such as the Flims rockslide on the Rhine River in Switzerland, can create multiple or complex impoundments over time and undergo multiple episodes of partial breaching and sediment infilling (Wassmer et al., 2004; von Poschinger, 2011).

Although not considered in detail here, landslides can also cause floods by mechanisms other than blocking channels (Costa, 1991). Landslides have triggered breaches of natural and artificial dams (Hermanns et al., 2004), and in many mountainous environments, mass movements evolve into debris flows or sediment-laden floods (Eisbacher and Clague, 1984). In several instances, landsliding directly into lakes has triggered large waves or expelled water, causing downstream floods. Examples are the 1983 flood of Ophir Creek, Nevada (Glancy and Bell, 2000) and, more lethally, the 1963 Mount Toc landslide into the Vajont (Vaiont) Reservoir, Italy, displacing a 245-m wave over the 262-m-high concrete arched dam and killing more than 2000 downvalley inhabitants (Kilburn and Petley, 2003; Ghirotti, 2012).

Landslide dams are found in all mountainous areas in the world (Costa and Schuster, 1991; Ermini and Casagli, 2003; Korup and Tweed, 2007; Hewitt et al., 2008; Fan et al., 2020). Hundreds have been mapped in the Himalaya (Hewitt, 1998, 2006, 2011; Shroder, 1998; Delaney and Evans, 2011; Ruiz-Villanueva et al., 2017); Tibet and China (Li et al., 1986; Hejun et al., 1998; Chai et al., 2000; Shang et al., 2003; Fan et al., 2017; Liu et al., 2019); Europe (Eisbacher and Clague, 1984; Nicoletti and Parise, 2002; Tacconi Stefanelli et al., 2016); Japan (Swanson et al., 1986); New Zealand (Adams, 1981; Perrin and Hancox, 1992; Korup, 2002); the South America Cordillera (Plaza-Nieto and Zevallos, 1994; Schuster et al., 2002; Hermanns et al., 2011a; Tacconi Stefanelli et al., 2018); and the western North America Cordillera (Costa and Schuster, 1991; Clague and Evans, 1994; Safran et al., 2015). These dams are most common in mountainous regions because high relief promotes mass movements and confined valleys are readily blocked by landslide debris (Costa and Schuster, 1988). Korup et al. (2006, 2007) determined that the largest terrestrial landslides, those with volumes greater than 10^8 m^3 and forming dams hundreds of meters tall, are concentrated in tectonically active mountain belts and volcanic arcs. More than half of these mass movements were in the steepest parts of the surrounding landscape. Additionally, certain geological environments favor landslides and landslide dams by virtue of structural orientations or weaknesses (Alden, 1928), stratigraphy (Palmer, 1977; Safran et al., 2011), active volcanism (Meyer et al., 1986; Scott, 1989; Capra and Macías, 2002), seismicity (Davis and Karzulovíc, 1963; Nicoletti and Parise, 2002), and glacier retreat (Evans and Clague, 1994; Bovis and Jakob, 2000).

Volcanoes are also sources of large landslides or debris avalanches, which by blocking tributary valleys set the stage for landslide dam failures (Capra, 2011; Manville, 2015; Walsh et al., 2016; Fan et al., 2020). An example is the 1980 debris avalanche at Mount St. Helens, which carried 2.3×10^9 m^3 of the edifice into the North Fork Toutle River valley, impounding several tributary drainages and raising the height of the natural dam bounding Spirit Lake (Voight et al., 1981; Youd et al., 1981; Meyer et al., 1986). Scott (1989) documented previous debris-avalanche damming at Mount St. Helens ~2500 years ago, followed by a lake outbreak and downstream lahar with a peak discharge exceeding 2.5×10^5 m^3 s^{-1}. Some of the landslides associated with volcanoes, such as the case with Mount St. Helens, are triggered by eruptive activity. But many volcanic landslides and debris flows that lead to floods are not directly triggered by magmatic activity, an example being the debris flow from Mount Hood, Oregon, that temporarily dammed the East Fork Hood River in 1980 (Gallino and Pierson, 1985).

The engineering community has recognized the compound hazard posed by landslide dams and their impounded water bodies; consequently such dams and resulting outburst floods are typically studied as hazards rather than as geomorphic agents (Whitehouse and Griffiths, 1983; Schuster and Costa, 1986; Costa and Schuster, 1988; Webby and Jennings, 1994; Jakob and Jordan, 2001; Schuster and Highland, 2001; Risley et al., 2006; Hermanns et al., 2013). Recent work by geomorphologists, however, also demonstrates the important role of landslide dams and debris flows on the evolution of fluvial systems in many mountainous environments (Hewitt, 2006, 2009; Korup, 2006; Lancaster and Grant, 2006; Hewitt et al., 2008, 2011; Safran et al., 2011, 2015; Fan et al., 2020). These studies harken back to an idea advanced in 1830 by Charles Lyell in his *Principles of Geology* (vol. 1, pp. 192–193):

> The power which running water may exert, in the lapse of ages, in widening and deepening a valley, does not so much depend on the volume and velocity of the stream usually flowing in it, as on the number and magnitude of the obstructions which have, at different periods, opposed its free passage.

Landslide dams are vulnerable to breaching because they commonly consist of unconsolidated porous material and have no controlled outlet. Landslide dams that do breach typically do so within weeks or months of formation by overtopping and rapid erosion of an outlet channel (Costa and Schuster, 1988; Ermini and Casagli, 2003; Tacconi Stefanelli et al., 2018; Fan et al., 2020), sometimes in conjunction with upstream flooding caused by rainfall or snowmelt (Hancox et al., 2005). The review of Fan et al. (2020) suggests that certain types of landslide dams, particularly those formed of unconsolidated sediment are more prone to rapid failure than those emplaced by rock/debris avalanches and rockslides involving coherent blocks of bedrock.

Most landslide dams are triggered by precipitation, rapid snowmelt, volcanic activity, and earthquakes (Costa and Schuster, 1988; Peng and Zhang, 2012; Liu et al., 2019; Fan et al., 2020). Recent work has emphasized the role of earthquakes in generating

landslide dams, many of which are susceptible to catastrophic breaching (e.g., Xu et al., 2009; Fan et al., 2012, 2019). For example, the breach of a quake-triggered landslide dam on the Dadu River, China, in 1786 killed more than 100,000 people (Dai et al., 2005). Rarer are failures by ground-water piping or mass movement of the blockage itself (Costa and Schuster, 1988). Some breaches are triggered by large water waves overtopping the blockage, such as for the 1963 breach of the Issyk landslide dam in Kazakhstan (Gerasimov, 1965). Similarly, long-lasting landslide dams in the Argentine Andes apparently breached catastrophically by large waves triggered by rock avalanches into the impounded lakes (Hermanns et al., 2004).

Geological evidence of outburst floods and debris flows from breached landslide dams is becoming increasingly recognized in many mountainous environments. In most cases, bouldery fluvial or debris-flow deposits are traced to incised landslide masses filling valley bottoms (Selting and Keller, 2001; Beebee, 2003; O'Connor et al., 2003; Safran et al., 2015). The remnant landslide barriers and flood deposits can form persistent features in valley bottoms (Schuster, 2000; O'Connor et al., 2003; Korup and Tweed, 2007; Hewitt et al., 2008; Harrison et al., 2015; Fan et al., 2020).

Many landslide dams do not fail catastrophically; rather their lakes fill partly or wholly with sediment before the blockage is significantly eroded (Clague and Evans, 1994; Hewitt, 2006). Of the 340 landslide dams whose fate is documented in the Costa and Schuster (1991) global compilation, about 75% breached and produced downstream floods. Similarly, 67% of the 282 landslides dams in the similar but updated compilation by Ermini and Casagli (2003) breached cataclysmically. In both compilations, the failure percentages may be overestimates, because landslide dams that breach cataclysmically are more likely reported in the literature than those that do not. From a more systematic survey of 232 landslide dams in New Zealand, Korup (2004) reports that about 37% apparently have failed, although the analysis may not fully account for very short-lived blockages that left little lasting evidence.

Predicting the stability of landslide dams is challenging because of the many internal and external factors controlling dam stability and breach-triggering mechanisms (Costa and Schuster, 1988; Ermini and Casagli, 2003; Korup, 2004; Korup and Tweed, 2007; Dunning et al., 2005; Fan et al., 2017, 2020). Quantitative indices based on morphometric and watershed characteristics, including dam height and volume, impounded water volume, watershed area, and relief, have been successful locally in discriminating stable from unstable dams (Ermini and Casagli, 2003; Korup, 2004; Tacconi Stefanelli et al., 2016), but their predictive power is low and critical values separating stability domains seem to depend on regional conditions (Korup, 2004).

2.1.3 Volcanogenic dams

Volcanism can directly trigger large floods and debris flows by rapid melting of snow and ice; the floods include the large Icelandic *jökulhlaups* (Roberts, 2005; Björnsson, 2009), and volcanogenic debris flows are often referred to by the Indonesian term *lahar*. Large snow-and-ice augmented lahars have been documented for many of the tall stratovolcanoes of the Pacific Rim. The November 1985 lahar triggered by the eruption of Nevado del Ruiz, Colombia, killed more than 23,000 in the city of Armero (Pierson et al., 1990). In addition to lahars and floods produced directly by volcanism, many of which which may not strictly be outburst floods, eruptions can also indirectly cause floods by blocking drainages with primary volcanic materials such as lava, pyroclastic debris, lahars, and debris avalanches, which can lead to outburst floods (Umbal and Rodolfo, 1996; Capra, 2007, 2011; Manville, 2015; Fan et al., 2020).

These volcanogenic blockages share many similarities with landslide dams, although the materials are different. Macías et al. (2004) summarized volcanic dams and described the hot 1.1×10^4 m^3 s^{-1} flood that resulted from breaching a dam of pyroclastic flow material deposited in the April 3, 1982, eruption of El Chichón, Mexico. Also in Mexico, a late Pleistocene debris avalanche from Nevado de Colima volcano blocked the Naranjo River, forming a 1×10^9 m^3 lake, which then breached to produce a 3.5×10^6 m^3 s^{-1} debris flow downstream (Capra and Macías, 2002). Another large lake ($\sim 1 \times 10^9$ m^3) was impounded behind a welded block-and-ash breccia that blocked the Lillooet River in British Columbia, Canada, about 2350 year BP. This lake breached cataclysmically, transporting still-hot blocks as large as 15-m in diameter up to 3.5 km downstream (Hickson et al., 1999; Andrews et al., 2014). Several outburst floods from breached lahar dams and volcanogenic debris-avalanche deposits probably have coursed down the Chakachatna River, which drains the Mt. Spurr volcanic complex in south-central Alaska (Waythomas, 2001), and similar events have caused large floods in Japan (Kataoka et al., 2008). Two floods resulted from breaching of volcanogenic deposits blocking the outlet of Lake Tarawera, North Island, New Zealand, including a ca. AD 1315 flood with a peak discharge of $5–10 \times 10^4$ m^3 s^{-1} (Hodgson and Nairn, 2005). Multiple lake break-out floods followed repeated damming of tributaries by aggradational lahar deposits and secondary pyroclastic flows in the aftermath of the 1991 eruption of Mt. Pinatubo in the Philippines (Umbal and Rodolfo, 1996). Similar floods resulted from pyroclastic flows shed during the 7.7 ka climactic eruption of Mount Mazama, Oregon, which blocked the Williamson River (Conaway, 1999; Cummings and Conaway, 2009). The Rhine River, Germany, was apparently blocked repeatedly by Plinian pumice fallout during the 12.9 ka Laacher See eruptions (Park and Schmincke, 2020a,b). These blockages, formed of grounded and floating rafts of pumice, formed transient blockages similar to ice jams, yet impounded up to 8×10^8 m^3 of water and pumice. Breakouts, apparently during pauses in eruptive activity, produced floods overtopping downstream floodplains by as much as 10 m. Such dams of pyroclastic material are particularly susceptible to breaching because they erode quickly once overtopped or possibly floated by rising upstream water levels.

Dams composed of lava flows are less easily breached. Many valley-filling lava flows have blocked drainages, but very few are known to have breached cataclysmically. Examples include the breach of the Lagunas del Blanquillo, dammed by lava flows from the 1846–47 eruptions of Volcán Quizapu in Chile but breached and drained in 1932 by incursion of a lahar (Manville, 2015). Quaternary lava flows cascading into western Grand Canyon, Arizona, repeatedly blocked the Colorado River, possibly leading to as many as five outburst floods (Hamblin, 1994; Fenton et al., 2002, 2004, 2006). The best documented is the flood from the 165 ka

"hyaloclastite" dam, which was more than 140 m high and breached to produce a flood with a peak discharge of 2.3–5.3 × 10^5 m^3 s^{-1}. Crow et al. (2008), however, offer alternative interpretations not requiring outburst floods from the Grand Canyon lava dams. Another example of catastrophic failure of a lava flow blockage occurred at Laguna del Maule caldera in Chile. Emplacement of the Espejos rhyolite at 19.0 ± 0.7 ka dammed the northern outlet to the nearly 400 km^2 basin and raised the level of the lake by 200-m to form a prominent shoreline before breaching at ca. 9.4 ka and releasing ca. 1.5 × 10^{10} m^3 of water (Singer et al., 2018).

Lava-flow dams apparently breach cataclysmically only under special conditions, as exemplified by the Grand Canyon case. In the Grand Canyon, basalt poured into a steep-walled canyon occupied by a large river. The resulting lava dams were buttressed by unconsolidated talus and were composed partly of material that brecciated when the lava entered the river (Fenton et al., 2006). By contrast, most lava flows entering valleys or canyons in the western US formed long-lived blockages that did not breach cataclysmically; instead rivers were diverted into the more erodible materials forming the paleo-valley walls (Stearns, 1931; Malde, 1982; Howard et al., 1982; O'Connor et al., 2003; Duffield et al., 2006; Ely et al., 2012). Many of these lava flows travelled several kilometers down river valleys and formed massive and lengthy dams of solid lava resistant to breaching.

In some instances, volcanic cones themselves block drainages, leading to outburst floods. An example is the growth of Antuco volcano in Chile during the Pleistocene. The growing cone blocked Rio Laja, creating a lake >250 m deep. Collapse of the volcanic cone during a Bandai-type eruption and debris avalanche at about 7200 years ago completely emptied the lake, releasing 1.5–1.8 × 10^{10} m^3 of water and generating an outburst flood that deposited a 3000 km^2 alluvial plain in the Central Andean Depression. Growth of the Antuco-2 cone in the collapse amphitheater has since re-dammed the basin and progressively refilled Lago Laja to a depth of over 134 m (Thiele et al., 1998; Melnick et al., 2006).

2.1.4 Constructed dams

Floods from constructed dams (Fig. 5) are a process of human origin but they nonetheless pose significant hazards and can accomplish substantial geomorphic work (Costa, 1988). From a global database, Jansen (1980) reports over 2000 failures of constructed dams since AD 1100, resulting in more than 11,000 fatalities. Additionally, Liu et al. (2019) reports 3520 constructed-dam failures in China between 1954 and 2012. At least four constructed-dam failures since 1889 in China have each claimed more than 2000 lives, topped by the 1975 failure of Banqiao dam on the Ru River, China, which directly killed 26,000 by flooding and a subsequent 145,000 by resulting famine and disease (Costa, 1988; Si, 1998).

Most constructed dams are embankment dams composed of compacted fill and rock; other types include concrete or masonry structures relying on gravity, buttresses, and arch-shaped planforms to counter the reservoir mass (Costa, 1988). Tailings dams, which are embankments for storing mill byproducts and waste rock from mining activities, constitute another class of dams with significant outburst flood potential (Rico et al., 2008).

The largest reported peak discharge from a constructed dam failure was 7.8 × 10^4 m^3 s^{-1} released by Banqiao dam failure in China on 7 August 1975 (Table 1). This rock-fill dam was overtopped in the aftermath of super typhoon Lianna (Liu et al., 2019). Of similar magnitude was the 5 June 1976 piping failure of the 100-m-high earth-fill Teton Dam in Idaho; the flood had a peak discharge of 6.5 × 10^4 m^3 s^{-1} about 0.4 km downstream from the dam (Ray and Kjelström, 1978). Other large discharges are 3.7 × 10^4 m^3 s^{-1} from the 12–13 March 1928 failure of the masonry St. Francis Dam in California (Outland, 1963; Rogers, 1992), 2.8 × 10^4 m^3 s^{-1} from the 2 December 1959 breach of the concrete arch Malpasset Dam in France (Costa, 1988), 2.5 × 10^5 m^3 s^{-1} from the 8 June 1964 failure of Swift Reservoir, Montana (Boner and Stermitz, 1967), and 8.2 × 10^3 m^3 s^{-1} from the 14 December 2005 failure of the Taum Sauk reservoir, Missouri (Rydlund, 2006). A recent large dam failure was the breach an earthen saddle dam impounding a reservoir in the Mekong River basin, southern Laos, on 23 July 2018, which released 3.5 × 10^8 m^3 of water at a peak discharge of 8.5 × 10^3 m^3 s^{-1} (Latrubesse et al., 2020).

Some floods from constructed dams are intentional, part of the recent spate of dam decommissioning (e.g., Foley et al., 2017). A well-documented example is the 2011 breaching of Condit Dam on the White Salmon River, Washington State, which produced a peak discharge of about 420 m^3 s^{-1} and an ensuing hyperconcentrated flow, as about 10% of the sediment impounded in the reservoir liquefied and moved down the channel (Wilcox et al., 2014a). So far, such intentional outburst floods from breaching constructed dams have been small, but they do provide excellent opportunities to study the short- and long-term consequences of dam breaching (e.g., Major et al., 2012).

2.1.5 Other types of valley blockages

Other types of valley blockages affect fluvial systems, but rarely produce outburst floods of great hazard or geomorphic significance. Beaver dams and resulting ponds were pervasive across North America prior to 16th–19th century trapping. Substantial valley aggradation has been attributed to beaver dams (Ruedemann and Schoonmaker, 1938; Gurnell, 1998) but documentation of outburst floods from beaver dam failures is rare. An exception is Butler and Malanson's (2005) compilation of several outburst floods, including four resulting in fatalities. In most cases, because of the small sizes of beaver dams and their impoundments, damage and geomorphic consequences are localized, although an exception is the 15 m^3 s^{-1} flood from a breached beaver dam in Alberta, Canada, which greatly exceeded meteorological floods in the watershed and significantly affected the riparian corridor (Table 1; Hillman, 1998).

Breaching of beach-barrier spits, especially where they impound small drainages or estuaries, can cause small outburst floods (Kraus et al., 2002). Such blockages are typically formed of littoral or eolian sand and occur on steep beaches where high wave run-up can form sand barriers two or more meters above typical high tide levels. These littoral processes most effectively impound water

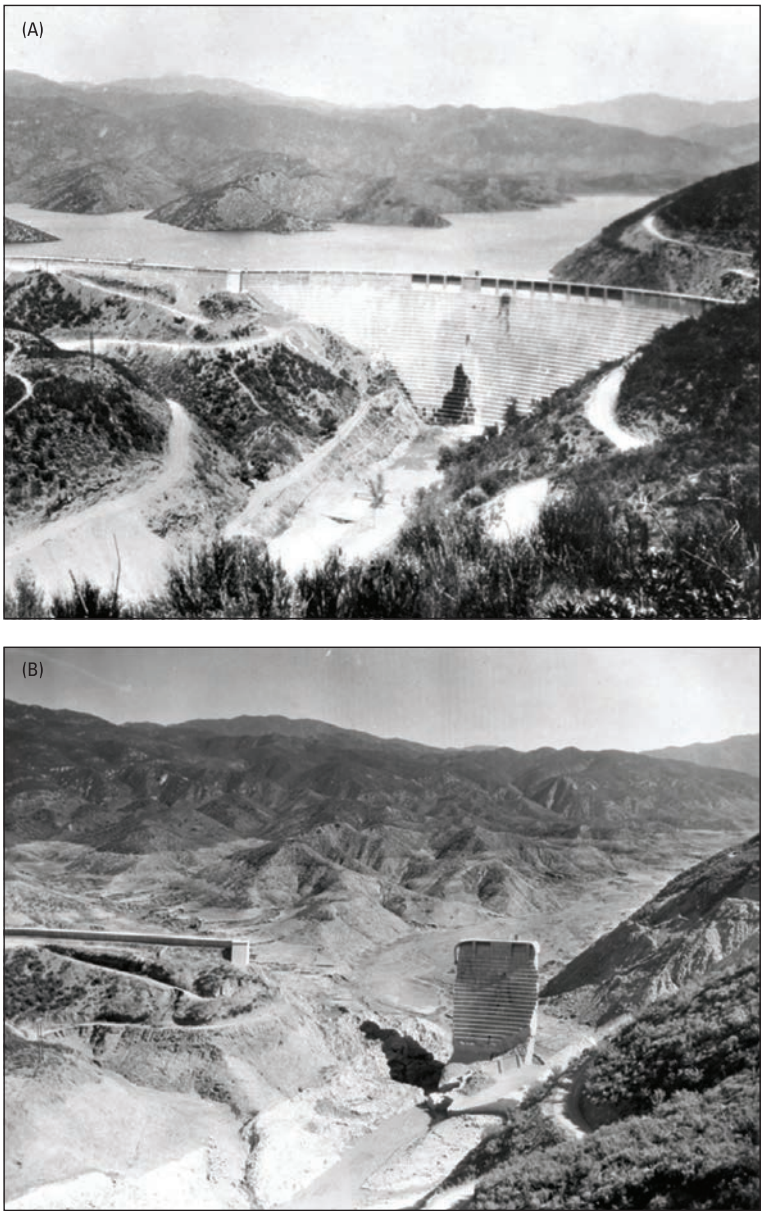

Fig. 5 Before and after views of the 12–13 March 1928 failure of St. Francis Dam, San Francisquito Canyon, California, United States. The masonry dam was 60 m high and impounded 4.71×10^7 m^3 of water at the time of failure. Peak discharge was 3.7×10^4 m^3 s^{-1}. The flood killed about 450 people (Outland, 1963; Rogers, 1992). (A) View of St. Francis Dam prior to failure. Photograph by Los Angeles Bureau of Power and Light and is part of H.T. Stearns USGS photograph collection. http://libraryphoto.cr.usgs.gov/; accessed 21 May 2011. (B) Photograph from the same location taken on 17 March 1928 by H.T. Stearns (USGS). http://libraryphoto.cr.usgs.gov/; accessed 21 May 2011.

bodies either where the tidal prism is small or river flow is low (Stretch and Parkinson, 2006; Parkinson and Stretch, 2007). In a global survey, McSweeney et al. (2017) identified nearly 1500 estuaries intermittently blocked by sand berms, mostly on wave dominated coastlines with small tidal ranges. Such blockages and breaches have been reported in Australia (Gordon, 1990), South Africa (Parkinson and Stretch, 2007), India and Sri Lanka (Ranasinghe and Pattiaratchi, 2003) and the west coast of the United States (Kraus et al., 2002; Behrens et al., 2013). Many breaches, known locally as "pond lettings" (Kraus et al., 2002), are intentional to control coastal or estuary flooding. But some breaches are uncontrolled and result from either seaward or landward causes. Seaward breaches typically happen when storm surges or large ocean waves overtop and incise the barrier, whereas landward breaches typically result from high flows that fill the blocked estuary or inlet and overtop the barrier. Seepage and piping can contribute to failure of these sandy barriers (Kraus et al., 2002). Because the maximum blockage height is typically less than 3 m, floods from breached beach barriers are small—the largest documented had a peak discharge of 4.1×10^2 m^3 s^{-1}. Yet they can cause substantial geomorphic, ecologic, and economic consequences by altering estuary and tidal inlet geometry (Van Niekerk et al., 2005; Parkinson and Stretch, 2007).

A large Holocene flood on the Sycan River, Oregon, may have resulted from blockage of the river by an eolian dune in a canyon reach near the outlet of a large tectonic basin (Table 1; Lind et al., 2007; Lind, 2009). In this case, a flood of about 5.8×10^3 m^3 s^{-1}, about 25 times larger than the largest historical flood, swept down the Sycan River shortly after the 7.7 ka eruption of Mount Mazama blanketed the surrounding landscape with up to 50 cm of coarse pumice. Extensive, now-vegetated dunes composed of this pumice cover the region. A dune, perhaps only a few meters high, at the seasonally dry and confined outlet of the extensive Sycan Marsh probably impounded a shallow lake that was the flood source.

2.2 Floods from breached basins

Overflow from tectonic basins, moraine-rimmed lakes, lakes in volcanic calderas and craters, and basins formed along isostatically depressed margins of large ice sheets can involve tremendous water volumes and cause major changes to drainage networks. For example, the Bonneville Flood from the tectonic basin of Great Salt Lake of the western US, with a total volume of 4.75×10^{12} m^3, is one of the largest known freshwater floods in Earth history (Table 1; O'Connor et al., 2002). Similarly, the late Miocene filling of the Mediterranean Sea basin from the Atlantic (Hsü, 1983; Garcia-Castellanos et al., 2009, 2020) is the largest known cataclysmic marine incursion (Fig. 1). Several processes can form basins that later fill and overflow. The material and geometry of the basin divide determine whether and how rapidly a breach may form, as well as the ultimate depth of outlet incision.

2.2.1 Basins marginal to ice sheets

Extensive lakes formed at the periphery of Pleistocene ice sheets, occupying basins partly resulting from crustal depression by the mass of ice but also commonly rimmed by morainal ridges. The best-known examples are the extensive ice-marginal lakes and resulting outburst floods along the southern margin of the Laurentide Ice Sheet in North America during and after the last glacial maximum (Teller et al., 2002; Teller, 2003; Kehew et al., 2009). In other locations, Pleistocene lakes formed as ice sheets encroached upon and blocked the lower parts of large drainages, such as the north-flowing Yenisei, Ob, Pechora, and Mezen rivers in Siberia (Grosswald, 1980; Mangerud et al., 2004; Yanchilina et al., 2019).

Pleistocene ice-marginal lakes are some of the largest known freshwater lakes in Earth history. Many of these lakes generated huge outburst floods. Lake Agassiz, which existed at the southwest margin of the Laurentide Ice Sheet between 13,000 and 8000 years ago, covered 1.5×10^{12} m^2 at its maximum and contained up to 1.5×10^{14} m^3 of water (Clarke et al., 2004; Teller et al., 2002; Teller and Leverington, 2004). Kehew et al. (2009) tabulated at least 35 large floods from the margin of the Laurentide Ice Sheet near the end of the last glacial period, several with peak discharges exceeding 1×10^6 m^3 s^{-1}. Similarly, ice-dammed lakes inundated 6×10^{11} m^2 (Mangerud et al., 2004) and possibly as much as 1.2×10^{12} m^2 of the Siberian plain with 7.5×10^{13} m^3 of water (Grosswald, 1980; Arkhipov et al., 1995; Yanchilina et al., 2019). Middle Pleistocene ice-marginal lakes flanking the Scandinavian ice sheet in north-central Europe contained up to 5×10^{11} m^3 of water. Some produced outbursts that flooded the lower Rhine River embayment and flowed into the North Sea, and possibly involved lake volumes as great as $\sim 2 \times 10^{11}$ m^3 and peak discharges of $\sim$500,000 m^3 s^{-1} (Winsemann et al., 2016; Lang et al., 2019; Winsemann and Lang, 2020). Smaller lakes formed where continental ice sheets impinged on mountain ranges and blocked valleys, as in the central Appalachians where a Middle Pleistocene ice sheet impounded several lakes containing as much as 1×10^9 m^3 of water (Kochel et al., 2009).

Ice-marginal lakes are unstable and can fail by (1) overtopping and breaching of moraine or rock basin divides at the outer margins of the lakes, (2) subglacial drainage under or along the ice-sheet margin, or (3) uncovering of new lower outlets as the glacier retreats. All such processes probably operated along the Laurentide Ice Sheet margin. Many large floods breached outer moraines rimming high proglacial lakes in the Great Lakes basins; many others issued from Lake Agassiz when progressively lower outlets were uncovered as the ice sheet margin retreated northward (Teller et al., 2002; Kehew et al., 2009); and some resulted from subglacial drainage (Clarke et al., 2004). Similarly, glacial Lake Purcell, holding about 1.4×10^{11} m^3 in the Columbia River basin, Canada, apparently emptied cataclysmically as the Purcell Trench ice lobe melted back at the end of the last glacial period and uncovered an outlet via the Kootenay River valley (Peters and Brennand, 2020). Large Siberian lakes, such as $\sim$90 ka Lake Komi in the Pechora River basin of western Russia, found progressively lower outlets through low passes into other basins as ice margins retreated. Lake Komi discharged to the west into the Baltic Sea, whereas the large ice-marginal lake in the blocked Ob and Yenisei drainages apparently had its outlet to the south, into the Aral and Caspian seas (Mangerud et al., 2004).

Some floods from ice-marginal lakes may have initiated new continental-scale drainage paths, such as in north-central Europe (Lang et al., 2019). Moreover, compelling evidence shows that these floods substantially affected climate during the waning stage of the last glacial period. For example, the $\sim$1300-year-long Younger Dryas cold event, which began about 13,000 years ago, has been attributed to a 9.5×10^{12} m^3 outburst from glacial Lake Agassiz into the Arctic Ocean that altered oceanic thermohaline circulation and induced global cooling (Teller et al., 2002; Murton et al., 2010; Teller, 2012; Condron and Winsor, 2012). Similarly, abrupt cooling that affected the northern hemisphere between 8400 and 8000 years ago has been attributed to a final outburst of glacial lakes Agassiz and Ojibway into Hudson Bay and the Labrador Sea, perhaps involving a volume exceeding 1.6×10^{14} m^3 (Barber et al., 1999; Clarke et al., 2004; Alley and Ágústsdóttir, 2005; Teller et al., 2002).

2.2.2 Moraine-rimmed basins

Basins formed by moraines include (1) river valleys blocked by lateral and end moraines and (2) closed depressions formed by ice retreat from moraines formed during times of advanced ice (Fig. 6). The former are probably more appropriately classified as valley blockages, similar in morphology and behavior to landslide dams; the latter result in far more outburst floods. Moraine-dammed

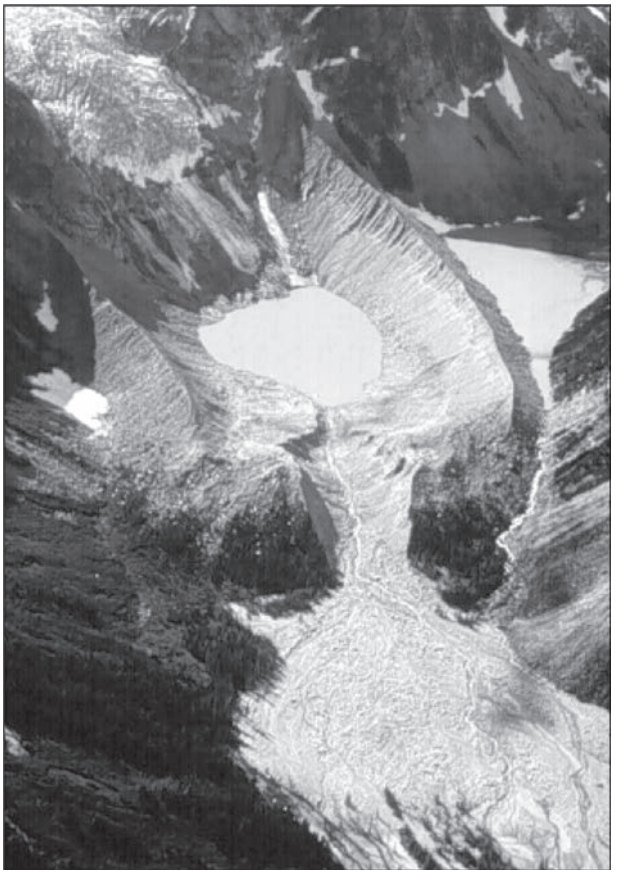

Fig. 6 Breached Neoglacial moraine of Cumberland Glacier and remnant Nostetuko Lake, British Columbia, Canada, after 19 July 1983 outburst flood. The lake level dropped 28.4 m, releasing 6.5×10^6 m^3 of water (Blown and Church, 1985; Clague and Evans, 1994). August 1984 photograph by J. J. Clague.

lakes and resulting floods are commonly categorized under the more general heading of "glacial lakes" and "glacial outburst floods" (e.g., Carrivick and Tweed, 2013, 2016; Emmer, 2018; Veh et al., 2020). Floods from moraine-dammed lakes (Table 1) have been extensively studied for several decades because they are an alpine hazard and important geomorphological agent. Releases from moraine-dammed lakes are sudden and rapid and thus produce impressive erosional and depositional features far from the lakes (e.g., Cook et al., 2018). The phenomenon was first documented comprehensively in the Cordillera Blanca of Peru, where resulting debris flows and floods are known as *aluviones* (Lliboutry et al., 1977) and caused nearly 6000 fatalities between 1941 and 1960 (Carey, 2005; Emmer, 2017). They are now commonly termed *GLOFs*, short for glacial lake outburst floods. Summaries of moraine-dammed lakes and their outbursts are provided by Cenderelli (2000), Clague and Evans (2000), Richardson and Reynolds (2000), Kattelmann (2003), Carrivick and Tweed (2013, 2016), Allen et al. (2016a), Wang and Jiao (2015), Emmer (2017), Harrison et al. (2018), Erokhin et al. (2018), Neupane et al. (2019), Liu et al. (2019), Emmer et al. (2020), and Clague and O'Connor (2020). The assessment of Harrison et al. (2018) provides a comprehensive global inventory of historical outburst floods from moraine-dammed lakes.

Large moraine-dammed lakes formed in the late Pleistocene where large valley glaciers built terminal moraines at the mouths of confined valleys. Documented floods from these moraine impoundments include the late Pleistocene breaching of the moraine rimming Lake Zurich, Switzerland (Strasser et al., 2008) and the historical emptying of Keppel Cove Tarn in the United Kingdom, which was probably human-caused (Carling and Glaister, 1987). Blair (2001) and Benn et al. (2006) report outburst-flood deposits that may have resulted from a breached late Pleistocene moraine in the Sierra Nevada of California. In contrast to the few documented incidents of breached Pleistocene moraines, scores of large floods and debris flows resulted from rapid breaching of late Holocene moraines. Harrison et al. (2018) document 165 moraine-dam outburst floods worldwide since the beginning of the 19th century. These floods cause substantial death and destruction (Carrivick and Tweed, 2016), including more than 5000 fatalities from the 1941 Huaraz outburst flood in Peru (Carey, 2005) and, more recently, more than 6000 deaths from the 2013 outburst that devastated the Indian Himalayan village of Kedernath (Allen et al., 2016b).

Moraine dams form in the wake of retreating glaciers. They have become a subject of particular and increasing interest because of 20th century warming (Lliboutry et al., 1977; Liu and Sharma, 1988; O'Connor and Costa, 1993; Clague and Evans, 1994;

O'Connor et al., 2001; Kattelmann, 2003; Wang et al., 2014; Veh et al., 2020; Emmer et al., 2020). The rapidly expanding literature and its geographic distribution are documented by the bibliometric analysis of Emmer (2018). Most moraine dams that have breached in recent decades formed in the 17th, 18th, and 19th centuries, the time of most extensive glaciation of the late Holocene Neoglacial period (Porter and Denton, 1967). During this period, valley and cirque glaciers built moraines up to 100 m high. By the late-1800s and through most of the 20th century, glaciers substantially retreated from their advanced Little Ice Age positions, allowing lakes with volumes up to $1{\cdot}10^8$ m^3 and depths of nearly 100 m to form in the vacated basin between moraines and the retreating ice (Fig. 6). Tens to thousands of Little Ice Age moraine-dammed lakes have been mapped in glaciated regions such as the Himalaya (Liu and Sharma, 1988; Yamada and Sharma, 1993; Richardson and Reynolds, 2000; Fujita et al., 2013; Worni et al., 2013; Wang and Jiao, 2015; Wang et al., 2015; Gurung et al., 2017; Nie et al., 2017; Veh et al., 2019, 2020), central Asia (Janský et al., 2010), South America (Lliboutry et al., 1977; Reynolds, 1992; Carey, 2005; Anacona et al., 2015a,b; Emmer et al., 2016a,b, 2020), the European Alps (Haeberli, 1983; Emmer et al., 2015), southern British Columbia, Canada (Clague and Evans, 1994; McKillop and Clague, 2007a,b), and the Cascade Range of Oregon and Washington, USA (O'Connor et al., 2001). More proglacial lakes are likely to form as glaciers continue to retreat, as predicted by most climate models (e.g., Emmer et al., 2020; Magnin et al., 2020).

Many Little Ice Age moraines enclosing lakes are susceptible to breaching because of their geotechnical characteristics and the trigger mechanisms provided by adjacent steep terrain. Young moraines commonly are perched on steep mountain slopes, are sparsely vegetated, and consist of loose and poorly sorted glacial sediment deposited at slopes as steep as 40 degree—all characteristics facilitating rapid erosion once overtopped. Breaching can be triggered by periods of rapid snowmelt or intense rainfall that either lead to overflow of the moraine rim or initiate outlet erosion (e.g., Allen et al., 2016a). The most common failure mechanism, however, is ice- or rock-fall into the lake from the glacier or surrounding rock slopes, which generates waves that overtop the moraine and initiate breaching (Costa and Schuster, 1988; Clague and Evans, 2000, Kershaw et al., 2005; Westoby et al., 2014; Nie et al., 2017; Harrison et al., 2018). Breaching in some cases may be facilitated by a slow lowering of the moraine crest due to melting ice cores (Reynolds, 1992) or interstitial ice. Maximum historical breakout volumes have approached 7×10^7 m^3 with breach depths of up to 50 m (O'Connor and Beebee, 2009; Veh et al., 2020).

Some moraine rims breach soon after the lake first forms (O'Connor et al., 2001), but most fail years or decades later depending on the time required to fill the lake basin or the incidence of breach-triggering processes such as rock-fall or ice avalanches. In general, the likelihood of breaching increases as lakes get larger and then decreases gradually as moraine dams age and presumably consolidate (Clague and Evans, 2000). For example, in the Oregon Cascade Range, 13 moraine-dammed lakes formed between 1924 and 1956, by which time they had reached their maximum size. Eight of these lakes produced floods and debris flows from four complete and seven partial dam breaches between 1934 and 1987, with one small partial breach subsequently in 2012 (O'Connor et al., 2001; Sherrod and Wills, 2014). Globally, the frequency of outburst floods is similar—a substantial increase in outburst flood frequency between 1930 and 1970 followed by a decline (Carrivick and Tweed, 2016; Harrison et al., 2018). An exception may be the Himalayan region where incidence of moraine breaches in the Himalaya has not slowed (Harrison et al., 2018), in part signaled by large and lethal outbursts in 2013 and 2016 (Allen et al., 2016b; Cook et al., 2018; Veh et al., 2019), and where lakes continue to grow in the wake of retreating glaciers (Liu and Sharma, 1988; Mool, 1995; Richardson and Reynolds, 2000; Kattelmann, 2003; Fujita et al., 2013; Wang and Jiao, 2015; Nie et al., 2017).

Not all moraine dams breach cataclysmically. The large number of existing lakes impounded by Pleistocene moraines attests to long-term stability of some moraine dams. Likewise, many Neoglacial moraine dams have persisted without breaching. In an inventory of moraine-dammed lakes in southern British Columbia, Canada, McKillop and Clague (2007a) found only 10 of 175 moraine-rimmed lakes had drained partly or completely. For some lakes, stability is promoted by outlet channels formed in rock or armored by coarse material. Others are stable because low-gradient outlet channels drain the lakes (Clague and Evans, 2000). Logistic analysis of the stable and breached moraine dams in British Columbia showed that four factors were correlated with increased likelihood for breaching: large moraine height-to-width ratio, presence of ice-free moraines, large lake area, and moraines composed of sedimentary rock types (McKillop and Clague, 2007a). Moraine dams formed on stratovolcanoes may be particularly susceptible to breaching because they are generally tall and are located on steep slopes—on the central Oregon Cascade Range volcanoes, 8 out of 13 Neoglacial-age moraine dams have partly or completely breached (O'Connor et al., 2001), a failure rate far surpassing the 6% that have failed in the mostly crystalline and sedimentary rocks of the British Columbia Coast Mountains (McKillop and Clague, 2007a).

2.2.3 Tectonic basins

Large tectonic basins that fill with water and cataclysmically drain have been the source of many great floods, primarily because of the immense volumes of water involved (Table 1; O'Connor and Costa, 2004). For example, Pleistocene Lake Bonneville at its maximum contained 1×10^{13} m^3 of water and was 330 m deep. Floods from basin spills generally overwhelm pre-existing drainages, leaving pronounced flood features. Such floods commonly lower local base levels and alter hydrological pathways, initiating landscape and ecological adjustments. Consequences may include drainage integration, regional incision (House et al., 2009; Hilgendorf et al., 2020) and changed migration pathways for aquatic organisms (Reheis et al., 2002). Tectonic basins may also have been the source of large outburst floods on Mars (Irwin and Grant, 2009; Burr, 2010).

A common flood-causing scenario for tectonic basins is the filling and overtopping of hydrologically closed basins, either because of climate change or because geological events increase the contributing drainage area or cause a sudden influx of water. Upon overtopping the basin divide, flow rapidly erodes an outlet channel, partly or completely emptying the lake. Such was the case

for the Bonneville Flood in western North America (Fig. 7; Gilbert, 1890; Malde, 1968; O'Connor, 1993, 2016). Pleistocene Lake Bonneville filled the closed basin of Great Salt Lake, overtopped and eroded the alluvium and poorly consolidated rock forming the drainage divide at Red Rock Pass, Idaho, and then spilled northward into the Snake River basin. Gilbert (1890, p. 175) described evidence pointing to a "veritable debacle" as about 5×10^{12} m^3 of water flowed out of the basin with a peak discharge of 1×10^6 m^3 s^{-1} while incising the basin divide ~108 m. Late Pleistocene outburst floods from Issyk Kul, Krygyzstan, may have involved a similar overflow scenario (Rosenwinkel et al., 2017).

Similar floods elsewhere in western North America are indicated by incision of surface overflow channels at basin rims (Currey, 1990; Reheis et al., 2002) or by downstream deposits of fluvially transported boulders (Anderson, 1998; Reheis et al., 2002). Two such floods from overflowing basins have been documented in Oregon: (1) overflow of Pleistocene Lake Alvord into Crooked Creek of the Snake River drainage (Hemphill-Haley et al., 1999; Carter et al., 2006); and (2) overflow of a Pleistocene lake in the Millican basin into the Crooked River, central Oregon (Vanaman et al., 2006).

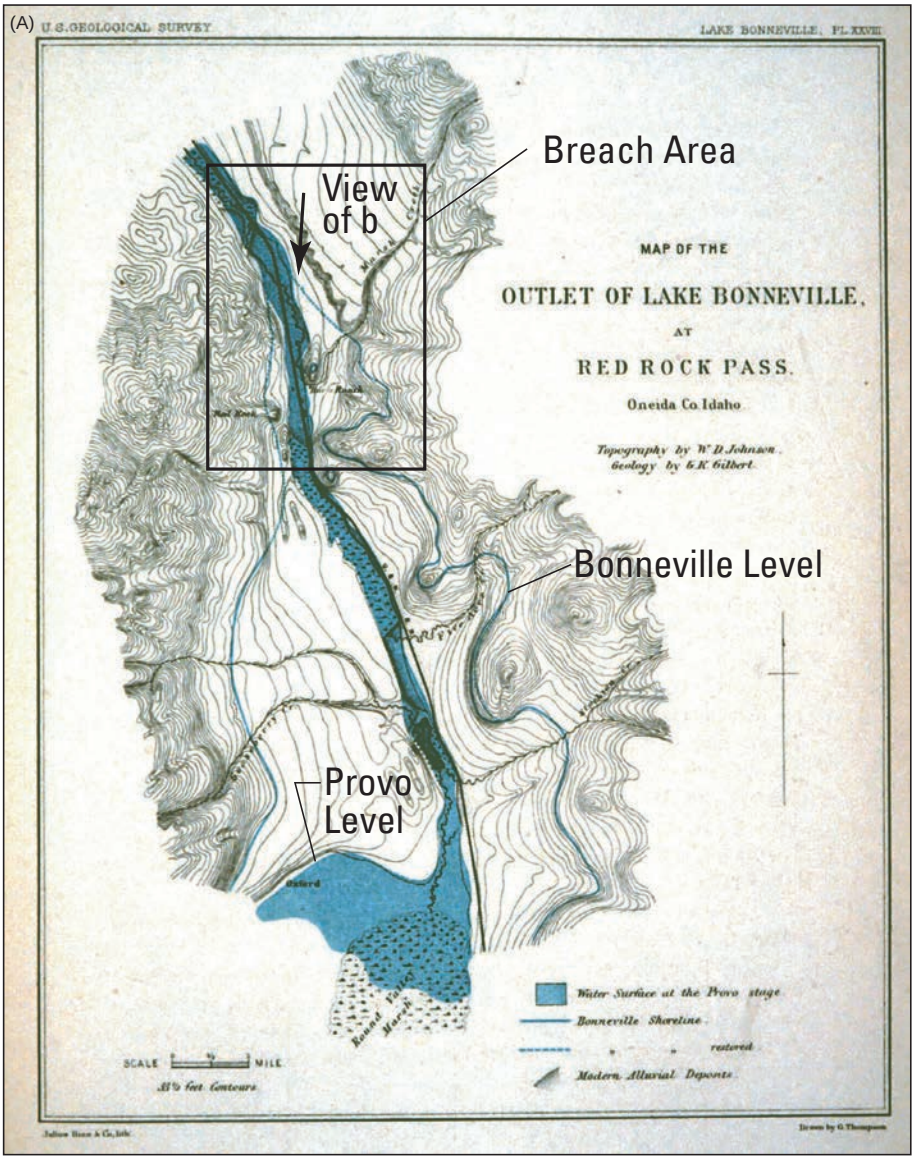

Fig. 7 Figures adapted from Gilbert (1890) showing conditions at the outlet of pluvial Lake Bonneville near Red Rock Pass, Utah. (A) Map showing maximum elevation (1552 m asl) of pluvial Lake Bonneville and subsequent Provo shoreline (1444 m asl) after breaching and release of 4.75×10^{12} m^3 of water about 17,000 years ago. The alluvial fan of Marsh Creek formed the divide between the closed basin of Great Salt Lake and the Snake River watershed. Overtopping resulted in rapid incision of 108 m to underlying bedrock at Red Rock Pass, where downcutting ceased. The resulting outburst flood had a peak discharge of 1.0×10^6 m^3 s^{-1} (O'Connor, 1993). (B) Sketch of view south (upstream) toward Red Rock Pass from the surface of March Creek fan, showing breach channel formed during incision of the fan.

Continued

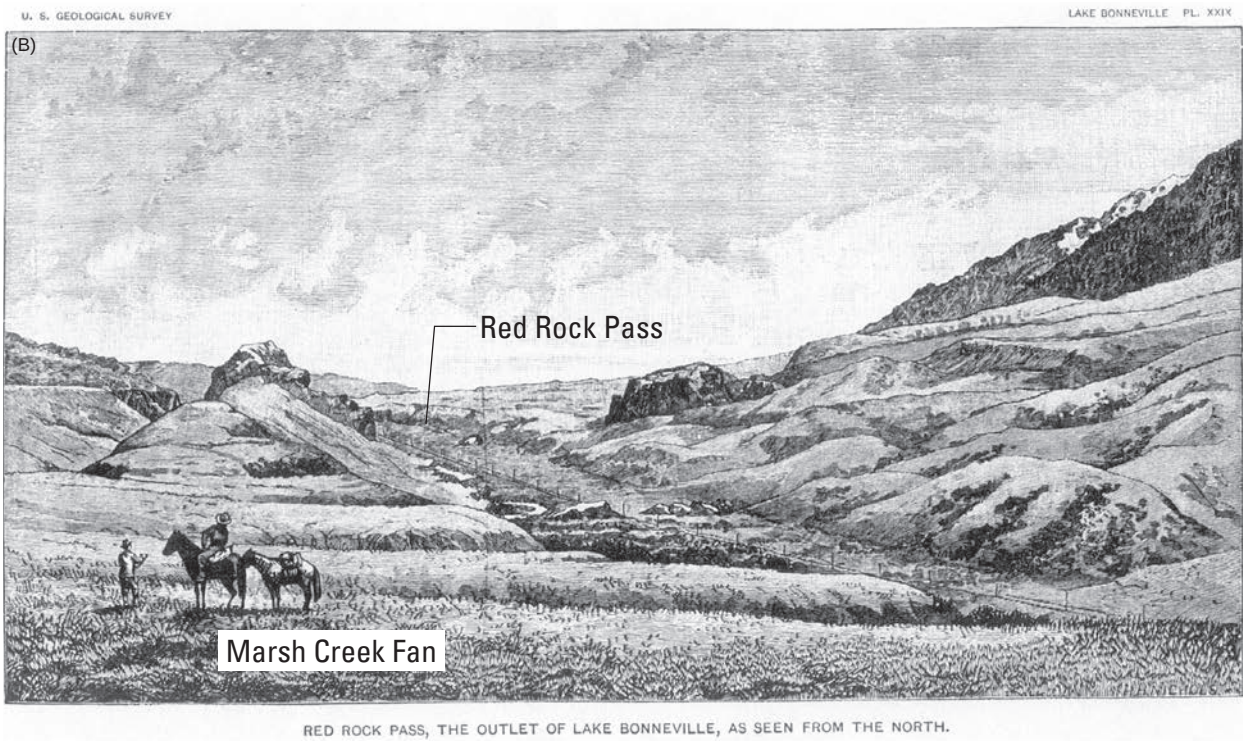

Fig. 7, Cont'd

The Lake Bonneville flood, other U.S. Great Basin spillovers, and the Oregon floods are examples of closed basins filling during wetter periods. Accounts also show that rapid emptying of some closed basins resulted from sudden water inputs caused by upstream drainage basin changes. For example, floodwater from breaches of ice-dammed and proglacial lakes may have entered the Pleistocene predecessor of the Caspian Sea, filling the basin and incising its outlet in the Manych Strait, releasing >25,000 km^3 into the Black Sea basin (Yanchilina et al., 2019). Similarly, House et al. (2009) concluded that the lower Colorado River became connected with the upper Colorado drainage at about 5 Ma owing to chain-reaction breaching of upstream basin divides. Boulder deposits downstream of breached divides indicate that some of these Colorado basin breaches caused large floods. Similar sequences about 2 Ma may have led to integration of the Snake River watershed into the Columbia River basin and incision of Hells Canyon and the western Snake River Plain of Idaho (Othberg, 1994; Wood and Clemens, 2002), as well as the integration of the upper Yellow River in Tibet (Craddock et al., 2010). Such spillovers, whether by flood or gradual outlet incision, are an important mechanism of drainage integration and modulate overall fluvial response to regional uplift (Meek, 2019; Hilgendorf et al., 2020).

Even larger marine floods into closed tectonic basins have likely resulted from eustatic sea-level rise or tectonic activity at basin margins. Hsü (1983) suggested that a desiccated Mediterranean basin was filled rapidly about 5.3 Ma by breaching at the present-day Strait of Gibraltar, a flood estimated by Garcia-Castellanos et al. (2009, 2020) and Abril-Hernández and Periáñez (2016) as having a peak discharge of 10^8 m^3 s^{-1} and a volume of 3.7×10^{15} m^3, nearly 1000 times larger than the Lake Bonneville flood. Garcia-Castellanos et al. (2020)relate the flood to long-held legends of southern Iberia, including that of Hercules cutting the breach with his sword, enabling the ocean to flow into the Mediterranean basin. This event, termed the Zanclean flood, lowered global sea level by about 10 m and is correlated with a mass extinction event that marks the Miocene-Pliocene boundary. Similarly, Quaternary breaching of a resistant chalk ridge formerly spanning the Dover Strait led to outburst flooding from a proglacial lake that occupied the southern part of the present-day North Sea (Gupta et al., 2007, 2017). Erosion of this channel separated Britain from the continent. Ryan et al. (1997, 2003) proposed that the rising Mediterranean Sea overtopped and eroded a divide at the Bosporus Strait, Turkey, about 9300 years ago, rapidly filling the Black Sea—from the direction opposite that of the last glacial flooding from the Caspian Sea (Ryan et al., 2003; Ryan, 2007; Yanchilina et al., 2017). This flooding perhaps engendered the story of the Biblical Flood (Ryan and Pitman, 1999), although the exact scenario remains controversial (Baker, 2009; Brückner and Engel, 2020).

Large floods involving tectonic basins typically occur in semi-arid environments during times of changing hydrological conditions. Very large terrestrial freshwater floods result from sustained wet periods that allow closed basins to fill. During the Quaternary, filling episodes were mostly during pluvial periods during times of glaciation (Baker, 1983; Reheis et al., 2002). Likewise, marine waters are most likely to flood continental basins during times of rising sea level driven by climate warming, sudden inputs from large terrestrial lakes, and melting of ice sheets and glaciers. Large closed basins are common in tectonically

active regions and especially within the arid and semi-arid subtropical belts, such as Africa, Australia, and the Basin-and-Range Province of western North America. In these areas, millenia-long dry periods allow closed basins to form without continuous overflow and drainage integration, creating the possibility for large water volumes to flow over steep basin margins during singular episodes of basin filling. About 20% of the global continental land surface is internally drained under present climate (Lee, 2018), indicating the broad potential for such processes. Marine floods into closed basins are also more likely in environments of negative water balance, where deep and isolated they will remain dry or contain endorheic lakes substantially below sea level, thus providing the hydraulic head for cataclysmic marine inflow (O'Connor et al., 2002).

2.2.4 Volcanic basins

Large floods from basins formed by volcanic activity, in particular caldera and crater lakes, are increasingly recognized as a hazard in volcanic landscapes (Lockwood et al., 1988; Waythomas et al., 1996; Manville et al., 1999, 2007; Wolfe and Begét, 2002; Manville, 2010a, 2015; Singer et al., 2018; Yi et al., 2019). Calderas and volcanic craters are formed by a combination of explosive volcanism and volcano-tectonic collapse (Williams, 1941). More than 200 Late Pleistocene or younger calderas sit high in volcanic landscapes world-wide (Manville, 2010a).

Some calderas and crater lakes contain large volumes of water—for example, Lake Taupo, New Zealand, holds $\sim 6 \times 10^{10}$ m^3 (Manville et al., 1999); Lake Atitlán, Guatemala, holds $\sim 4 \times 10^{10}$ m^3 (Newhall et al., 1987); and Crater Lake, Oregon, is nearly 600 m deep and contains 1.7×10^{10} m^3 (Johnson et al., 1985). The largest caldera lake in the world is Lake Toba in Indonesia, which contains 2.4×10^{11} m^3 of water (Chesner and Rose, 1991). Although two orders of magnitude smaller than the largest tectonic basins, large caldera and crater lakes may be more likely to produce large outburst floods than basins of other origins because (1) they form rapidly and without water outlets, (2) they are commonly at high elevations with substantial local relief and therefore high potential energy, (3) they are commonly rimmed by heterogeneous and structurally weak lava flows and unconsolidated pyroclastic material, (4) they are susceptible to draining during renewed volcanic activity, and (5) they are located in volcanic arcs that, because of their elevated positions commonly near ocean moisture sources, may fill rapidly from precipitation. Breaching may be triggered by volcanism producing displacements or waves that overtop and breach outlets (Richer et al., 2004; Stelling et al., 2005), or by overtopping by rapid melting of snow and ice (Donnelly-Nolan and Nolan, 1986). Breaching might not be directly related to volcanism but instead triggered by overtopping of weak rims (e.g., Waythomas et al., 1996), piping (e.g., Massey et al., 2010), and headward erosion (Karátson et al., 1999). More than 20 such floods are listed in the compilation by Manville (2015).

The largest well-documented outburst flood from a caldera lake is the post-3.4 ka flood from Aniakchak Volcano, Alaska (Fig. 8; McGimsey et al., 1994; Waythomas et al., 1996). The caldera at Aniakchak formed from a large eruption about 3.4 ka and subsequently filled with about 3.7×10^9 m^3 of water to an average depth of $\sim$98 m. Shorelines near the elevation of the inferred low point in the rim indicate that the lake may have overflowed the basin rim for some time before rapidly breaching. Once breached, almost the entire lake emptied into the Aniakchak River valley at a peak discharge of about 1×10^6 m^3 s^{-1}, producing one of the largest known Holocene floods on Earth (Waythomas et al., 1996).

Several large floods from caldera and crater lakes have been documented in New Zealand, including the 13 March 2007 partial breach of the 1.3×10^7 m^3 crater lake at Mount Ruapehu (Table 1; Manville and Cronin, 2007; Graettinger et al., 2010; Procter et al., 2010; Manville, 2010b, 2015). A post-1.8 ka partial breach of Lake Taupo emptied 2.0×10^{10} m^3 of water with a peak discharge of 1.7–3.5×10^5 m^3 s^{-1} (Manville et al., 1999). The worst volcanic disaster in New Zealand resulted from a breach at Mount Ruapehu on 24 December 1953, when 1.8×10^6 m^3 of water emptied rapidly from the summit crater lake into the headwaters of the Whangaehu River. The flood incorporated volcaniclastic debris from the steep upper slopes of the volcano and transformed into a lahar with a peak discharge of $\sim 2 \times 10^3$ m^3 s^{-1} that destroyed a railroad bridge 39 km downstream, minutes before arrival of a passenger train, resulting in 151 deaths (Manville, 2004).

Other documented caldera-breach floods include the 15–12 ka breach of Towada Caldera in Japan, which released 6×10^9 m^3 into the Oirase River (Kataoka, 2011); the 1.5 ka cataclysmic emptying of a $\sim$100 m-deep lake in Fisher Caldera, Alaska, apparently triggered by an eruption-generated wave (Stelling et al., 2005); two breaches from Okmok Caldera, Umnak Island, Alaska since 1.6 ka, including one that emptied 5.8×10^9 m^3 of water from a 150 m-deep lake filling a caldera formed about 2 ka (Wolfe and Begét, 2002; Begét et al., 2005); the 9.4 ka breach of Laguna del Maule caldera in Chile, which released $\sim 1.5 \times 10^{10}$ m^3 of water when a lava flow emplaced across the outlet at 19.0 ± 0.7 ka failed catastrophically (Singer et al., 2018); breaching of the 5 km diameter caldera lake at the summit of Changbaishan (Tianchi/Baitoushan) on the North Korea/China border, which emplaced 0.8–1.8×10^{10} m^3 of water into the Erdaobaihe River following its formation during the 946 ± 20 CE Millennium eruption (Yi et al., 2019); and a July 2002 flood of 6.5×10^7 m^3 of water from the summit caldera formed by the 1991 eruption at Pinatubo, Philippines (Lagmay et al., 2007). In the Cascade Range of western North America, documented outburst floods from crater and calderas include a post-4.7 ka partial breach of Paulina Lake at Newberry Volcano, Oregon (Chitwood and Jensen, 2000), and a $\sim 3.3 \times 10^3$ m^3 s^{-1} late Pleistocene flood from a possibly ice-covered caldera lake on Medicine Lake volcano, California (Donnelly-Nolan and Nolan, 1986).

An additional dimension to hazards of outburst floods from volcanic basins is provided by Schaefer et al. (2008). They describe a May 2005 breach of a sulfurous crater lake at the summit of Chiginagak volcano, Alaska, resulting in a highly acidic lahar and flood that killed all aquatic life along its 27-km-long path. In addition to the lahar and flood, the breach was accompanied by a flow of acidic aerosols, causing substantial plant death and damage over a 29 km^2 area flanking the flood path at heights up to 150 m above the channel.

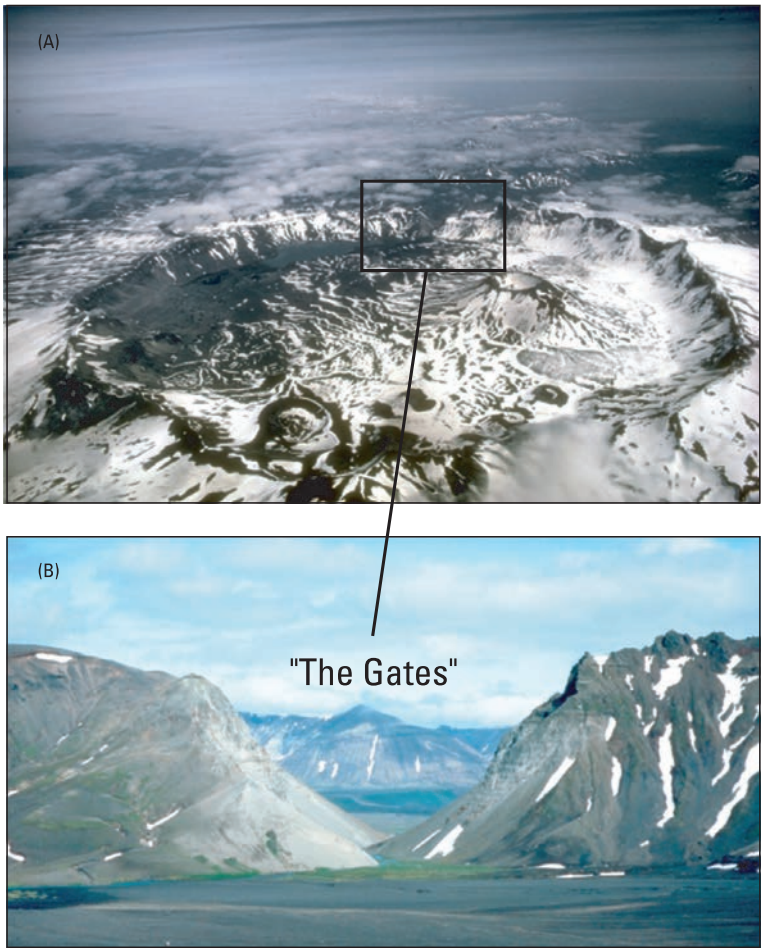

Fig. 8 Aniakchak caldera, Alaska, which breached sometime after 3400 years ago, producing one of the largest terrestrial floods of the Holocene (Waythomas et al., 1996). (A) Aerial view east of Aniakchak caldera. The caldera is about 10 km across and an average of 500 m deep. After formation, the caldera filled to a maximum depth of 183 m before breaching through a low point on the western caldera rim, incising "The Gates" and releasing 3.7×10^9 m^3 of water with a peak discharge of 1×10^6 m^3 s^{-1}. (B) View east of "The Gates," the ~200-m-deep breach formed in the rim of Aniakchak Caldera. (A) Photograph by M. Williams, National Park Service, 1977. (B) Photograph 3 July 1992 by C.A. Neal, U.S. Geological Survey.

Like outbursts from other types of breached basins, crater and caldera lake floods are restricted geographically—obviously in this case to volcanic provinces, mainly volcanic arcs flanking subduction zones and less commonly in rift valleys (Manville, 2010a, 2015). Larson (1989) identified 88 lakes in 75 calderas with diameters >2 km in 31 volcanic regions globally. The largest caldera and crater lakes, and those more likely to overflow, are associated with explosive silicic volcanism (Manville, 2010a). These lakes are bounded by relatively impermeable pyroclastic material. In contrast, lakes on more mafic basaltic and andesitic volcanoes formed primarily of lava flows (such as Crater Lake, Oregon) are more likely to drain by subterranean outflow through permeable lava flows. The filling and breaching of caldera and crater lakes also may be restricted to humid environments or times of local positive moisture balance because most such lakes have small drainage areas relative to their size.

2.2.5 Meteorite craters

Outburst floods from breached impact craters channeled the surface of Mars during wetter periods (Irwin and Grant, 2009; Burr, 2010; Coleman, 2013, 2015; Goudge et al., 2016, 2018; Goudge and Fassett, 2018), and perhaps also on early Earth. Some of these Martian floods involved outburst volumes exceeding 10^{14} m^3 (about five times the combined volume of the Great Lakes) and breach depths of nearly a kilometer (Coleman, 2015; Goudge et al., 2018). Examples include Morella Crater (Coleman, 2013), shown in Fig. 9, and Galilaei Crater, a 960-m-deep, 137-km-diameter impact crater that filled with 1.1×10^{13} m^3 of water (similar to Lake Superior) before breaching with a peak discharge possibly as large as 8.4×10^7 m^3 s^{-1} (Coleman, 2015), a flood volume and discharge about five times the largest Missoula flood (Table 1).

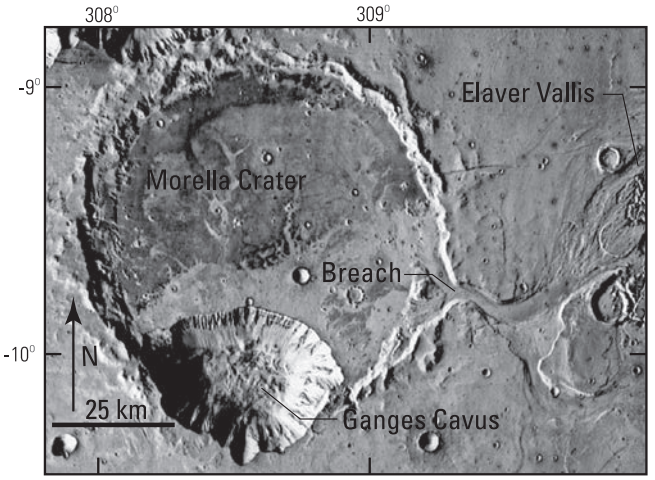

Fig. 9 Morella Crater and the head of the Elaver Vallis channel system in the circum-Chryse region of Mars, showing an outflow channel emanating from breached Morella Crater. Coleman (2013) inferred that groundwater discharged from Ganges Cavus, filling the crater until it overtopped. From breach geometry and crater topography, they estimated 2×10^{12} m^3 of water escaped at a peak discharge as great as 2×10^7 m^3 s^{-1} while the lake level dropped 530 m. Daytime infrared mosaic from THEMIS Public Data Releases, Planetary Data System node, Arizona State University (http://themis.mars.asu.edu/feature/16).

2.3 Floods from release of subglacial and subterranean storage

Water release from beneath and within glaciers has caused floods, including relatively small releases from alpine glaciers that nonetheless create hazards in developed mountainous areas (Haeberli, 1983; Walder and Driedger, 1994), and much larger Holocene flows—up to 7×10^5 m^3 s^{-1}—from volcanic eruptions under ice sheets in Iceland (Waitt, 2002; Alho et al., 2005; Carrivick, 2006, 2007, 2009; Björnsson, 2009; Carrivick and Tweed, 2019). The 1918 Katla jökulhlaup in Iceland had a peak discharge of about 3×10^5 m^3 s^{-1} (Tómasson, 1996). Some of these Icelandic floods involved water evacuated from subglacial calderas. Tremendous Pleistocene floods may have resulted from rapid emptying of water stored within or under continental ice sheets (Shaw, 1983; Munro-Stasiuk et al., 2009). On Mars, even larger floods were possibly generated by catastrophic releases of pressurized groundwater (Carr, 1979; Manga, 2004; Burr et al., 2009; Coleman and Baker, 2009; Burr, 2010).

2.3.1 Subglacial and englacial impoundments

Outburst floods from subglacial and englacial water bodies have long been noted as a source of damaging floods and debris flows in areas of alpine glaciers (Richardson, 1968; Haeberli, 1983; Driedger and Fountain, 1989; Walder and Driedger, 1994; Roberts, 2005; Björnsson, 2009). Haeberli (1983) documented more than 26 outburst floods from glacial "water pockets" in the Swiss Alps, involving water volumes as great as 2.7×10^6 m^3. Similarly, water stored in subglacial or englacial cavities in glaciers on Mount Rainier, Washington, have been the source of dozens of 20th century outburst floods, including some with peak discharges as great as 1×10^4 m^3 s^{-1} and volumes of up to 3×10^5 m^3 (Driedger and Fountain, 1989; Walder and Driedger, 1994). A recent example was the June 2016 outburst from Lhotse Glacier in the Everest region of Nepal, where a peak discharge of about 210 m^3 s^{-1} emerged from breached englacial conduits (Rounce et al., 2017).

Some of the floods in the Alps and on Mount Rainier were associated with rainstorms, but many happened during dry warm periods (Haeberli, 1983; Walder and Driedger, 1994). Driedger and Fountain (1989) reviewed the physical conditions associated with the outburst floods on Mount Rainier and concluded that rapid outbursts likely result from sudden emptying of a single or a few large pressurized water-filled cavities into low-pressure, subglacial drainage pathways. These breaches possibly resulted from cavity enlargement, glacier movement, or by addition of water from the surface during periods of rain or melting. Once sub- or englacial cavities connect, pressure differences drive flow that thermally and mechanically enlarges pathways in a manner similar to tunneling flow under and through ice dams (Nye, 1976; Clarke, 1982). Formation of pressurized subglacial and englacial water-filled cavities is an outcome of glacier flow over steep and stepped beds (Driedger and Fountain, 1989), consistent with the observation of Haeberli (1983) that many of the Swiss outburst floods came from relatively steep glaciers.

Some of the most spectacular floods from glacial water sources have been the Icelandic jökulhlaups (literally "glacier-burst"). Immense floods—on the order of two floods per century with discharges exceeding 10^5 m^3 s^{-1}—have resulted from subglacial water melted by geothermal heat and volcanism (Tómasson, 2002; Björnsson, 1974, 2009, 2010; Carrivick et al., 2004; Roberts, 2005; Russell et al., 2010; Björnsson, 2010; Baynes et al., 2015a,b). These floods have emanated from the subglacial cauldrons, crater lakes and calderas of the ice-capped Icelandic rift valleys. The largest historical outburst flood resulted from the eruption of Katla volcano underneath Mýrdalsjökull (*jökull* is Icelandic for "glacier") and had a peak discharge of 3×10^5 m^3 s^{-1} (Tómasson, 1996). The largest Icelandic jökulhlaups of the Holocene have been along Jökulsá á Fjöllum in northeastern Iceland. The exact eruptive and outburst sequence of many of these floods is uncertain (Carrivick et al., 2004; Carrivick and Tweed, 2019) but they all likely

involved subglacial volcanism associated with one or more volcanic centers under Vatnajökull. One such flood had a discharge of 9×10^5 m^3 s^{-1} (Alho et al., 2005). Similarly, volcano and ice interactions may have been a mechanism for producing large floods on Mars (Chapman et al., 2003).

A large flood in 1996, triggered by eruptions from the Grímsvötn caldera lake beneath Vatnajökull, travelled down Jökulsá á Fjöllum with a peak discharge 5×10^4 m^3 s^{-1} (Björnsson, 2009). This flood is one of several 20th century floods emanating from six subglacial lakes beneath Vatnajökull. Many of these floods, however, were not triggered by eruptions, but rather by geothermal melting of ice at the glacier bed, pressurizing subglacial water accumulations until lifting of the capping ice enabled rapid water escape (Björnsson, 2009).

Large water bodies, some perhaps associated with floods, underlie ice sheets in Antarctica (Wingham et al., 2006; Fricker et al., 2007). A sequence of immense subglacially derived floods eroded scabland terrain, channels, potholes, and left giant current dunes in the Dry Valleys, Antarctica, during the Miocene (Marchant et al., 2011).

More controversial (Baker, 2009; Baker, 2020; Munro-Stasiuk et al., 2009) is the hypothesis of great outburst floods from under the large ice sheets of the late Pleistocene. Shaw (1983, 2002) proposed that many subglacial landforms, such as drumlins, are the product of immense subglacial sheet floods from under the Laurentide Ice Sheet, some with discharges exceeding 10^6 m^3 s^{-1}. Grosswald (1999, cited in Baker, 2009) extended this idea to relate the topography of much of central Russia to immense water flows under an ice cap covering the Arctic Ocean. Similar floods, with sources beneath the Cordilleran Ice Sheet in the Okanagan Valley of British Columbia, have been proposed by Lesemann and Brennand (2009). This idea is broadly consistent with the Shaw et al. (1999) proposal that at least some of the water that eroded the Channeled Scabland of eastern Washington—generally attributed to outburst flooding from ice-dammed Glacial Lake Missoula—actually came from a hypothesized 10^{14} m^3 accumulation of water under the Cordilleran Ice Sheet in British Columbia. This scenario has been discounted specifically for the Channeled Scabland by Atwater et al. (2000) and on more general physical principles by Walder (1994) and Clarke et al. (2005).

2.3.2 Groundwater

Although groundwater commonly contributes to flooding, it is not typically considered a source for terrestrial outburst floods. Aside from the Biblical "fountains of the great deep" (Genesis 7:11, King James Version, Cambridge Edition) as a source of Noah's Flood, few riverine floods have been documented from rapidly expelled groundwater on Earth. The most notable examples involve releases of groundwater from volcanic edifices during gravitational collapse to form debris avalanches, or from faulting during tectonic or volcanic activity. Delcamp et al. (2016) demonstrated that volcanic edifices can efficiently store large volumes of groundwater in perched aquifers formed by layers of different porosity and permeability and intrusion networks. Rapid release of this stored water, which can reach up to 30% volume of the rock mass, can occur either through dewatering of the debris avalanche as was observed at Mount St. Helens (Janda et al., 1981), or by seepage from the avalanche scar (Delcamp et al., 2016), evident at Mount Meager following the 2010 collapse (Guthrie et al., 2012) and inferred at Mt. Meru, Tanzania. At Nevado del Huila, Colombia, two small phreatic eruptions in February 2007 were accompanied by large lahars in the Páez and Simbola Rivers (Johnson et al., 2018). Large fissures in the summit region, up to 2-km long and 50–80-m wide, appear to be the source of much of the water in the lahars seemingly too voluminous to have been derived from melting of snow and ice, and were likely sourced from hydrothermal reservoirs within the volcano (Pulgarín et al., 2007). Model calculations indicate groundwater expulsion of possibly $\sim 10^3$ m^3·per meter of crack within tens of minutes, possibly but not necessarily aided by volcanic pressurization. Peak discharge 24 km from source was estimated at 1.35×10^4 m^3 s^{-1} for the larger flow with a total volume of 5×10^7 m^3 (Worni et al., 2012b). Another possible groundwater-sourced flood is hypothesized by Amidon and Clark (2015), invoking floods emerging from the Snake River Plain aquifer in Idaho, United States, to have eroded amphitheater-headed canyons carved into the basalt plain.

In contrast to the rarity of groundwater outburst floods on Earth, releases of water from pressurized aquifers is a strongly supported mechanism for generating the tremendous water flows on Mars (Fig. 10; Baker and Milton, 1974; Carr, 1979; Burr et al., 2002a,b, 2009; Wilson et al., 2009; Salese et al., 2019), although several alternative mechanisms—some involving surface water—have also been advanced (Roda et al., 2014; Cassanelli and Head, 2018). The largest Martian flood channels were formed during the Hesperian epoch (3.7–3.0 Ga) by floods with volumes of 10^{15} m^3 (e.g., Roda et al., 2014) and discharges exceeding 10^9 m^3 s^{-1}—two orders of magnitude larger than the largest freshwater floods on Earth (Burr, 2010). These flows probably resulted from release of vast accumulations of groundwater confined by the overlying cryosphere, leaving so-called chaotic terrain at the head of outflow channels that run for thousands of kilometers and are locally more than one kilometer deep (Baker, 2001). Rupture and release of this groundwater was likely triggered by magmatic intrusions, but tectonic fracturing and landslides may also have triggered these and later Martian floods (Burr et al., 2009; Coleman and Baker, 2009; Montgomery et al., 2009).

2.4 Floods from unusual sources

Costa (1988) summarized some unusual outburst floods, including *bog bursts* in the United Kingdom and Republic of Ireland resulting from rapid escape of water accumulations trapped between impermeable glacial till and thick overlying thick peat layers (Colhoun et al., 1965). This phenomenon also has been described in the Falklands (Dyer, 1886). Notable outburst floods of even more bizarre flavors include "Boston's Great Molasses Flood" of 15 January 1919, in which 900 m^3 of molasses escaped a storage tank, inundated nearby streets and killed 21 people (Hartley, 1981); a 15-m-high torrent of beer from a catastrophically ruptured fermentation tank flood in London in 1814, causing 8 fatalities (https://www.thehistorypress.co.uk/articles/the-london-beer-flood,

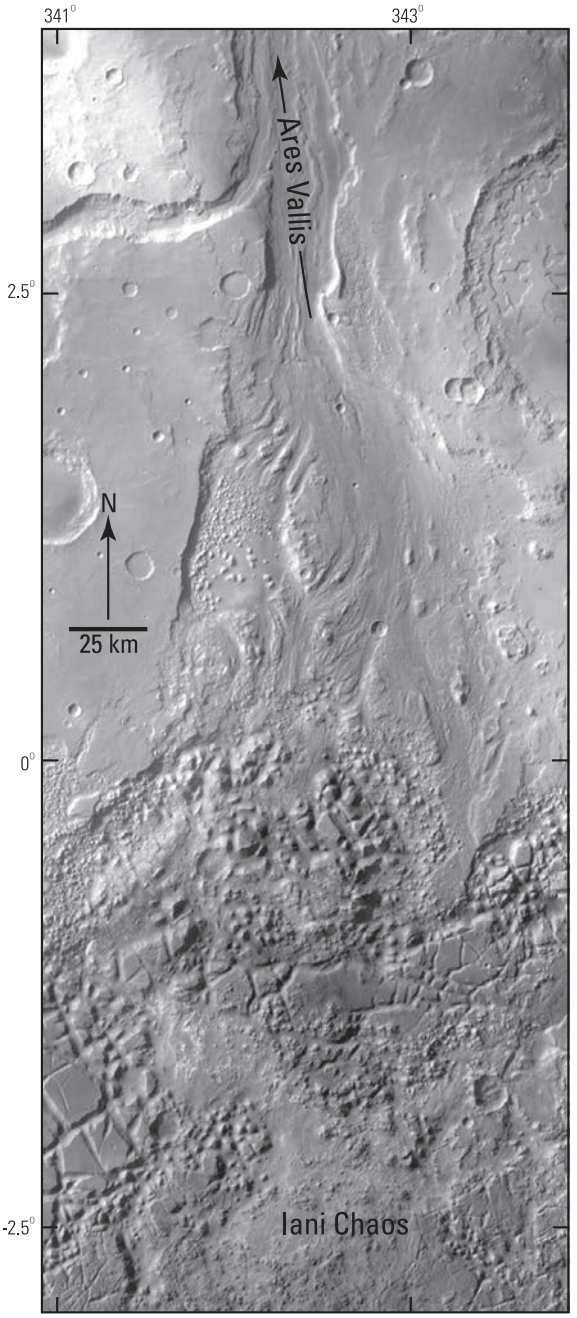

Fig. 10 Iani Chaos and Ares Vallis in the circum-Chryse region of Mars. The Ares Valles may have carried 1–6 $\times$ 10^8 m^3 s^{-1} of water derived from a variety of sources, including the Iani Chaos terrain at the bottom of the image, which is inferred to have resulted from ground-water discharge and consequent disruption of the surface (Coleman and Baker, 2009). Modified from image produced by European Space Agency (ESA/DLR/FU Berlin [G. Neukum]; http://www.esa.int/esaCP/index.html, accessed 24 May 2011).

accessed 15 April 2020); and more recently, a 28,000 m^3 outburst of Pepsi fruit drink in 2017 from collapsed storage containers warehoused in Lebedyan, Russia (https://www.britannica.com/list/7-strange-disasters, accessed 15 April 2020).

3 Outburst flood magnitude and behavior

Outburst floods profoundly affect landscapes and socioeconomic systems, motivating focused research into their triggers and downstream behavior. Early outburst-flood studies emphasized mapping and qualitative descriptions (e.g., Hewitt, 1968, 1982;

Lliboutry et al., 1977). Later and more quantitative hazard assessments adopted empirical analysis and modeling techniques for assessing magnitude and inundation, such as Clague and Mathews (1973), Costa (1988), Costa and Schuster (1988), and Fread (1988, 1991, 1993). In recent years, this work has involved sophisticated multi-dimensional and multi-component modeling and statistical approaches (e.g., Denlinger and O'Connell, 2010; Westoby et al., 2014; Worni et al., 2014; Garcia-Castellanos et al., 2020; Sattar et al., 2020; Veh et al., 2020). For constructed dams, extensive research has evaluated dam-failure processes and downstream flooding because of the common risks to downstream population centers (recently, for example: Capart, 2013; Brunner, 2014; Froehlich, 2016; Eghbali et al., 2017; Morris et al., 2018; Wang et al., 2018; Zhong et al., 2020). Additionally, geologists have long recognized the persistent landscape effects of outburst floods (e.g., Lyell, 1830, p. 192; Bretz, 1923a,b), currently reflected in a rapidly expanding literature addressing the "geomorphic work" and erosional and depositional processes of outburst floods on Earth as well as other planets (e.g., O'Connor, 1993; Benito, 1997; Montgomery et al., 2004; Lamb and Fonstad, 2010; Baynes et al., 2015a,b; Lapotre et al., 2016; Emmer, 2017; Cook et al., 2018; Goudge et al., 2018; Keisling et al., 2020).

The important factors controlling outburst flood likelihood and magnitude for all types of barriers are (1) the stability the blockage or divide in relation to plausible triggering processes, (2) the speed and depth of breach or outlet growth, and therefore the volume, rate, and duration of escaping water and entrained sediment, and (3) downstream water and sediment interactions that may change the volume, peak discharge, and type of flow. Each component of this "process cascade" has many complicated aspects and uncertainties, challenging geoscientists and engineers faced with predicting the likelihood, magnitude, and downstream evolution of dam-break floods (Westoby et al., 2014: Worni et al., 2014). These same factors complicate interpretation of past events from geological evidence, even for historic floods (e.g., Manville, 2004). Analysis is also hindered by the few detailed observations of dam failures. Consequently, approaches to assessing hazards and landscape effects are quite variable, ranging from maps and descriptions (e.g., Malde, 1968), to empirical assessments of historical data (e.g., Wang et al., 2018; Veh et al., 2020), to forward computational process modeling (e.g., Westoby et al., 2014; Worni et al., 2014; Kropáĉek et al., 2015; Somos-Valenzuela et al., 2016; Lala et al., 2018; Begam et al., 2018; Abril-Hernández et al., 2018). Summaries and examples of approaches to assessing the likelihood and magnitude of outburst floods from constructed and natural dam failures are provided by Clague and Evans (1994, 2000), Froehlich (1995, 2008, 2016), Walder and Costa (1996), Walder and O'Connor (1997), Cenderelli (2000), Korup (2002), Huggel et al. (2002, 2003a,b, 2004), Ermini and Casagli (2003), Manga (2004), Wahl (2004), Roberts (2005), Korup and Tweed (2007), Manville et al. (2007), McKillop and Clague (2007a,b), Tweed and Russell (1999), Manville (2010a, 2015), Wang et al. (2012), Westoby et al. (2014), Worni et al. (2014), Herget (2015), Walder et al. (2015), Rounce et al. (2016), Somos-Valenzuela et al. (2016), Wang et al. (2018), Shen et al. (2020), Veh et al. (2020), and Zhong et al. (2020).

3.1 Triggers and breach processes

Rates and processes of breaching control outburst flood magnitude and behavior. Natural and constructed dams may fail by intrinsic instability, exogenous triggers, or by some combination of factors. As a basin or valley impoundment fills, several processes that facilitate breaching begin to operate. Impounded water may (1) overtop and erode an outlet, (2) impart lateral forces that exceed the strength of the dam strength or buoyantly lift it, or (3) produce piezometric gradients through the barrier sufficient to promote piping, retrograde erosion of sapping channels, or mass failure. At high lake levels, rapid water rise or waves triggered by large inflows, wind, and mass movements may overtop dams and blockages, thereby initiating overflow and incision. In the case of ice dams, water levels approaching the top of the dam induce lateral stresses and possibly buoyancy, leading to tunneling, fracturing, or catastrophic collapse. For constructed dams, the main causes of uncontrolled releases are (1) overtopping, typically resulting from flows exceeding spillway capacity, (2) foundation failure, and (3) piping and seepage through the structure (Costa, 1988). Failure at first filling—by subglacial drainage, piping, outlet erosion, or some combination of these processes—is particularly common for landslide and ice dams (Costa and Schuster, 1988; Tweed and Russell, 1999; Carrivick and Tweed, 2016; Shen et al., 2020). Of landslide dams that have produced outburst floods, about 80% did so within a year of formation (Fan et al., 2020). Even some constructed dams fail at first filling; both the St. Francis and Teton dams failed during or soon after completion (Table 1).

Exogenic mechanisms also trigger breaches, especially in the case of moraine impoundments for which most breaches have been triggered by overtopping waves from ice or rock avalanches into the impounded lake (O'Connor and Beebee, 2009; Westoby et al., 2014; Herget, 2015; Emmer, 2017; Liu et al., 2019). Volcanism is a common trigger of Icelandic jökulhlaups (Roberts, 2005; Björnsson, 2009; Dunning et al., 2013; Carrivick and Tweed, 2019). Floods entering impounded waterbodies also have triggered natural dam failures, mainly by initiating rapid expansion of existing outlet channels. In many cases, the first seasonal flood triggers dam overflow and failure (e.g., Webby and Jennings, 1994), but in some cases exceptional floods were required to trigger erosion of outlets that had been stable for years or decades (e.g., Nash et al., 2010). An example of the latter is the Gros Ventre landslide dam failure, described by Alden (1928). In a few instances, upstream dam-break floods have triggered downstream breaches of dams. Examples include the upstream moraine-dam failure that led to breaching of landslide-dammed Lake Issyk, Kazakhstan (Gerasimov, 1965), and the breaching of lava-dammed Pleistocene American Falls Lake, Idaho, during the Bonneville Flood (O'Connor and Beebee, 2009). Earthquakes have triggered numerous landslide- and moraine-dam failures (Lliboutry et al., 1977; Costa and Schuster, 1991; Dai et al., 2005; Strasser et al., 2008; Emmer, 2017), and some caldera lake breaches may have been caused by intra-caldera volcanic activity (Waythomas et al., 1996; Manville, 2015). Human intervention also inadvertently caused the failure of some moraine and landslide dams in Peru (Lliboutry et al., 1977; Costa and Schuster, 1991; Reynolds, 1992), commonly during construction of outlet works at the blockages but also in the course of nearby construction and water diversion activities. Purposeful "pond letting" of some dammed estuaries (Kraus et al., 2002) and breaching of constructed dams (Major et al.,

2012; Herget and Gregori, 2020) have also caused floods. Longer-term exogenous processes indirectly trigger natural dam failure or basin breaching. For example, climate change leading to higher effective moisture regimes can fill and overtop closed basins.

The likelihood of breaching of natural dams or basin rims depends on the physical characteristics of the blockage and the probability of likely triggering processes (reviewed by Westoby et al., 2014). Important blockage characteristics are volume, height, shape, particle-size distribution, and layering. Engineering-style stability assessments, including subsurface material investigations, are generally feasible or justified only for large landslide dams for which several months or years may pass before the barrier is overtopped and where downstream flooding poses a significant hazard (Meyer et al., 1985; Hanisch and Söder, 2000; Risley et al., 2006), or for long-lived moraine dams (e.g., Lala et al., 2018; Falatkova et al., 2019). For many newly formed natural dams, stability assessments are necessarily qualitative and based on local topographic and glaciologic conditions (Lliboutry et al., 1977; Clague and Evans, 2000; O'Connor et al., 2001; Rounce et al., 2016; Fan et al., 2020), partly because it is difficult to obtain the pertinent data in the short time available for hazard assessment. This is particularly the case for small landslide dams, which commonly fail soon after they form but still can pose major downstream flood hazards (Hancox et al., 2005). Recent empirical studies of the likelihood of natural-dam failure offer potential for broad-scale quantification of the main breaching factors, including stability indices for landslide dams (e.g., Ermini and Casagli, 2003; Korup, 2004; Tacconi Stefanelli et al., 2016, 2018; Fan et al., 2020) and regional statistical likelihood assessments for moraine dams (e.g., McKillop and Clague, 2007a,b; Veh et al., 2020). Rule-based procedures have also provided estimates of the hazard for moraine-dam failures and ensuing debris flows (Huggel et al., 2004); McKillop and Clague, 2007a,b; Emmer and Vilimek, 2014; and Rounce et al. (2016). Similarly, Wang et al. (2012) proposed an objective "event-tree" breach probability assessment for moraine-dammed lakes in the Chinese Himalayas.

Many impoundments do not breach cataclysmically to produce floods. Instead, the blockages slowly incise, or the impounded water body completely fills in with sediment. A recent example of a gradually incised landslide dam was the barrier on the Stillaquamish River in Washington State created by the Oso landslide on March 22, 2014. After overtopping within 25 h of blockage, the river steadily incised a new channel to its near-original grade through the center of the landslide mass during the ensuing 2 months (Anderson et al., 2017). In addition to hazard implications, this observation has implications for the long-term geomorphic effects of natural dams on valley morphology and incision (Fan et al., 2020). For example, landslide blockages composed of rock debris, while perhaps not producing outburst floods as frequently or as large as glacier blockages (which nearly always fail catastrophically), may nevertheless leave a long landscape legacy of upstream valley fill deposits in addition to coarse lag deposits at the blockage site (Hewitt et al., 2008; Hewitt, 2009). Similarly, impoundments behind lava dams commonly fill with sediment (e.g., Ely et al., 2012). Even for beaver dams, long-term dam stability and resulting sediment filling is a key and widespread process affecting floodplain and valley morphology (Butler and Malanson, 2005).

For many outburst floods, initial incision of an overtopped blockage proceeds as a series of knickpoints or headcuts migrating up the downstream face of the barrier, with coincident channel enlargement as small landslides widen the banks of the deepening outlet channel (Lee and Duncan, 1975; Gordon, 1990; O'Connor, 1993; Plaza-Nieto and Zevallos, 1994; Dwivedi et al., 2000; Worni et al., 2012a,b; Ancey et al., 2019). Rapid outflow only begins once such retrogressively eroding headcuts intercept the breach crest, which then acts as a hydraulic weir. This sequence, which introduces uncertainty into predicting the timing of peak outflow, is well demonstrated by experimental and controlled breaches of earthen dams (Temple et al., 2010; Major et al., 2012; Walder et al., 2015). These processes may also transform what is commonly a clear-water flow at the breach crest to a turbid, sediment-laden flood or debris flow at the downstream end of the impoundment.

Once sufficient discharge through an outlet begins, tractive sediment entrainment, mass movements, or thermal ice erosion enlarges the overflow channel or conduit, increasing flow in a self-enhancing process (e.g., Clarke, 1982; Walder et al., 2015; Abril-Hernández et al., 2018). In most cases, the outlet rapidly enlarges until (1) the water supply diminishes or drops below the outlet elevation, (2) the outlet channel is armored sufficiently by coarse materials within the blockage to halt erosion, or, in the case of ice dams, (3) ice deformation or collapse closes the conduit. For valley blockages, the ultimate outlet elevation may be higher, the same, or lower than the pre-impoundment blockage elevation (O'Connor and Beebee, 2009).

Breach depth is a key factor controlling both peak discharge and ultimate flood volume for constructed and natural dams (Webby, 1996; Peng and Zhang, 2012; Begam et al., 2018). In the case of constructed earth-fill dams, breaching nearly always results in erosion to an elevation near the previous river level and, consequently, outflow of all the impounded water. For natural dams and basins, however, breaching may erode only part way through the blockage, to the base of the blockage, or in much rarer cases, deeper than the blockage. Most, however, erode only a fraction of the maximum impoundment depth (O'Connor and Beebee, 2009). Geological conditions typically will control breach depth of tectonic or volcanic basins (e.g., Garcia-Castellanos and O'Connor, 2018; Garcia-Castellanos et al., 2020). Resistant or hard materials halt erosion, generally at levels substantially above the bottom of the impoundment. But for landslide, volcaniclastic, and moraine dams formed of unconsolidated debris, the character of the blockage materials is important and the interplay between outflow rates and breach deepening, widening, and armoring will dictate the rate of breach growth, ultimate breach geometry, and possibly downstream flow rheology (Clague and Evans, 1992).

Breaching rates, geometry, and hydraulic conditions at the outlet nearly always control the outflow hydrograph (e.g., Walder et al., 2015). Analyses focused on outlet conditions, however, may overestimate peak discharges if (1) downstream "tailwater" (backwater from downstream ponding) slows outflow, or (2) the geometry of the waterbody inhibits movement of water to the outlet, either because of impoundment length or by internal lake constrictions limiting flow to the outlet (e.g., Abril-Hernández et al., 2018).

3.2 Peak discharge

Peak discharge is perhaps the most important attribute of outburst floods in terms of hazards and geomorphic consequences. Consequently, documenting, estimating, and predicting peak discharges and hydrographs of dam-failure floods, especially for constructed dams, has been a major focus of research in the engineering community (Ponce and Tsivoglou, 1981; Macdonald and Langridge-Monopolis, 1984; Froehlich, 1987, 1995, 2008, 2016; Fread, 1988, 1991; Singh et al., 1988; Macchione and Sirangelo, 1990; Wahl, 1998, 2004; Hanson et al., 2005; Macchione, 2008; Xu and Zhang, 2009; Temple et al., 2010; Thornton et al., 2011; Eghbali et al., 2017; Wang et al., 2018; Zhong et al., 2020). Hydrologists, glaciologists, and geologists interested in natural dam failures have extended this work substantially (Clague and Mathews, 1973; Nye, 1976; Clarke, 1982; Evans, 1986; Costa, 1988; Costa and Schuster, 1988; Björnsson, 1992, 2010; Walder and Costa, 1996; Walder and O'Connor, 1997; Tweed and Russell, 1999; Manville, 2001; Roberts, 2005; Risley et al., 2006; Davies et al., 2007; Manville et al., 2007; O'Connor and Beebee, 2009; Carrivick, 2010; Peng and Zhang, 2012; Herget et al., 2015; Walder et al., 2015, Liu et al., 2019, Sattar et al., 2020).

Three main approaches are commonly applied to predict (and retrodict) peak discharge from breached dams and basins: (1) regression analyses; (2) parametric or analytical assessments relying on basic physical principles in combination with prescribed geometric and temporal evolution of outlet conditions; and more recently (3) application of physically based morphodynamic models coupling flow, sediment transport, and mass movements that predict flow and breach evolution from initial conditions. Westoby et al. (2014), Worni et al. (2014), and Walder et al. (2015) describe key differences among these approaches.

Peak flood discharge scales with the size and geometry of the impoundment (Fig. 11). This observation has prompted numerous regression equations based on predictor variables such as impoundment volume and impoundment depth to provide a simple and frequently used approach to estimating peak discharge from natural dam failures (Clague and Mathews, 1973; Evans, 1986; Costa and Schuster, 1988; Walder and Costa, 1996; Walder and O'Connor, 1997; Cenderelli, 2000; Ng and Björnsson, 2003; Peng and Zhang, 2012; Westoby et al., 2014; Herget et al., 2015; Liu et al., 2019). Regression-based approaches that rely on dimensional analysis as a basis for identifying predictor variables (Froehlich, 1987, 1995, 2008; Webby and Jennings, 1994; and Webby, 1996; Xu and Zhang, 2009; Peng and Zhang, 2012; Zhong et al., 2020) are the most successful for predicting peak outflow from breached earth-fill dams (Wahl, 2004). However, as summarized by Walder and O'Connor (1997) and Wahl (2004) and is apparent from the spread of observations shown in Fig. 11, regression equations as well as bounding envelope curves derived from these analyses only give order-of-magnitude estimates of peak discharge. Recent examples of such regressions are given for several types of dam failures in China by Liu et al. (2019), for landslide dams by Peng and Zhang (2012), for ice dams by Walder and Costa (1996), for moraine and ice dams by Herget et al. (2015); and for constructed earthen dams by Froehlich (2016), Wang et al. (2018), and Zhong et al. (2020).

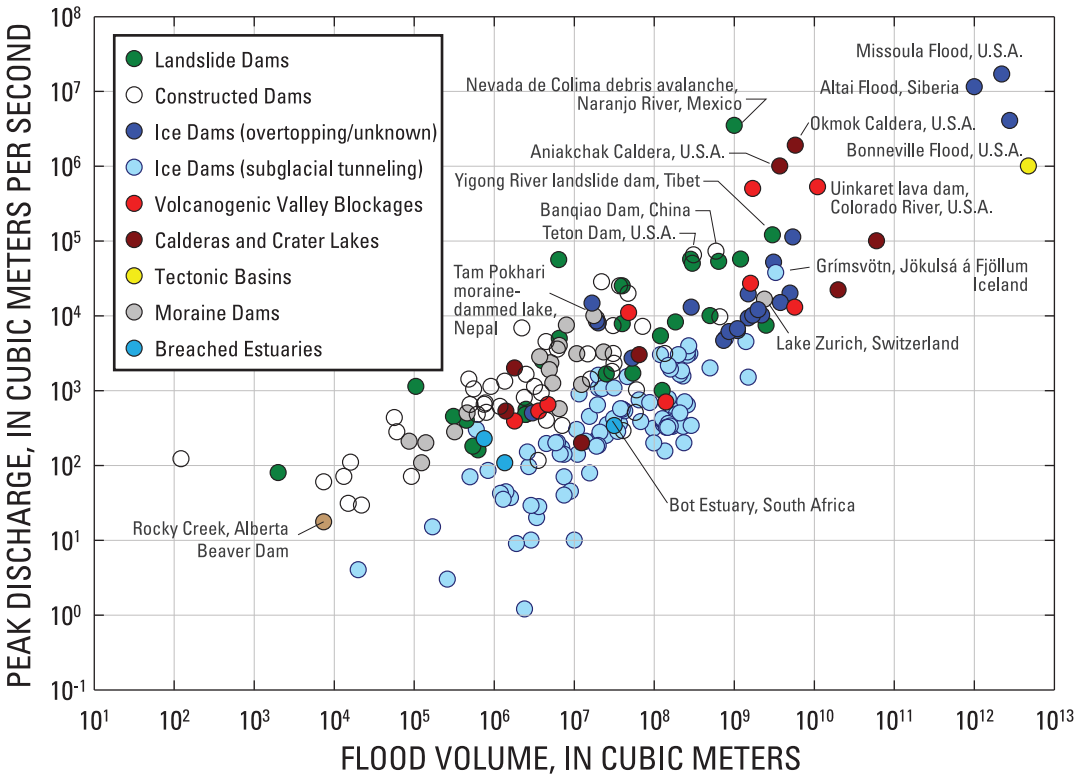

Fig. 11 Terrestrial freshwater outburst floods of known flood volume and peak discharge (discharge either measured or indirectly estimated from downstream flood evidence). Largest floods of each type are labeled. Data from Walder and Costa (1996), O'Connor and Beebee (2009), and Table 1.

Although expeditious, such regressions rarely give precise predictions (Walder and O'Connor, 1997; Wahl, 2004; Westoby et al., 2014). Contributing to the large uncertainty of these regression relations is the common large uncertainty in the discharge observations. They are typically estimated by a variety of methods—commonly with highly uncertain hydraulic parameters—at different distances downstream from the breach. And as the flood moves downstream beyond the breach, peak discharge may diminish due to flow-storage attenuation or increase due to sediment entrainment (O'Connor and Beebee, 2009; Herget et al., 2015; Erokhin et al., 2018), hence the measured discharge may be very different than the peak discharge at the outlet. The primary limitation of the regression approach, however, is that other factors besides impoundment volume and depth, such as hydraulic controls and breach erosion rates, strongly influence outflow (Walder and O'Connor, 1997; Peng and Zhang, 2012; De Lorenzo and Macchione, 2014; Sattar et al., 2020).

Parametric and morphodynamic approaches to estimating outflow hydrograph characteristics are, by necessity, specific to the processes by which impounded water evacuates. Outburst floods most commonly result from overtopping and breaching of barriers. For these types of breaches, peak discharge is nearly always controlled by the interplay between erosion and enlargement of the outflow channel (the "breach") and drawdown of the impounded water body (Fig. 12). This coupling between breach development, especially depth, and drawdown of the impounded waterbody forms the basis for several parameterized and physically based approaches to assessing peak discharges and outflow hydrographs from both natural-dam and constructed-dam failures (Ponce and Tsivoglou, 1981; Froehlich, 1987, 1995, 2008, 2016; Singh et al., 1988; Fread, 1991; Webby and Jennings, 1994; Webby, 1996; Walder and O'Connor, 1997; Manville, 2001; Marche et al., 2006, Peng and Zhang, 2012; Capart, 2013; Froehlich, 2016). Physically based parametric approaches consider outflow to be hydraulically critical, commonly specified as flow over a broad-crested weir. Breach growth is either parameterized by shape and time functions (Fread, 1988; Walder and O'Connor, 1997) or by physically based sediment transport and mass movement rules (Fread, 1991; Singh et al., 1988; Marche et al., 2006; Macchione, 2008; Capart, 2013; Wu, 2013). Failure by piping has been similarly evaluated (e.g., Wu, 2013; De Lorenzo and Macchione, 2014). Commonly, model parameters are iteratively fitted in order to match measured and calculated hydrographs.

More complex morphodynamic models attempt to fully couple breach flow hydraulics, sediment transport, and breach erosion processes, including lateral erosion processes. Such modeling is challenged by the exceptionally complicated and varied characteristics of natural dams, triggering mechanisms, and breaching dynamics (Westoby et al., 2014; Worni et al., 2014). This complexity is especially evident in field-scale experimental studies (e.g., Coleman et al., 2002; Hanson et al., 2005; Morris et al., 2007; Zhang et al., 2009; Pickert et al., 2011; Walder et al., 2015). Important factors include (1) uncertainty and diversity in materials forming natural blockages (Casagli et al., 2003); (2) the highly transient, non-equilibrium, and complex coupling of mass movement and fluvial erosion processes initiating and enlarging breach channels (e.g., Walder et al., 2015); and (3) the sensitivity of predictions to formulations, such as the bed-load transport equation, chosen to account for these processes (Cencetti et al., 2006). Nevertheless, such analyses are likely to become more common for outburst floods, spurred by advances in computational capacity. Recent examples incorporating elements of this approach include Worni et al. (2012a), Kropáĉek et al. (2015), Abril-Hernández et al. (2018), Begam et al. (2018), and Lala et al. (2018).

A consideration, especially for natural dam breaches, is Walder and O'Connor (1997) distinction between "large" and "small" impoundments (see also O'Connor and Beebee, 2009, as well as the similar formulation by Macchione and Rino, 2008). "Large" impoundments are those in which the breach develops fully before significant lake drawdown, either because the lake volume is very large relative to the breach depth or because the breach develops rapidly. In these cases, peak outflow is closely approximated by critical flow through the final breach geometry with $h = D$ (unless hindered by tailwater or reservoir routing effects). For cross-section shapes where width is approximately equal to depth,

$$Q \approx g^{\frac{1}{2}} h^{\frac{5}{2}} \tag{1}$$

where Q is the peak outflow discharge, g is gravitational acceleration, and h is the difference between the surface elevation of the impounded water body and the bottom of the breach at the outflow point, generally equivalent to the drop in water surface during the course of the outflow event. For wider breaches, peak discharge will be larger by a factor approximating b/h, where b is the breach width. The strong dependence on breach depth clarifies why deep lakes can produce such large peak discharges. Tectonic basins and caldera lakes can nearly always be considered "large" basins, and consequently, their peak discharges, where independently estimated, mostly range between 1 and 20 $g^{1/2}h^{5/2}$ (O'Connor and Beebee, 2009). Even for many moraine impoundments, lake volume and breach depth are the most important parameters influencing peak discharge (Begam et al., 2018). This basic dependence on flow depth within the outlet explains why uncertainty in the final breach depth—a common situation for many natural dams—complicates predictions of flood magnitude (e.g., Sattar et al., 2020).

"Small" impoundments, as classified by Walder and O'Connor (1997), are those for which there is significant water-surface drawdown during breach development. In these cases, the peak discharge is generally achieved before full development of the breach and is strongly dependent on the vertical erosion rate. Because observed vertical erosion rates for natural dam failures span nearly three orders of magnitude—4×10^{-4} to 1×10^{-1} m s^{-1} (O'Connor and Beebee, 2009)—predicting peak discharges from "small" impoundments is challenging (e.g., Sattar et al., 2020). Such is commonly the case for landslide dams (e.g., Peng and Zhang, 2012) and moraine impoundments, which typically block high-relief valleys and produce deep lakes with relatively small volumes (Davies et al., 2007). Veh et al. (2020) adopt a Bayesian approach in combination with the Walder and O'Connor (1997) formulation for estimating potential peak discharges from moraine-dammed lakes in the Himalaya, many of which straddle the imprecise boundary between "small" and "large."

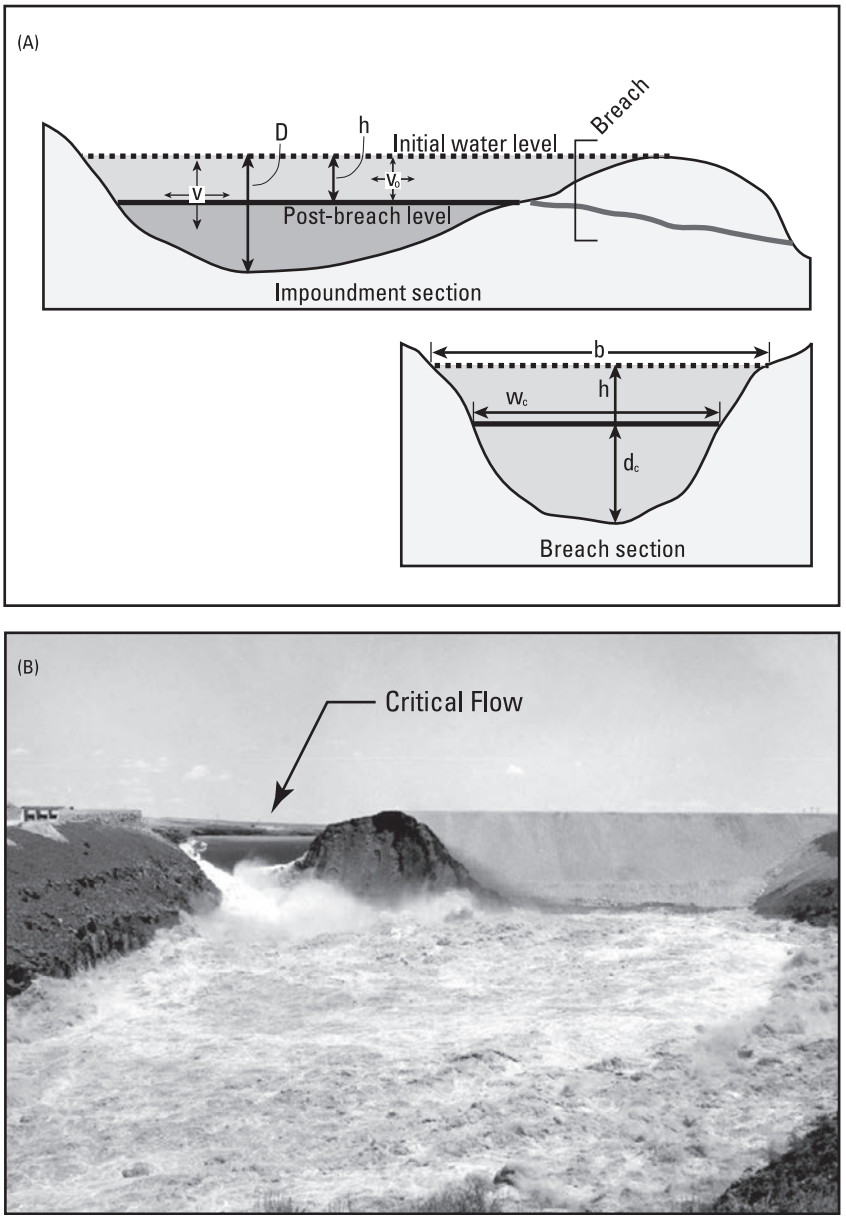

Fig. 12 Breach geometry and associated hydraulic conditions. (A) Definition diagram for impoundment and breach geometry. V is the total impoundment volume; V_0 is the volume released during the breach event; D is the maximum impoundment depth; h is the change in impoundment level during the breach event and is approximately equal to the maximum possible specific energy of flow through the breach; b is the breach width at the maximum impoundment elevation, w_c is the breach width at flow stage d_c associated with critical flow [$v = (gd)^{1/2}$] through the breach section with specific energy h. (B) View of outburst flood from failing Teton Dam on the Teton River, Idaho, on 5 June 1976. Teton Dam was a 100-m-high earth-fill dam that failed during first filling. Failure began by piping, which ultimately led to collapse and breaching of the dam crest. The smooth tongue of flow leading to intense waves and turbulence is evidence of critical flow through the breach. Peak outflow was 65,120 $m^3 s^{-1}$ (Ray and Kjelström, 1978) and 3.1×10^8 m^3 of water was released. U.S. Bureau of Reclamation Photograph P549–100-992. http://www.usbr.gov, accessed 21 May 2011.

For ice-dammed lakes and englacial waterbodies, physically based approaches for estimating peak discharges of outburst floods must consider processes distinct from overtopping because of the special properties of ice, especially in dynamic glacial environments (e.g., Carrivick et al., 2017). As noted by Ancey et al. (2019), much less literature has been devoted to breach and outflow mechanics associated with ice-dammed lakes. Much of the present understanding derives from analysis of Icelandic jökulhlaups, in part beginning with Thórarinsson's (1939) recognition that because of the lower density of ice relative to water, dams formed of ice are subject to local buoyancy due to hydrostatic stress before impounded water overtops the ice dam (Roberts, 2005; Björnsson, 2010). This explains why few ice dams fail by overtopping (Walder and Costa, 1996), but does not fully explain the triggers, peak discharges, and hydrographs of observed jökulhlaups (Ng and Björnsson, 2003). Glen (1954) and Liestøl (1956) proposed that subglacial tunneling may be an important process, followed by Mathews' (1973) inference that tunnels enlarge by thermal erosion

with the energy supplied by the potential energy of the impounded lake, thereby explaining the relatively slow but exponential rise in discharge measured for many jökulhlaups. Drainage of supraglacial lakes has been modeled by overtopping and thermal erosion of the outlet channel (Kingslake et al., 2015).

The overall physics of ice-tunneling were explained by Nye (1976). While this model has been elaborated and refined (Spring and Hutter, 1981, 1982; Clarke, 1982, 2003; Björnsson, 2010; Carrivick et al., 2017), the basic tenets endure: within an existing conduit or tunnel, sensible heat from water entering from the impounded waterbody is transferred to the ice walls by conduction, leading to conduit widening, thereby increasing flow, which in turns leads to more sensible heat transfer and to heat convection and associated thermal erosion due to viscous heat derived from friction associated with turbulent flow through the tunnel. This thermodynamic positive feedback process results in exponentially rising discharge through an enlarging conduit (Clarke, 1982; Björnsson, 1992, 2010; Carrivick et al., 2017). This process generally enlarges outlet channels more slowly than breaching of rock-material natural and constructed dams, thus peak discharges from ice-tunneling failures are typically smaller than those for rock-material dams involving similar impoundment volumes (Fig. 11).

Although the tunnel enlargement process has solid theoretical underpinnings, initiation and cessation conditions are less understood. Opening of a conduit may stem in part to ice flotation when water depth approaches 0.9 times the ice depth in the vicinity of the "seal" (Thórarinsson, 1939; Carrivick et al., 2017), but many examples show that conduit flow leading to outburst floods can begin at much lower lake levels than required for hydrostatic flotation, indicating that other factors related to glacier and drainage conditions are important, as summarized by Roberts (2005).

Similarly, jökulhlaup cessation is not entirely predictable. In some instances, termination of a jökulhlaup coincides with emptying of the waterbody (Clarke, 1982), but in many others, especially those emerging from conduits under thick glaciers (>80 m ice thickness), ice deformation may seal outlets before complete lake emptying (Nye, 1976; Roberts, 2005). And in the case of thinner glaciers, mechanical blockage may close conduits (Mathews, 1973; Sturm and Benson, 1985) in a manner similar to armoring of a breach eroded into rock-material dams. For the recent Russell Glacier, Greenland, outburst floods studied by Carrivick et al. (2017), floods terminated abruptly, apparently from lake levels falling below the conduit elevation rather than by viscous closure.

Some englacial or subglacial waterbodies produce outburst floods that seemingly peak too rapidly to be the result of simple conduit widening (Björnsson, 1977, 1992, 2009, 2010; Haeberli, 1983, Walder and Driedger, 1995; Walder and Fountain, 1997; Roberts, 2005). The generation and hydrodynamics of such floods are not well understood and may involve sudden rupture of pressurized water-filled englacial cavities (Walder and Fountain, 1997), pervasive hydro-fracturing at the base of an ice dam as a consequence of increasing hydrostatic pressure (Glen, 1954; Fowler, 1999), and in some instances, rapid generation of meltwater by hydrothermal or volcanic processes (Roberts, 2005). Peak flows in such situations may involve complex interactions between glacier drainage systems and transient hydraulic conditions (Roberts, 2005; Björnsson, 2009). Volcanogenic jökulhlaups may involve a sheet of water covering a large fraction of the glacier bed rather than channelized drainage channels (Björnsson et al., 2001; Johannesson, 2002; Flowers et al., 2004).

Some ice dams associated with subaerial water impoundments do fail by overtopping or ice-marginal drainage, similar to outburst floods associated with non-ice dams (Walder and Costa, 1996). These outbursts typically have much larger peak discharges than floods resulting from thermal erosion of subglacial conduits, and closer to those associated with failure of constructed dams (Fig. 11). Such was the case for the ice-avalanche dam in the Drance Valley, Switzerland, that failed in 1818 (Table 1). This similarity to rapidly failed constructed dams is reasonable because peak discharge from an overtopped ice dam will also approximate critical flow through a breach channel enlarging by thermal erosion in addition to mechanical erosion. Overtopping failures of ice dams are typically associated with glaciers flowing down tributary valleys to dam lakes in mainstem valleys (Walder and Costa, 1996). Haeberli (1983) and Carling (2013) describe how outburst flood hydrographs might vary with different types of ice-dam failures.

Few other processes besides overtopping and subglacial tunneling produce large terrestrial outburst floods. In some cases, outburst floods may begin by piping, groundwater sapping, or retrogressive landsliding (Costa, 1988; Massey et al., 2010), but in most instances, these processes lead to formation of an overflow channel that ultimately produces the peak discharge (Costa and Schuster, 1988, 1991; Temple et al., 2010).

On Mars, however, rapid release of pressurized groundwater is a likely source of outburst floods (Carr, 1979; Burr, 2010). Factors controlling the peak discharges of these floods relate to factors controlling groundwater flow through fissures (Head et al., 2003; Manga, 2004; Hanna and Phillips, 2005, 2006; Andrews-Hanna and Phillips, 2007). As described by Manga (2004), the geometric factors controlling peak discharge and flood volume are the hydraulic head, permeability, specific storage of the aquifer, and the fissure width, length, and associated friction factors. Peak discharges are greatest for wide fissures intercepting highly pressurized aquifers with high permeabilities. Flood volumes depend on the volume stored in the aquifer and the length of time the fissure remains open. Some Martian groundwater outbursts may have been triggered by volcanic melting and pressurization of frozen groundwater (Montgomery et al., 2009). Within some stress regimes, the tectonic environment may control both aquifer pressurization and fissure development (Hanna and Phillips, 2006), but in others, pressurization and release processes may be independent.

3.3 Downstream flood behavior

Large Pleistocene outburst floods travelled thousands of kilometers across landscapes down river valleys, some even leaving marks far out to sea (e.g., Zuffa et al., 2000; O'Connor et al., 2020). Historical natural dam failures have also produced far-travelled floods

(Delaney and Evans, 2011; Fan et al., 2020), such as the 1967 breaching of the Tanggudong landslide dam on the Yangtze River, raising river level 16.5 m as far as 560 km downstream (Liu et al., 2019). The records of these floods, preserved by oral stories, written records, and geologic evidence, hint at flood dynamics and potential hazards. But fuller, quantitative, understanding is hindered by the difficulty of making measurements, both because of the great energy of most outburst floods and to some degree their unpredictability. The few cases of well measured outburst floods, such as the 2007 Crater Lake breach from Mount Ruapehu, New Zealand (Procter et al., 2010), require tremendous effort and risk. Hence, the most common approach to assessing downstream outburst flood behavior—past or future—is by applying flow models of different types and comparing such model predictions to human and geologic accounts of their effects.

As described above, the flow hydrograph, including flow peak and duration, at the outlet depends chiefly on the geometry of the blockage and impounded water body, and the rates and processes of outlet enlargement processes. For overtopping failures, critical factors are the ultimate breach depth, and in many cases, the vertical breach erosion rate. Likewise, downstream flood behavior depends on several factors, including those common to all types of floods such as the outflow hydrograph shape and channel and valley geometries. In addition, many outburst floods erode and deposit substantial volumes of sediment, which can significantly affect flow behavior and have important geomorphological consequences. These factors pose serious challenges to characterizing and predicting the downstream behavior of outburst floods (Dunning et al., 2013; Westoby et al., 2014; Herget et al., 2015; Mergili et al., 2018). Nevertheless, new modeling techniques, increased availability of high-resolution topographic data, and more interdisciplinary attention have led to increased modeling capability as well as better understanding of downstream flood dynamics and resulting erosional and depositional processes.

Many breached landslide and moraine dams produce downstream debris flows, mainly by entrainment of material from the breached landslide mass or moraine by floodwaters, but also by incorporation of downstream bank and bed materials (Lliboutry et al., 1977; Eisbacher and Clague, 1984; Clague et al., 1985; King et al., 1989; Clague and Evans, 1994; Gallino and Pierson, 1985; Schuster, 2000; Huggel et al., 2003a, 2004; McKillop and Clague, 2007b; Breien et al., 2008; Carrivick et al., 2010; Procter et al., 2010; Emmer, 2017; Erokhin, et al., 2018; Liu et al., 2019). Such transformations have also been associated with glacial outburst floods, particularly in volcanic alpine environments (Walder and Driedger, 1994, 1995), but also in other steep environments (Jackson, 1979; Haeberli, 1983). Sediment-laden floods have also been reported from constructed- and ice-dam breaches, sometimes resulting from incorporation of fine-grained sediment liquefied or eroded from the rapidly drained and incised impoundment (Carling et al., 2009b; Wilcox et al., 2014a; Zhang et al., 2019). Transformation to debris flow has been most commonly documented for outbursts from moraine basins, where flow bulking can increase peak discharge of the water and entrained debris by an order of magnitude or more (Fig. 13), as well as increasing total flow volume. An extreme example is the August 1985 Dig Tsho outburst in Nepal, where 5.1×10^6 m^3 of water entrained $\sim 0.9 \times 10^6$ m^3 of sediment from the bounding moraine and ultimately incorporated and redeposited $\sim 3.3 \times 10^6$ m^3 of sediment over a 40-km distance downstream (Vuichard and Zimmermann, 1987). Similarly, peak discharge from a breach of a moraine-rimmed lake at the foot of Collier Glacier, Oregon, increased by a factor of 3 from less than 1.4×10^2 m^3 s^{-1} at the outlet to more than 5×10^2 m^3 s^{-1} 1 km downstream (O'Connor et al., 2001).

Outbursts from crater lakes and volcanic impoundments, especially on steep stratovolcanoes or in tephra-mantled or eruption-devastated landscapes, can also incorporate materials from channel beds and banks and develop into debris flows (Scott, 1988; Capra and Macías, 2002; Manville, 2004, 2010b, 2015; Schaefer et al., 2008; Procter et al., 2010; Capra, 2011; Yi et al., 2019). The 2007 crater-lake outburst flood on Mount Ruapehu, New Zealand, grew from a starting water volume of 1.3×10^6 m^3 to a lahar of 4.4×10^6 m^3 (Procter et al., 2010). These bulked-up volcanic lake breakouts are responsible for some of the largest and most lethal historic floods from natural dam breaches (e.g., Manville, 2004). Systematic analysis is difficult because of the few descriptions of flow rheology, but it is clear that steep channel slopes are required to sustain debris flows, generally slopes greater than 0.10–0.15 (Clague and Evans, 1994; O'Connor et al., 2001; McKillop and Clague, 2007b; Procter et al., 2010; Erokhin, et al., 2018), although less for large outbursts in volcanically devastated terrains (Scott, 1988). Plots of downstream peak-discharge changes (Fig. 13) show that most flow bulking is within the first 10 km of the breach, consistent with entrainment requiring steep channel slopes found in basin headwaters where many landslide and moraine dams form.

Flood behavior downstream of the breach depends on the flow rheology, outflow hydrograph, and downstream channel and valley geometry. Outburst floods that evolve into debris flows near the breach, resulting in increased peak discharges and flow volumes in steep and confined channel sections, will deposit in unconfined reaches and lower gradient reaches. Sediment deposition may sequester part or all of the initial water release, resulting in smaller downstream flood volumes compared to a clear-water flood and perhaps in more rapid rates of flow attenuation (O'Connor et al., 2001). In most instances, however, floods that become debris flows in their upper reaches continue downstream on lower gradients as sediment-laden water floods with total flood volumes about the same as the release volume (Manville, 2004). Even for outbursts that do not become debris flows, extensive erosion and deposition is common, in places contributing more to economic damage than inundation (e.g., Ruiz-Villanueva et al., 2017; Cook, et al., 2018).

Downstream propagation of outburst floods affects hazards as well as the distribution and magnitude of the resulting flood features. Consequently, understanding downstream flood behavior, chiefly by flood modeling, has been a significant recent research emphasis. Modeling is done both predictively, mainly to assess hazard, and after-the-fact, chiefly to understand processes. In particular, hydraulic models are commonly used to estimate outburst flood discharges of prehistorical floods and for floods for which other means of flow measurements are unavailable (e.g., O'Connor and Baker, 1992; Herget and Gregori, 2020). Most downstream flood models are separate from those assessing the outflow hydrograph, which is typically specified as an input

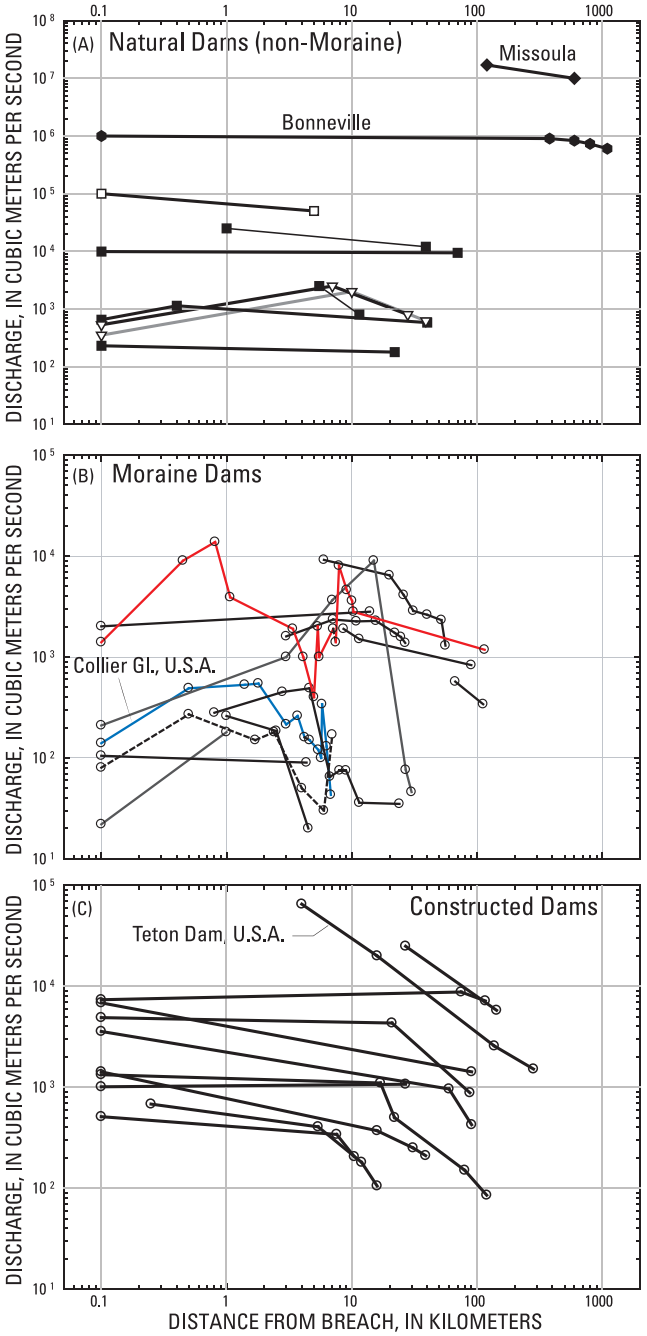

Fig. 13 Outburst flood attenuation shown as plots of peak discharge versus distance from the breach. Estimates of breach outflow are plotted at 0.1 km for portrayal on log axes. (A) Non-moraine natural dam failures. (B) Floods from moraine-rimmed lakes, showing rapid downstream increases and decreases in peak discharge, chiefly owing to entrainment and deposition. (C) Floods from breached embankment dams. Modified from O'Connor JE, Beebee RA (2009). Floods from natural rock-material dams. In: Burr DM, Carling PA, Baker VR (eds.), Megaflooding on Earth and Mars. pp. 128–171. United Kingdom: Cambridge University Press, http://refhub.elsevier.com/S0012-8252(20)30223-3/rf9017. (A) Data from sources in O'Connor JE, Beebee RA (2009). Floods from natural rock-material dams. In: Burr DM, Carling PA, Baker VR (eds.), Megaflooding on Earth and Mars. pp. 128–171. United Kingdom: Cambridge University Press, http://refhub.elsevier.com/S0012-8252(20)30223-3/rf9017; (B) data primarily from O'Connor JE, Hardison III JH, Costa JE (2001) Debris Flows From Failures of Neoglacial Moraine Dams in the Three Sisters and Mt. Jefferson Wilderness Areas, Oregon. U.S. Geological Survey Professional Paper 1608, 93 pp.; (C) data chiefly from sources in O'Connor JE, Beebee RA (2009). Floods from natural rock-material dams. In: Burr DM, Carling PA, Baker VR (eds.), Megaflooding on Earth and Mars. pp. 128–171. United Kingdom: Cambridge University Press, http://refhub.elsevier.com/S0012-8252(20)30223-3/rf9017 and Costa JE (1988) Floods from dam failures. In: Baker VR, Kochel RC, Patton PC (eds.), Flood Geomorphology. pp. 439–469. New York: John Wiley and Sons.

condition (e.g., Westoby et al., 2014; Lang et al., 2019; Turzewski et al., 2019; Latrubesse et al., 2020; Sattar et al., 2020). Yet some models do couple both components (e.g., Worni et al., 2012a; Vetsch et al., https://basement.ethz.ch/). Flood models include those employing constitutive equations applicable to water and debris flows (e.g., Mergili et al., 2018), and some are capable of coupling flow and sediment transport (e.g., Carrivick et al., 2010). Not yet applied, to our knowledge, are fully morphodynamic models integrating flow, sediment transport, and concurrent channel change for field-scale outburst floods. Many recent applications are fully two-dimensional, able to take advantage of increasingly available high-resolution digital topography. Recent summaries of flow models applied to outburst floods, including key issues and uncertainties, are given by Carling et al. (2003), Worni et al. (2014), Herget et al. (2015), Mergili et al. (2018), Bohorquez et al. (2019a), Neupane et al. (2019), and Turzewski et al. (2019). A recent comprehensive review of flood inundation modeling in general is given by Teng et al. (2017).

Some recent examples of diverse applications of flow models to evaluate downstream effects of outburst floods include:

- The coupled flow and sediment erosion and deposition model applied to Carrivick et al. (2010) to the 2007 lahar resulting from the Crater Lake breakout at Mt. Ruapehu, New Zealand.
- The prospective hazard assessment by Sattar et al. (2020) for moraine-dammed Safed Lake in the Indian Himalaya using HEC-RAS 2D, a widely used two-dimensional flow model (Brunner, 2016). Similar prospective hazard assessments for moraine-dammed lakes employing flood modeling have been conducted by Kougkoulos et al. (2018), Lala et al. (2018), and Wang et al. (2018). An early such analysis was performed by Laenan et al. (1987).
- Prediction of downstream flooding from the hypothetical breaching of the 550-m-tall Usoi landslide dam, Tajikistan (Risley et al., 2006).
- The Zanclean flood filling the Mediterranean basin, for which Abril-Hernández and Periáñez (2016) used a two-dimensional hydrodynamic model incorporating lateral and vertical erosion to estimate water passing through and enlarging the Strait of Gilbraltar as the previously isolated Mediterranean basin was rapidly filled by rapid influx from the Atlantic Ocean. Abril-Hernández et al. (2018) used a similar model to estimate outflow of pluvial Lake Bonneville during the Bonneville flood in western North America.
- Use of the open-source GeoClaw model (Berger et al., 2011) to assess hydraulics and geomorphic effects from the 2000 Yigong River landslide dam outburst flood in the Himalaya of Tibet (Turzewski et al., 2019). A version of this model was also applied to the Malpasset constructed dam failure in southern France (George, 2011).
- Single cross-section calculations and historical documentation to evaluate the downstream flood wave resulting from Allied bombing of the Möhne Reservoir in the Ruhr Valley, Germany (Herget and Gregori, 2020).
- Large Holocene subglacial releases at Kverkfjöll, Iceland, modeled by Carrivick (2006). Similarly, Alho et al. (2005) modeled the largest Holocene jökulhlaup at Jökulsá á Fjöllum, Iceland.
- The channels of Mars, including two-dimensional modeling of flows within Athabasca Valle, an outflow channel possibly formed by groundwater outflow from the Cerberus Fossae (Keszthelyi et al., 2007).
- Many modeling efforts focused on the Missoula floods in western North America, some motivated to estimate peak discharge (e.g., O'Connor and Baker, 1992), but more recent two-dimensional modeling to evaluate the interaction among the plexus of flow routes downstream of the failed ice dam (e.g., Alho et al., 2010; Denlinger and O'Connell, 2010; Denlinger et al., 2020).
- Other glacial megafloods: for example, Bohorquez et al. (2019b) applied a two-dimensional hydrodynamic model to retrodict downstream flood inundation from large Pleistocene ice-dammed lakes in the Altai Mountains, central Asia; and Winsemann et al. (2016), Lang et al. (2019) and Winsemann and Lang (2020) evaluated magnitudes and effects of Middle Pleistocene glacial lake outburst floods from the margin of the Fenno-Scandinavian ice sheet in north-central Europe.
- Two-dimensional modeling in conjunction with a bedrock erosion model to evaluate the potential for episodic incision within a Missoula flood pathway in Washington State, United States (Larsen and Lamb, 2016).
- Evaluation of the hydraulics and bedrock erosion processes causing rapid canyon incision during 2002 overtopping of the Canyon Lake reservoir, Texas, USA (Lamb and Fonstad, 2010).
- Submarine density current modeling for turbidity currents produced by sediment-laden Missoula floods entering the eastern Pacific Ocean (Beeson et al., 2017).

4 Signs left behind—Erosional and depositional features

Like the floods themselves, marks of outburst floods imprint cultures and language. *Scabland*, a term applied to the scabbly landscape carved by the Missoula floods, is widely used to denote flood-eroded landscapes, even in Antarctica (e.g., Cotton, 1965; Marchant et al., 2011). Other regional place names evoke flood features: Devils Corral, a cataract complex cut by the Bonneville flood; Dry Falls, Devils Coulee, and Potholes Coulee, all within the Channeled Scabland. Indeed, early maps showing the unusual topography (and perhaps the name) of Potholes Coulee motivated J Harlen Bretz's investigation of the Channeled Scabland, thus launching outburst floods into the scientific discourse of landscape evolution (Fig. 14; Baker, 2008). Even depositional features, like flood bars and boulder deposits inspire local names, such as Big Bar and Melon Valley along the Bonneville flood route. Such names reflect the unique flood-formed landscapes—typically terrain bedeviling settlement and cultivation—in turn signaling the capacity of outburst floods to make and erode landforms.

Fig. 14 Erosional features in northwestern United States left by the late Pleistocene Missoula floods and the Bonneville flood. (A) Aerial view northeast of Potholes Coulee and Columbia River showing pair of cataract-headed canyons cut by floods spilling 220 m down into the Columbia Valley; photograph by Bruce Bjornstad; inset shows part of 1910 USGS Quincy topographic map that inspired Bretz's investigations of the Channeled Scabland (squares are surveyed sections, each square is 1.6 km on the side). (B) Aerial view west and downstream from near Twin Falls, showing scabland and cataracts of the Devils Corral area carved by upland flow of the Bonneville flood reentering the Snake River; photograph by Bruce Bjornstad. (C) Ground view of abraded and fluted basalt near the outlet of pluvial Lake Bonneville; shovel handle 0.5 m. Photograph by Jim E. O'Connor.

The signs stand out because outburst flood magnitudes typically exceed those of meteorologically generated floods, sometimes by orders of magnitude. Hence outburst floods produce bigger landforms, they entrain, carry, and deposit more and larger materials, and may carve and bury broad swaths of valleys and channels (Fig. 14). From a large variety of terrestrial, subaqueous, and planetary environments, descriptions of flood and debris flow features resulting from outburst floods include Bretz (1923a,b, 1924, 1928, 1932), Malde (1968), Scott and Gravlee (1968), Baker (1973), Costa (1984), Blair (1987, 2001), Scott (1988), O'Connor (1993), Carling (1996, 2013), Cenderelli and Wohl (1998), Benito and O'Connor (2003), Manville (2004), Herget (2005), Kershaw et al. (2005), Carling et al. (2009a,b), Lamb and Fonstad (2010), Munro-Stasiuk et al. (2009), Burr (2010), Marchant et al. (2011), Carling (2013), Coleman (2013), Baynes et al. (2015b), Lapotre et al. (2016), Emmer (2017), Gupta et al. (2017), Carrivick and Tweed (2019), Goudge et al. (2018), Lang et al. (2019), and Carling and Fan (2020).

In general, flood effects and resulting landforms scale with flood force and the related quantity of flood energy. Following Carling and Fan (2020), the kinetic energy of flowing water per unit volume is given by:

$$E = \tfrac{1}{2}\rho v^2 \tag{2}$$

where E is the kinetic energy of the fluid in joules per cubic meter (J m^{-3}), ρ is the fluid density in kilograms per cubic meter (kg m^{-3}), and v is flow velocity in meters per second (m s^{-1}). Flow power owing to kinetic energy, Ω, equating to the time rate of energy expenditures in Watts per cubic meter (W m^{-3}), is given by:

$$\Omega = \tfrac{1}{2}\rho A v^3 \tag{3}$$

where A is the flow cross-sectional area in square meters. Apparent from these relations is the highly non-linear relation between flow velocity and power. Large and deep outburst floods may produce velocities of 40 m s^{-1} (e.g., Carrivick and Rushmer, 2006). For comparison, maximum measured velocities in rapids of Colorado River in Grand Canyon were 6.5 m s^{-1} (Magirl et al., 2009), and perhaps as high as 10 m s^{-1} in gorges of the Indus River (Whipple et al., 2000). Hence, outburst floods may generate shear stresses and stream powers 1–2 orders of magnitude greater than meteorological flows, thus the spectacular flood features.

Most assessments of outburst flood features and their relation to flow strength are based on related measures of shear stress and stream power per unit area of channel boundary. Shear stress, τ, expressed in Newtons per square meter (N m^{-2}), is the tangential force applied to the bed per unit area and for hydrostatic conditions can be calculated as:

$$\tau = \rho g d_f S \tag{4}$$

where d_f is flow depth and S is the local flow energy gradient, which for steady and uniform flow corresponds to channel slope. Unit stream power, ω (Bagnold, 1966, p. 5–6), expressed in watts per square meter (W m^{-2}), is the power developed per unit area of bed and can be expressed as

$$\omega = \rho g d_f v S = \tau v \tag{5}$$

These properties are best viewed as crude indices of the potential to produce geomorphic work. For most natural flows, only a portion of available mechanical energy is expended in accomplishing geomorphological work; the remainder is dissipated in other forms of energy loss. In addition, the formulations of Eqs. (4) and (5) are for hydrostatic conditions, thereby ignoring transient vertical and horizontal accelerations that can produce stresses of the same order as the hydrostatic forces (Iverson, 2006; Yager et al., 2018). Nevertheless, many studies have shown that the volume and caliber of entrained sediment, as well as the distribution of erosional features, broadly relate to the distribution of shear stress and stream power magnitudes (Baker, 1973; O'Connor, 1993; Benito, 1997; Cenderelli and Wohl, 2003; Carrivick, 2007, 2009; Denlinger and O'Connell, 2010; Lamb and Fonstad, 2010; Larsen and Lamb, 2016; Winsemann and Lang, 2020).

Chiefly because of high velocities and great depths, outburst floods generate exceptional shear stresses and stream powers (Baker and Costa, 1987; Carrivick and Rushmer, 2006; Carling, 2013). For example, the largest unit stream power values reconstructed from U.S. Geological Survey discharge measurements of meteorological floods, which result from flash floods in steep basins, are about 2×10^4 W m^{-2}, a value similar to that attained during the Teton Dam failure in Idaho (Costa and O'Connor, 1995). In comparison, maximum unit stream power values locally exceeded 10^5–10^6 W m^{-2} for the Bonneville flood (O'Connor, 1993) and the largest Missoula floods (O'Connor and Waitt, 1995; Benito, 1997; Denlinger and O'Connell, 2010), and 8×10^5 W m^{-2} for jökulhlaups from Kverkfjöll volcano, Iceland (Carrivick, 2007, 2009). Local unit stream-power values as high as 5×10^6 W m^{-2} may have been attained during Holocene floods from breached ice dams in the Tsangpo River gorge, Tibet (Montgomery et al., 2004).

4.1 Erosional features and processes

High shear stress and stream-power values create impressive erosional features (Fig. 14)—a hallmark of outburst floods (Carling et al., 2009b). Outburst floods typically erode at or near the outlet and in downstream energetic reaches, especially in near-glacial and volcanic environments of steep slopes and abundant unconsolidated debris. Erosion can also extend back into impoundments, as exemplified by the Condit Dam removal in Washington State where lacustrine sediments liquefied and passed through the breach (Wilcox et al., 2014a). Common erosional features include anastomosing channel networks, in places separated by streamlined "islands" of uplands (Baker, 1973); trenched valleys (commonly with hanging tributary valleys); cataracts, "dry falls," and amphitheater headed canyons; rock surfaces eroded into fantastic forms, such as basin-and-butte scabland and giant potholes (O'Connor, 1993); and fluted and streamlined rock surfaces.

Plucking, toppling, and abrasion are primary processes eroding rock during outburst floods (Bretz, 1924; Baker, 1973; Richardson and Carling, 2005; Carling et al., 2009b; Lamb and Fonstad, 2010; Lapotre et al., 2016; Larsen and Lamb, 2016). Vortices or kolks may facilitate plucking for some rock types (Baker, 1973). Recent mechanistic analyses of these processes (e.g., Whipple et al., 2000; Carling et al., 2002; Lamb and Fonstad, 2010; Lapotre et al., 2016) offer potential for better understanding of the spatial and temporal rates of flood erosion. Cavitation is an intensely energetic and potentially highly erosive process affecting engineering structures but unlikely to be effective for most river flows (Carling et al., 2017). Yet conditions conducive to cavitation may have been attained by some outburst floods on Earth (Baker, 1984; O'Connor, 1993) and Mars (Wilson et al., 2009).

Example studies of diverse approaches investigating erosional processes associated with outburst floods include:

- Empirical and semi-theoretical broad-scale assessments of the relations among shear stress, stream power, and the distribution and intensity of erosional features, including O'Connor (1993), Benito (1997), Carrivick (2007), Carrivick et al. (2013), and Turzewski et al. (2019).
- Examination of hydraulic conditions associated with streamlined flood forms (Komar, 1983, 1984).
- Assessments of block entrainment thresholds, including by plucking and toppling, such as by Carling et al. (2002), Lamb and Fonstad (2010), Lamb et al. (2015), and Carling and Fan (2020).
- Investigations of flood carved cataracts and amphitheater-headed canyons (e.g., Lamb et al., 2008, 2014; Baynes et al., 2015a; Lapotre et al., 2016).
- Numerous breach erosion studies, including experimental (e.g., Hanson et al., 2005; Walder et al., 2015; Zhou et al., 2019) and morphometric, such as the Goudge et al. (2018) analysis of breached Martian craters.
- Volumetric flood erosion estimates, such as Scott and Gravlee (1968), Baynes et al. (2015a), and Cook et al. (2018).
- Examination of rock resistance to erosion (Garcia-Castellanos and O'Connor, 2018).

4.2 Depositional features and processes

Erosion leads to sediment transport and ultimately deposition. Depositional landforms (Fig. 15) reflect transport processes, including those involving mass transport such as by mass movement and debris flow, suspended sediment and bedload in dominantly water flows, and hyperpycnal currents within large waterbodies. Some common features associated with outburst floods include: expansive debris fans downstream of breaches (e.g., Kershaw et al., 2005); immense boulder and gravel bars of a variety of forms and position relative to flood flow (e.g., Bretz, 1928; Scott and Gravlee, 1968; Malde, 1968; O'Connor, 1993; Herget, 2005; Baynes et al., 2015a), some of which are mantled with giant current dunes (e.g., Baker, 1973; Carling, 1996); extensive slackwater sediment accumulations in back-flooded areas (e.g., Waitt, 1980; Lang et al., 2013); coarse deltas where floods enter lake or marine basins (e.g., Winsemann et al., 2016), and widespread turbidity deposits where floods generate hyperpycnal currents (e.g., Zuffa et al., 2000). Reviews of debris flow and lahar processes and deposits relevant to outburst floods are given by Iverson (1997) and Vallance and Iverson (2015). Reviews of megaflood sediment transport processes and deposits—widely applicable to outburst floods—are given by Carling et al. (2009a), Carling (2013), and Carling and Fan (2020).

Outburst floods deposits commonly are distinguished by large constituent clasts (Fig. 15). Some terrestrial flood deposits from natural and constructed dam failures contain clasts with intermediate diameters exceeding 10 m (Baker, 1973; Rogers, 1992; Herget, 2005). Theoretical considerations and empirical studies (Baker and Ritter, 1975; Komar, 1987; Costa, 1983; Williams, 1983; O'Connor, 1993; Carling et al., 2009a; Lamb and Fonstad, 2010) demonstrate that tractive boulder entrainment scales with local flow strength. The empirical analyses by Williams (1983) and Costa (1983) indicate that entraining a 1 m intermediate-diameter boulder requires local stream power values of about 5×10^2 W m^2. Based on a reconstruction of local hydraulic conditions for the Bonneville Flood, O'Connor (1993) estimated that a 5 m boulder requires about 5×10^3 W m^2 for transport, a value rarely attained by meteorological floods (Baker and Costa, 1987). More recently, Lamb and Fonstad (2010) developed a threshold shear stress approach based on the Shields criterion. While subject to many uncertainties (Jacobson et al., 2016), these types of flow competence relations have been used for many paleohydraulic analyses of outburst floods (e.g., Lord and Kehew, 1987; Waythomas et al., 1996; Manville et al., 1999; Hodgson and Nairn, 2005; Carrivick, 2009; Lang et al., 2013; Baynes et al., 2015a).

Example studies of diverse investigations of depositional processes and landforms associated with outburst floods include:

- Empirical and semi-theoretical broad-scale assessments of the relations among velocity, shear stress, stream power, and the size of tractively transported clasts, including entrainment and depositional thresholds (e.g., Baker, 1973; O'Connor, 1993; Lamb and Fonstad, 2010; reviewed by Carling and Fan, 2020).
- Examination of the potential caliber of suspended load transported by floods (e.g., Komar 1980, 1988).
- The evaluation of flood deposit sedimentology in relation to high-energy process by Carling (2013).
- Evaluation of particle comminution in relation to flood energy (Carling and Fan, 2020).
- Assessment of the distribution and processes leading to formation and preservation of giant current dunes (e.g., Thiel, 1932; Baker, 1973; Carling, 1996; Herget and Carling, 2004; Bohorquez et al., 2019a).

4.3 Outburst floods and landscape evolution

Signs left by outburst floods are commonly dramatic, but do they matter in terms of long-term landscape evolution? This question has stalked studies of outburst floods for more than 50 years (e.g., Scott and Gravlee, 1968). And even earlier, Charles Lyell (1830, p. 192), the uniformitarian, hypothesized that "lake bursts" and their resulting floods may be a primary fluvial force excavating valleys. Clear is that the large Pleistocene outburst floods from ice-dammed lakes and pluvial lake spillovers have had long-lasting landscape effects, essentially setting the stages for Holocene processes and landforms in many areas (Figs. 14 and 15). It is not yet so clear for other environments, where meteorological floods compete with natural dams and outburst floods in pacing landscape evolution (Montgomery et al., 2004; Korup and Tweed, 2007; Baynes et al., 2015a; Safran et al., 2015; Cook et al., 2018; Fan et al., 2020). The question is increasingly relevant as landscape evolution models attempt to parameterize critical processes shaping continents. But because most such models relate landscape erosion to river flows and stream power indexed to

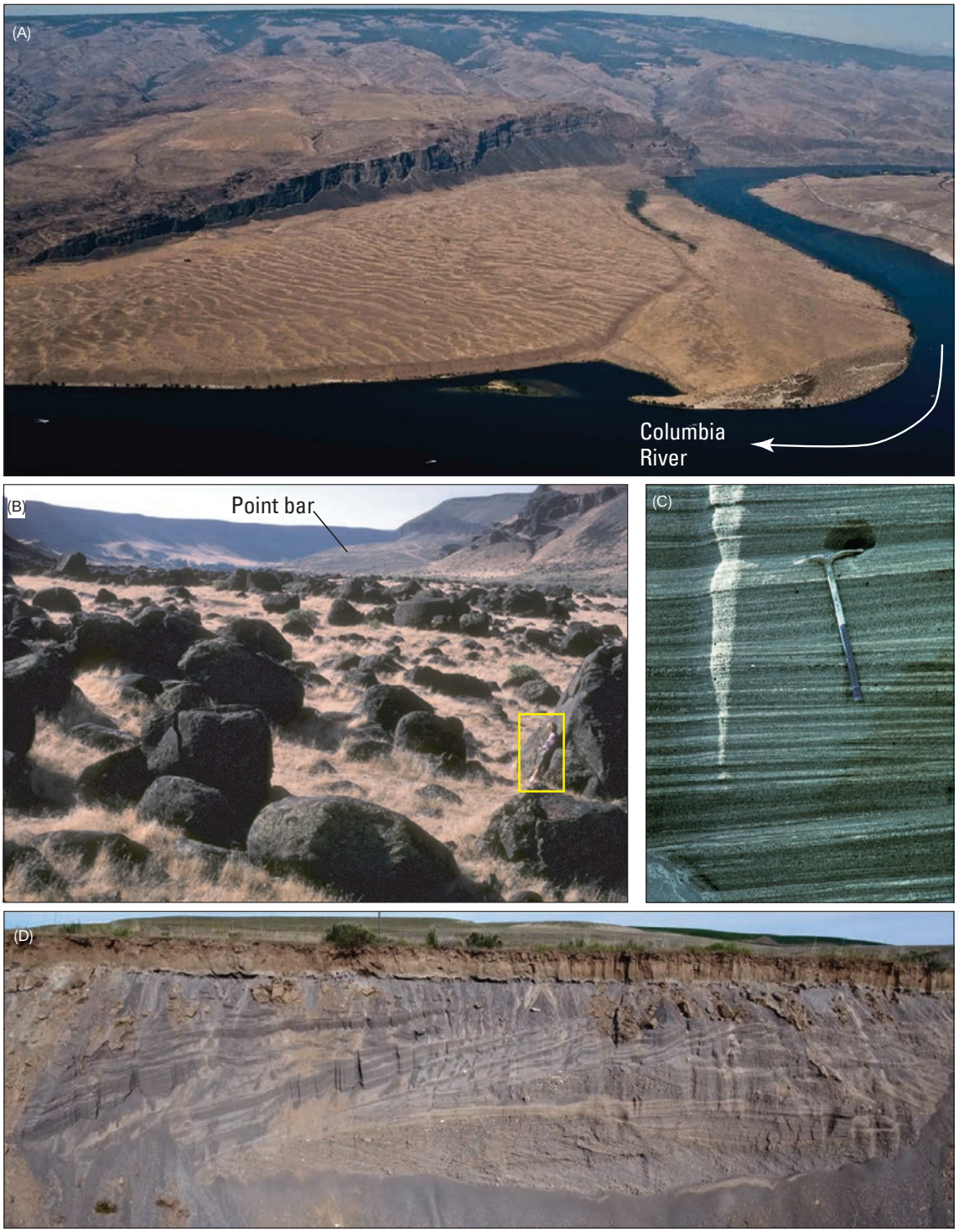

Fig. 15 Depositional landforms of late Pleistocene outburst floods in the northwestern United States. (A) Upstream aerial view of rippled West Bar along the Columbia River, Washington. This surface is inferred to have been formed by an outburst of glacial Lake Columbia. The bar surface stands 60 m above Columbia River pool level. Inset into West Bar is another flood bar, possibly left by an outburst from glacial Lake Kootenay (Waitt, 2016). (B) View upstream of large and rounded boulders deposited by the Bonneville Flood where the flow was wholly contained within the Snake River canyon in southwestern Idaho. Person for scale; many of the boulders have long diameters exceeding 10 m; a 100-m-tall point bar is visible against the canyon wall upstream. (C) Sand and fine gravel deposited from suspended load of the Bonneville flood in an eddy bar in southern Idaho. Pick is 0.7 m long. (D) Exposed flood bar within the Channeled Scabland of eastern Washington, capped by 2 m of brown loess; variously oriented gravel foresets indicate swirling flow directions. (A) Photograph by Bruce Bjornstad, modified from O'Connor JE, Baker VR, Waitt RB, Smith, LN, Cannon CM, George DL, Denlinger RP (2020) The Missoula and Bonneville floods—A review of ice-age Megafloods in the Columbia River Basin. *Earth-Science Reviews*. https://doi.org/10.1016/j.earscirev.2020.103181; (B) Photograph by Jim O'Connor; (C) photograph by Jim O'Connor; (D) photograph by Bruce Bjornstad.

Fig. 16 Areas of erosion and deposition from Oct. 7, 1966, moraine-dammed-lake outburst at terminus of East Bend Glacier at Broken Top volcano, central Oregon Cascade Range, United States. (A) Downstream view of fan of 1–2 m boulders deposited about 2.1 km downstream of breach. (B) Evident erosion, probably by plucking and toppling, of jointed basaltic andesite flows along the valley bottom, about 1.6 km downstream from the breach; flow left to right. Modified from O'Connor JE, Hardison III JH, Costa JE (2001) Debris Flows From Failures of Neoglacial Moraine Dams in the Three Sisters and Mt. Jefferson Wilderness Areas, Oregon. U.S. Geological Survey Professional Paper 1608, 93pp.

contributing basin area (e.g., Whipple and Tucker, 1999), the effects of valley blockages and related outburst floods may not be fully accounted for (e.g., Korup et al., 2010; Fan et al., 2020).

Such accounting is probably important in many environments. Because of their immense power, outburst floods can be of long-lasting influence along flood tracts (Korup and Tweed, 2007). Their energy levels commonly exceed rock erosion thresholds out of reach to meteorological floods, thereby producing substantial valley erosion (e.g., Montgomery et al., 2004; Lang et al., 2013; Cook et al., 2018). And their depositional products, especially coarse flood bars and fans, may be too large to be mobilized by subsequent meteorological floods, thus forming persistent landscape elements (e.g., O'Connor et al., 2003; Fan et al., 2020). For many mountainous regions, outbursts from landslide-, ice-, and moraine-dammed lakes may be key drivers of long-term erosion and sediment transport (Fig. 16; Cenderelli and Wohl, 2003; Montgomery et al., 2004; Korup and Tweed, 2007; Cook et al., 2018; Turzewski et al., 2019; Fan et al., 2020). Similarly, for the glacial rivers of Iceland and Greenland, floods from ice-dammed and subglacial water accumulations may be the primary erosional process (e.g., Baynes et al., 2015a,b; Carrivick and Tweed, 2019). But the accounting is complicated by few measurements quantifying erosion by outburst floods (e.g., Lamb and Fonstad, 2010), their uncertain frequency (e.g., Montgomery et al., 2004), how frequency over geologic (or shorter) time scales might change (e.g., Emmer et al., 2020; Veh et al., 2020), and the role of contingency in controlling the effects of both outburst and meteorological floods. These questions are active research fronts spurring much of the ongoing research on outburst floods.

5 Summary

Outburst floods can be large, hazardous, and geomorphically effective at local and planetary scales. The very largest floods on Earth in terms of peak discharge have been outbursts from ice-dammed and ice-marginal lakes during glacial epochs, but immense floods have also come from valleys temporally blocked by landslides and primary volcanic deposits and from basins formed by tectonism,

volcanism, and glacial moraines. The largest known freshwater floods by volume have been from Pleistocene ice-marginal lakes and may have involved as much 10^{13}–10^{14} m^3 of water with significant effects on oceanic circulation and global climate. The largest known non-ice-related outburst flood by volume was probably the late Pleistocene Bonneville flood from an overtopped tectonic basin. Immense Holocene floods have also issued from breached volcanic calderas. Large marine floods have inundated tectonic basins during periods of rising sea level. On Mars, even larger outburst floods resulted from cataclysmic release of pressurized ground water and from meteor craters that filled with water and then spilled. Failure of constructed dams is a more recent geological phenomenon, but is a significant hazard instigating much of the recent research on dam failure and breaching processes.

Outburst floods from natural dams result from specific geological, topographic, and climatic environments. Landslide dams and resulting floods are worldwide phenomena but are concentrated in mountainous regions where (1) relief promotes landslides and (2) confined valleys provide effective dam sites. Large floods and debris flows resulting directly or indirectly from volcanic processes, such as breaching of volcanically emplaced valley blockages and caldera and crater lakes, are restricted to volcanic environments and are well documented around the Pacific Rim in Alaska, New Zealand, Mexico, Japan, Chile, and the U.S. Pacific Northwest. Floods from tectonic basins are mostly in mid-latitude semiarid environments where periods of greater effective moisture fill closed basins. Most breached moraine-rimmed lakes have formed and emptied in the past 150 years because of rapid alpine glacier retreat from maximum Little Ice Age positions.

The peak discharge, duration, and volume of outburst floods are interrelated and depend chiefly on breach geometry and development rate and on the size and geometry of the impounded water body. In general, the largest floods result from breaching of tall blockages by large water bodies, such as the Pleistocene outbursts of Glacial Lake Missoula. Floods with large volumes relative to ultimate breach depth or where breaches erode rapidly generally will have peak discharges approximating critical flow through the final breach geometry. These discharges depend strongly on breach depth. Many floods from tectonic and volcanic basins and volcanic and ice blockages are of this type, including most of the largest documented terrestrial floods. Floods from blockages where the impounded volume is small relative to breach depth, or where erosion rates are low, have peak discharges strongly dependent on breach erosion rate. This is the case for the majority of breached landslide, moraine, and earth-fill dams.

Downstream flood behavior, including discharge, flow type, and depositional and erosional features, depends on the breach development processes, the rate and duration of flow out of the lake, and interactions with the channel and valley. Breaches that result in incorporation of great sediment volumes by the flow, either from the blockage itself or from downstream channel boundaries, may evolve into far-travelled debris flows. These debris flows may have peak discharges several times the peak outflow at the breach and substantially increase the flow volume. Debris flows attenuate rapidly downstream by deposition, particularly where slopes diminish below 0.15. This behavior is common for outbursts from moraine-rimmed and landslide-dammed impoundments, especially in volcanic environments.

Erosional and depositional features left by large floods, including gigantic bars and eroded channel tracts, reflect the depth and breadth of inundation as well as the large forces applied by deep high-velocity flow. Floods from natural dam failures can attain local stream power values of $\sim 10^{5\text{-}6}$ watts m^{-2}—one to two orders of magnitude greater than those generated by the most intense meteorological floods—and are capable of eroding bedrock channels and transporting clasts with diameters exceeding 10 m. These features and deposits, whether preserved as landforms or in stratigraphic records, are the persistent legacy of great floods, the largest of which on Earth result from failure of natural dams.

Table 1 Selected examples of well documented outburst floods; "n.d." no data; "n.a." not applicable.

	Flood	*Location*	*Approximate Outlet or Flood Location (WGS 84)*		*Date*	*Dam Height (Maximum Lake Depth), in Meters*	*Volume Impounded, in Cubic Meters*	*Breach Depth (Lake Level Fall), in meters*	*Volume Released, in Cubic Meters*	*Peak Discharge, in Cubic Meters per Second*	*References*	*Comments*
			Latitude	*Longitude*								
Valley Blockages	*Ice Dams*											
	Glacial Lake Missoula; Columbia River	USA, Idaho	47.8160	−119.9712	Pleistocene	650	$2.5 \cdot 10^{12}$	650	$2.5 \cdot 10^{12}$	$1.7 \cdot 10^{07}$	O'Connor and Baker (1992); O'Connor et al. (2020)	Multiple releases; failure mechanism unknown, but some probably involved subglacial tunneling
	Altai Mountains; River Ob	Russia	50.2500	87.6708	Pleistocene	650	$5.6 \cdot 10^{11}$	685	$5.6 \cdot 10^{11}$	$1.1 \cdot 10^{07}$	Bohorquez et al. (2019b)	Failure mechanism unknown
	Glacial Lake Vitim; Vitim and Lena Rivers	Russia	57.3930	116.4795	Pleistocene	490	$3.0 \cdot 10^{12}$	490	$3.0 \cdot 10^{12}$	$5.0 \cdot 10^{06}$	Margold et al. (2018)	Failure mechanism unknown; peak discharge estimate 4–6.5 $m^3 s^{-1}$
	Giétro Glacier, Drance River	Switzerland	45.9998	7.3507	June 15, 1818	80	$2.7 \cdot 10^{07}$	60	$1.6 \cdot 10^{07}$	$1.5 \cdot 10^{04}$	Ancey et al. (2019)	Rapid failure from retrograde incision; peak discharge estimated from parameterized breach conditions fit to observed lake-level fall
	Hubbard Glacier, Russell Fiord	USA, Alaska	59.9948	−139.4853	Oct. 8, 1986	25.5	$5.4 \cdot 10^{09}$	25.5	$5.4 \cdot 10^{09}$	$1.1 \cdot 10^{05}$	Mayo (1989); Trabant et al. (2003)	Probably failed by overtopping
	Chong Khumdan Glacier, Upper Shyok River	Pakistan	35.1740	77.7060	Aug. 15, 1920	120	$1.5 \cdot 10^{09}$	120	$1.5 \cdot 10^{09}$	$2.0 \cdot 10^{04}$	Hewitt (1968, 1982)	Subglacial tunneling, then collapse
	Lake George	USA, Alaska	61.3985	−148.5950	July 18, 1958	48.8	$2.2 \cdot 10^{09}$	48.8	$2.2 \cdot 10^{09}$	$1.0 \cdot 10^{04}$	Hulsing (1981); Lipscomb (1989)	Overtopping failure; peak lake stage attained July 13
	Strandline Lake	USA, Alaska	61.4811	−151.8830	Sept. 14–16 1984	149	$7.9 \cdot 10^{08}$	140	$7.1 \cdot 10^{08}$	$5.0 \cdot 10^{03}$	Sturm et al. (1987)	Subglacial tunneling; discharge value approximate; geometry estimated from fig. 3 of Sturm et al., 1987
	Lena River	Russia	64.3761	126.4314	June 6, 2001	n.d.	n.d.	n.d.	n.d.	$1.4 \cdot 10^{05}$	http://rims.unh.edu/data.shtml [accessed 30 may 2011]	Lena River at Kusur; flood peak from snowmelt and breached ice jam; discharge value obtained in 2011 no longer available from original source

Landslide Dams											
Naranjo River (Colima)	Mexico	19.4647	−103.4554	Pleistocene	150	$1.0 \cdot 10^{09}$	150	$1.0 \cdot 10^{09}$	$3.5 \cdot 10^{06}$	Capra and Macías (2002)	Volcanic debris avalanche filled canyon for 25 km; resulting breach resulted in debris flow; impoundment geometry estimated
Columbia River	USA, Washington	45.6551	−121.9080	circa 1450 AD	90	$1.7 \cdot 10^{10}$	75	$1.6 \cdot 10^{10}$	n.d.	O'Connor et al. (1996); O'Connor and Burns (2009)	Lake probably released in multiple events of unknown discharge
Indus River	Pakistan	35.4931	74.5997	June, 1841	150	$6.5 \cdot 10^{09}$	150	$6.5 \cdot 10^{09}$	$5.7 \cdot 10^{04}$	Hewitt (1968); Delaney and Evans (2011)	
Birehi Ganga River	India	30.3773	79.5009	Aug. 25, 1894	237	$4.4 \cdot 10^{08}$	120	$2.9 \cdot 10^{08}$	$5.7 \cdot 10^{04}$	Lubbock (1894), Strachey (1894), Malde (1968), Costa (1988), Costa and Schuster (1991)	
Gros Ventre River	USA, Wyoming	43.6308	−110.5504	May 18, 1927	70	$8.0 \cdot 10^{07}$	15	$5.4 \cdot 10^{07}$	$1.7 \cdot 10^{03}$	Malde (1968)	
Rio Mantaro	Peru	−12.6183	−74.6568	June 6, 1974	170	$6.7 \cdot 10^{08}$	107	$5.0 \cdot 10^{08}$	$1.0 \cdot 10^{04}$	Lee and Duncan (1975)	
Yigong River	Tibet	30.1738	94.9398	June 10, 2000	54	$2.3 \cdot 10^{09}$	58	$2.3 \cdot 10^{09}$	$1.2 \cdot 10^{05}$	Shang et al. (2003), Peng and Zhang (2012), and Delaney and Evans (2015)	Ovetopping; snowmelt induced; values from Liu et al. (2019)
Volcanogenic Dams											
Colorado River	USA, Arizona	36.1405	−113.2025	Pleistocene	302	$1.1 \cdot 10^{10}$	302	$1.1 \cdot 10^{10}$	$5.3 \cdot 10^{05}$	Fenton et al. (2006)	Lava flow into Grand Canyon
Williamson River	USA, Oregon	42.6940	−121.8210	7.7 ka	21	$6.5 \cdot 10^{09}$	17	$5.7 \cdot 10^{09}$	$1.3 \cdot 10^{04}$	Conaway (1999)	Lake dammed by pyroclastic flows from Mt. Mazama eruption
Tadami River (Numazawako)	Japan	37.4575	139.6134	5 ka	100	$1.7 \cdot 10^{09}$	70	$1.6 \cdot 10^{09}$	$2.7 \cdot 10^{04}$	Kataoka et al. (2008)	Pyroclastic flow into river valley
Tarawera River	New Zealand	−38.1831	176.5009	1305 AD	118	$4.0 \cdot 10^{09}$	40	$1.7 \cdot 10^{09}$	$5.0 \cdot 10^{05}$	Hodgson and Nairn (2005)	Existing lake dammed 30 m higher by pyroclastic flow
Marella River (Mapanuepe Lake)	Philipines	14.9875	120.2709	Sept. 21, 1991	24	$7.5 \cdot 10^{07}$	6.5	$4.7 \cdot 10^{06}$	$6.5 \cdot 10^{02}$	Umbal and Rodolfo (1996)	Dammed by lahars generated from Mt. Pinatubo pyroclastic flows
Constructed Dams											
South Fork (Johnstown)	USA, Pennsylvania	40.3475	−78.7744	May 31, 1889	24.6	$1.9 \cdot 10^{07}$	24.6	$1.9 \cdot 10^{07}$	$8.5 \cdot 10^{03}$	McCullough (1968)	Embankment dam; failed by overtopping

(*Continued*)

Table 1 (Continued)

	Flood	*Location*	*Approximate Outlet or Flood Location (WGS 84)*		*Date*	*Dam Height (Maximum Lake Depth), in Meters*	*Volume Impounded, in Cubic Meters*	*Breach Depth (Lake Level Fall), in meters*	*Volume Released, in Cubic Meters*	*Peak Discharge, in Cubic Meters per Second*	*References*	*Comments*
			Latitude	*Longitude*								
	St. Francis	USA, California	34.5468	−118.5125	Mar. 12, 1928	60	$4.7{\cdot}10^{07}$	60	$4.7{\cdot}10^{07}$	$3.7{\cdot}10^{04}$	Rogers (1992)	Gravity masonry dam; overtopping initiated by landslide
	Malpasset	France	43.5122	6.7567	Dec. 2, 1959	66.5	$5.5{\cdot}10^{07}$	66.5	$5.5{\cdot}10^{07}$	$4.5{\cdot}10^{04}$	Valiani et al. (2002)	Concrete arch, foundation failure
	Oros	Brazil	−6.2383	−38.9253	Mar. 26, 1960	35.8	$6.6{\cdot}10^{08}$	35.8	$6.6{\cdot}10^{08}$	$9.6{\cdot}10^{03}$	Costa (1988), Froelich (1995), and Wahl (1998)	Embankment dam; overtopped
	Hell Hole	USA, California	39.0581	−120.4097	Dec. 23, 1964	125	n.d.	35.1	$3.1{\cdot}10^{07}$	$7.4{\cdot}10^{03}$	Scott and Gravlee (1968) and Wahl (1998)	Rockfill dam failed by piping during construction
	Teton Dam	USA, Idaho	43.9119	−111.5393	June 5, 1976	n.d.	$3.1{\cdot}10^{08}$	77.4	$3.1{\cdot}10^{08}$	$6.5{\cdot}10^{04}$	Ray and Kjelström (1978), Costa (1988), and Froehlich (1995)	Embankment dam; failure began from piping, leading to formation of overflow breach
	Banqiao	China	32.9824	113.6233	Aug. 7, 1975		$6.1{\cdot}10^{08}$	24.8	$6.1{\cdot}10^{08}$	$7.8{\cdot}10^{04}$	Data summarized in Liu et al. (2019)	Rockfill dam; failed by overtopping after excessive rain from super typhoon Lianna; Froehlich (2016) provides alternate peak discharge estimate of 56,300 $m^3\ s^{-1}$
	Other Valley Blockages											
	Sycan River (eolian dune)	USA, Oregon	42.7170	−121.1709	7.7 ka	n.d.	n.d.	n.d.	n.d.	$5.8{\cdot}10^{03}$	Lind (2009)	Probable blockage of river canyon by eolian dune
	Bot Estuary (littoral sand ridge)	South Africa	−34.3669	19.0969	n.d.	2.7	$3.0{\cdot}10^{07}$	2.7	$3.0{\cdot}10^{07}$	2.5-$4.1{\cdot}10^{02}$	Van Niekerk et al. (2005)	Estuary blocked by coastal dunes; typical outburst flood characteristics (natural and human triggered)
	Rocky Creek (beaver dam)	Canada, Alberta	50.8278	−115.1207	June 8, 1994	3.2	$7.5{\cdot}10^{03}$	3.2	$7.5{\cdot}10^{03}$	$1.5{\cdot}10^{01}$	Hillman (1998)	
Basins	*Ice-Marginal Basins*											
	Glacial Lake Halle-Leipzig	Northwestern Germany, Netherlands	51.2062	11.7720	Middle Pleistocene	n.d.	$2.24{\cdot}10^{11}$	105	$2.24{\cdot}10^{11}$	4.6-$6.7{\cdot}10^{05}$	Lang et al. (2019)	Peak discharge estimated by breach modeling

Glacial Lakes Münsterland and Weser; Ruhr River valley	Northwestern Germany, Netherlands	51.7370	7.2020	Middle Pleistocene	150	$6.00 \cdot 10^{10}$	35	$9.00 \cdot 10^{10}$	1.7-3.7·10^{05}	Winsemann et al. (2016) and Winsemann and Lang (2020)	Possibly tanden lake breach; peak discharge estimated by breach modeling, ranges owe to uncertain ice margins and lake geometry; multiple outlets
Glacial Lake Regina	Canada, Saskatchewan; USA, North Dakota	49.6322	−103.8223	Late Pleistocene	n.d.	n.d.	n.d.	$7.4 \cdot 10^{10}$	5.8-8.2·10^{05}	Lord and Kehew (1987) and Kehew et al. (2009)	Multiple outlets
Glacial Lake Komi	Russia	62.0940	38.4330	Late Pleistocene	150	$2.1 \cdot 10^{12}$	150	$2.1 \cdot 10^{12}$	3-8.5·10^{05}	Mangerud et al. (2004)	Modeled subglacial release; 'best estimate;" depth estimated from source Fig. 2
Glacial Lake Agassiz into Mackenzie River	Canada, Saskatchewan	66.2440	−128.6960	13 ka	n.d.	n.d.	n.d.	$9.5 \cdot 10^{12}$	n.d.	Murton et al. (2010)	Possibly triggered Younger Dryas global cooling event
Glacial Lake Agassiz into Clearwater River	Canada, Saskatchewan	56.9620	−108.5300	11.5 ka	46	n.d.	n.d.	$1.6 \cdot 10^{13}$	$2.4 \cdot 10^{06}$	Smith and Fisher (1993)	
Glacial Lake Agassiz and Objibway into Hudson	Canada	58.5559	−95.9236	8.2 ka	230	$1.5 \cdot 10^{14}$	85	$7.1 \cdot 10^{13}$	$9.0 \cdot 10^{06}$	Clarke et al. (2004)	Modeled subglacial release; maximum case [C(230)]; release linked to 8.2 ka cold event
Moraine-Rimmed basins											
Lake Zurich	Switzerland	47.3687	8.5427	Pleistocene	147	n.d.	12	$2.5 \cdot 10^{09}$	$2.1 \cdot 10^{04}$	Strasser et al. (2008)	Discharge calculated by assuming critical flow through outlet; perhaps triggered by earthquake
Collier Gl.; White Branch	USA, Oregon	44.1857	−121.7920	July, 1942	10	$6.7 \cdot 10^{05}$	5.4	$4.6 \cdot 10^{05}$	$5.0 \cdot 10^{02}$	O'Connor et al. (2001)	Evolved into debris flow
Tam Pokhari Glacier Lake	Nepal	27.7386	86.8425	Sept. 3, 1998	60	$1.9 \cdot 10^{07}$	52	$1.8 \cdot 10^{07}$	$1.0 \cdot 10^{04}$	Dwivedi et al. (2000) and Dwivedi (writ. commun. with J.E. O'Connor, 2006)	Triggered by overtopping wave from ice fall. Minimum estimate of peak discharge
Laguna Jancaruish; Quebrada Los Cedros	Peru	−8.8508	−77.6753	Oct. 20, 1950	21	$8.0 \cdot 10^{06}$	21	$8.0 \cdot 10^{06}$	$7.5 \cdot 10^{03}$	Lliboutry et al. (1977)	Breached while outlet works under construction
Boqu River	Tibet	28.0713	86.0562	July 11, 1981	50	n.d.	32	$1.9 \cdot 10^{07}$	$9.2 \cdot 10^{03}$	Xu (1988) and Xu and Feng (1994)	Failure triggered by piping; evolved into debris flow; discharge estimated Manning equation 6 km below breac

(*Continued*)

Table 1 (Continued)

Flood	*Location*	*Approximate Outlet or Flood Location (WGS 84)*		*Date*	*Dam Height (Maximum Lake Depth), in Meters*	*Volume Impounded, in Cubic Meters*	*Breach Depth (Lake Level Fall), in meters*	*Volume Released, in Cubic Meters*	*Peak Discharge, in Cubic Meters per Second*	*References*	*Comments*
		Latitude	*Longitude*								
Lake Nostetuko	Canada, British Columbia	51.2110	−124.4151	July 19, 1983	n.d.	n.d.	38.4	$6.5 \cdot 10^{06}$	$5.7 \cdot 10^{02}$	Blown and Church (1985) and Clague and Evans (1994)	Peak discharge gaged 67 km downstream
Tectonic Basins											
Mediterranean Sea (Zanclean flood)	Gibraltar	35.9378	−5.5643	Miocene (5.3 Ma)	1500-2600	n.a.	240	$3.7 \cdot 10^{15}$	$1.0 \cdot 10^{08}$	Garcia-Castellanos et al. (2009, 2020) and Abril-Hernández and Periáñez (2016)	Marine incursion into Mediterranean basin
Lake Bonneville; Snake River	USA, Idaho	42.3564	−112.0469	Pleistocene	328	$1.0 \cdot 10^{13}$	108	$5.1 \cdot 10^{12}$	$1.0 \cdot 10^{06}$	O'Connor (1993) and O'Connor et al. (2020)	Discharge calculated by step-backwater modeling
Crooked Creek; Owyhee River	USA, Oregon	42.4870	−118.3860	Pleistocene	68	$4.0 \cdot 10^{10}$	12	$1.1 \cdot 10^{10}$	$1.0 \cdot 10^{04}$	Carter et al. (2006)	Maximum discharge calculated by assuming critical flow at outlet
Volcanic Basins											
Lake Taupo; Waikato River	New Zealand	38.6868	176.0638	Pleistocene	330	$1.1 \cdot 10^{11}$	80	$6.0 \cdot 10^{10}$	$1.0 \cdot 10^{05}$	Manville et al. (2007)	
Towada Caldera; Oirase River	Japan	40.4788	140.9421	Pleistocene	~400	$1.2 \cdot 10^{11}$	76	$6.0 \cdot 10^{09}$	$3.2 \cdot 10^{05}$	Kataoka (2011)	Caldera breakout flood; discharge estimated from boulder transport criteria
Aniakchak Caldera; Aniakchak River	USA, Alaska	56.9029	−158.0648	3.4 ka	183	$3.7 \cdot 10^{09}$	183	$3.7 \cdot 10^{09}$	$1.0 \cdot 10^{06}$	Waythomas et al. (1996)	Spillover of an caldera; discharge estimate from step-backwater calculation
Newberry Caldera, Paulina Lake; Paulina Creek	USA, Oregon	43.7170	−121.2793	4.7–1.7 ka	78	$3.2 \cdot 10^{08}$	2	$1.2 \cdot 10^{07}$	$2.0 \cdot 10^{02}$	Chitwood and Jensen (2000)	Critical flow measurement (110–280 $m^3 s^{-1}$) at downstream falls
Okmok Caldera; Umnak Island; Crater Creek	USA, Alaska	53.4681	−168.0913	1.5–1.0 ka	150	$5.8 \cdot 10^{09}$	150	$5.8 \cdot 10^{09}$	$1.9 \cdot 10^{06}$	Wolfe and Begét (2002)	"Maximum possible discharge" possibly estimated from critical flow calculation at breach
Pinatubo Caldera	Philippines	15.1488	120.3438	July 10, 2002	175	$1.6 \cdot 10^{08}$	23	$6.5 \cdot 10^{07}$	$3.0 \cdot 10^{03}$	Lagmay et al. (2007) and Antonia et al. (2003)	Geometry estimated from diagrams in Lagmay et al. (2007) and Stimac et al. (2004)

	Crater Lake, Mount Ruapehu; Whangaehu River	New Zealand	−39.2821	175.5682	Mar. 28, 2007	134	$1.3 \cdot 10^{07}$	6.3	$1.4 \cdot 10^{06}$	$5.3 \cdot 10^{02}$	Manville et al. (2007) and Manville and Cronin (2007)	Crater lake breach, tephra barrier eroded to lava-rock sill
	Impact Craters											
	Galilaei Crater	Mars			Hesperian	960	$1.1 \cdot 10^{13}$	960	$1.1 \cdot 10^{13}$	1.5-$8.4 \cdot 10^{7}$	Coleman (2015)	Maximum discharge estimated rapid breach formation by Walder and O'Connor (1997) method
Other	*Subglacial and Englacial Empoundments*											
	Jökulsá á Fjöllum	Iceland	64.7292	−16.6963	Holocene	n.a.	n.d.	n.a.	n.d.	$9.0 \cdot 10^{05}$	Alho et al. (2005)	Probably triggered by subglacial eruption under Vatnajökull
	Katla; Mýrdalsjökull	Iceland	63.5543	−18.8259	Oct. 12, 1918	n.a.	n.d.	n.a.	$5.0 \cdot 10^{09}$	$2.8 \cdot 10^{05}$	Tómasson (1996)	Volume estimated from hydrograph of Oct. 12 peak
	South Tacoma Glacier, Tahoma Creek	USA, Washington State	46.8050	−121.8482	July 26, 1988	n.a.	n.d.	n.a.	$3.0 \cdot 10^{05}$	$5.5 \cdot 10^{02}$	Walder and Driedger (1994)	Debris flow; peak water flow about 200 $m^3 s^{-1}$
	Grímsvötn; Jökulsá á Fjöllum	Iceland	64.3881	−17.3300	Nov. 5, 1996	n.a.	n.d.	175	$3.3 \cdot 10^{09}$	$5.3 \cdot 10^{04}$	Tweed and Russell (1999) and Björnsson (2009)	Triggered by Gjalp eruption
	Vadret da L'Albigna	Switzerland	46.3169	9.6476	1927	n.a.	n.d.	n.a.	$2.7 \cdot 10^{06}$	$1.3 \cdot 10^{02}$	Haeberli (1983)	Triggered by precipitation
	Ground Water											
	Cerebus Fossae; Athabasca Valles	Mars			Amazonian	n.a.	n.d.	n.a.	$4.5 \cdot 10^{10}$	$1.2 \cdot 10^{06}$	Burr et al. (2002a,b) and Manga (2004)	
	Other											
	Boston Molasses Flood	USA, Massachusetts			Jan. 15, 1919	15.2	$8.9 \cdot 10^{03}$	n.a.	n.d.	n.d.	Hartley (1981)	Molasses from breached storage tank; 21 fatalities

Acknowledgments

Partial support for this project was provided by the National Science Foundation award EAR-0617234. We have been aided by discussions with V.R. Baker, Paul Carling, Juergen Herget, and Devon Burr.

References

Abril-Hernández JM and Periáñez R (2016) Revisiting the time scale and size of the Zanclean flood of the Mediterranean (5.33 Ma) from CFD simulations. *Marine Geology* 382: 242–256. https://doi.org/10.1016/j.margeo.2016.10.008.

Abril-Hernández JM, Periáñez R, O'Connor JE, and Garcia-Castellanos D (2018) Computational fluid dynamics simulations of the late Pleistocene Lake Bonneville flood. *Journal of Hydrology* 561: 1–15. https://doi.org/10.1016/j.jhydrol.2018.03.065.

Adams JE (1981) Earthquake-dammed lakes in New Zealand. *Geology* 9: 215–219.

Alden WC (1928) Landslide and flood at Gros Ventre, Wyoming. *Transactions of the American Institute of Mining and Metallurgical Engineers* 76: 347–360.

Alho P, Russell AJ, Carrivick JL, and Käyhkö J (2005) Reconstruction of the largest Holocene jökulhlaup within Jökulsá á Fjöllum, NE Iceland. *Quaternary Science Reviews* 24: 2319–2334.

Alho P, Baker VR, and Smith LN (2010) Paleohydraulic reconstruction of the largest Glacial Lake Missoula draining(s). *Quaternary Science Reviews* 29: 3067–3078. https://doi.org/10.1016/j.quascirev.2010.07.015.

Allen SK, Linsbauer A, Randhawa SS, Huggel C, Rana P, and Kumari A (2016a) Glacial lake outburst flood risk in Himachal Pradesh, India: An integrative and anticipatory approach considering current and future threats. *Natural Hazards* 84: 1741–1763. https://doi.org/10.1007/s11069-016-2511-x.

Allen SK, Rastner P, Arora M, Huggel C, and Stoffel M (2016b) Lake outburst and debris flow disaster at Kedarnath, June 2013: Hydrometeorological triggering and topographic predisposition. *Landslides* 13: 1479–1491. https://doi.org/10.1007/s10346-015-0584-3.

Alley RB and Ágústsdóttir AM (2005) The 8k event: Cause and consequences of a major Holocene abrupt climate change. *Quaternary Science Reviews* 24: 1123–1149.

Amidon WH and Clark AC (2015) Interaction of outburst floods with basaltic aquifers on the Snake River Plain: Implications for Martian canyons. *Geological Society of America Bulletin* 127: 688–701. https://doi.org/10.1130/B31141.1.

Anacona PI, Mackintosh A, and Norton KP (2015a) Hazardous processes and events from glacier and permafrost areas: Lessons from the Chilean and Argentinean Andes. *Earth Surface Processes and Landforms* 40: 2–21. https://doi.org/10.1002/esp.3524.

Anacona PI, Mackintosh A, and Norton K (2015b) Reconstruction of a glacial lake outburst flood (GLOF) in the Engaño Valley, Chilean Patagonia: Lessons for GLOF risk management. *Science of the Total Environment* 527: 1–11. https://doi.org/10.1016/j.scitotenv.2015.04.096.

Ancey C, Bardou E, Funk M, Huss M, Werder MA, and Trewhela T (2019) Hydraulic reconstruction of the 1818 Giétro glacial lake outburst flood. *Water Resources Research* 55: 8840–8863. https://doi.org/10.1029/2019WR025274.

Anderson DE (1998) *Late Quaternary Paleohydrology, Lacustrine Stratigraphy, Fluvial Geomorphology and Modern Hydroclimatology of the Amargosa River/Death Valley Hydrologic System, California and Nevada*. Unpublished Ph.D. dissertation Riverside, CA: University of California Riverside.

Anderson SW, Keith MK, Magirl CS, Wallick JR, Mastin MC, and Foreman JR (2017) *Geomorphic Response of the North Fork Stillaguamish River to the State Route 530 Landslide Near Oso, Washington*. U.S. Geological Survey Scientific Investigations Report 2017–5055, 85. https://doi.org/10.3133/sir20175055.

Andrews GDM, Russell JK, and Stewart ML (2014) The history and dynamics of a welded pyroclastic dam and its failure. *Bulletin of Volcanology* 76: 811. https://doi.org/10.1007/s00445-014-0811-0.

Andrews-Hanna JC and Phillips RJ (2007) Hydrological modeling of outflow channels and chaos regions on Mars. *Journal of Geophysical Research, Planets* 112: E08001. https://doi.org/10.1029/2006JE002881.

Antonia M, Bornas V, and Newhall CG (2003) *The 10 July 2002 caldera-rim breach and breakout lahar from Mt. Pinatubo, Philippines: Results and lessons from attempting an artificial breach*. Programme and abstracts of the Volcanological Society of Japan, p. 91.

Arkhipov SA, Ehlers J, Johnson RG, and Wright HE Jr. (1995) Glacial drainage towards the Mediterranean during the Middle and Late Pleistocene. *Boreas* 24: 196–206.

Atwater BF (1986) *Pleistocene Glacial-Lake Deposits of the Sanpoil River Valley, Northeastern Washington*. U.S. Geological Survey Bulletin 1661, 39.

Atwater BF, Smith GA, and Waitt RB (2000) The Channeled Scabland: Back to Bretz? Comment and Reply. *Geology* 28: 574.

Bagnold RA (1966) *An Approach to the Sediment Transport Problem From General Physics*. U.S. Geological Survey Professional Paper 422-I, 37.

Baker VR (1973) *Paleohydrology and Sedimentology of Lake Missoula Flooding in Eastern Washington*. Geological Society of America Special Paper 144, 79.

Baker VR (1983) Late Pleistocene fluvial systems. In: Porter SC (ed.) *The Late Pleistocene, Volume 1 of Late-Quaternary Environments of the United States*, pp. 115–129. Minneapolis, Minnesota: University of Minnesota Press. Wright HE Jr (ed.).

Baker VR (1984) Flood sedimentation in bedrock fluvial systems. In: Koster EH and Steel RJ (eds.) *Sedimentology of Gravels and Conglomerates*, 87–98. Canadian Society of Petroleum Geologists Memoir 10: Calgary, Alberta.

Baker VR (2001) Water and the Martian landscape. *Nature* 412: 228–236. https://doi.org/10.1038/35084172.

Baker VR (2008) The Spokane Flood debates: Historical background and philosophical perspective. In: Grapes RH, Oldroyd D, and Grigelis A (eds.) *History of Geomorphology and Quaternary Geology*, 33–50. https://doi.org/10.1144/SP301.3. Geological Society of London Special Publications 301.

Baker VR (2009) Overview of megaflooding: Earth and Mars. In: Burr DM, Carling PA, and Baker VR (eds.) *Megaflooding on Earth and Mars*, pp. 1–12. Cambridge: Cambridge University Press.

Baker VR (2020) Global megaflood paleohydrology. In: Herget J and Fontana A (eds.) *Palaeohydrology: Geography of the Physical Environment*. Cham: Springer. https://doi.org/10.1007/978-3-030-23315-0_1.

Baker VR and Costa JE (1987) Floodpower. In: Mayer L and Nash D (eds.) *Catastrophic Flooding*, pp. 1–24. Boston, MA: Allen and Unwin.

Baker VR and Milton DJ (1974) Erosion by catastrophic floods on Mars and Earth. *Icarus* 23: 27–41. https://doi.org/10.1016/0019-1035(74)90101-8.

Baker VR and Ritter DF (1975) Competence of rivers to transport coarse bedload material. *Geological Society of America Bulletin* 86: 975–978.

Baker VR, Benito G, and Rudoy AN (1993) Paleohydrology of late Pleistocene Superflooding, Altay Mountains, Siberia. *Science* 259: 348–350.

Baker VR, Hamilton CW, Burr DM, Gulick VC, Komatsu F, Luo W, Rice JW Jr., and Rodriguez JAP (2015) Fluvial geomorphology on Earth-like planetary surfaces: A review. *Geomorphology* 245: 149–182. https://doi.org/10.1016/j.geomorph.2015.05.002.

Barber DC, Dyke A, Hillaire-Marcel C, Jennings AE, Andrews JT, Kerwin MW, Bilodeau G, McNeely R, Southon J, Morehead MD, and Gagnon J-M (1999) Forcing of the cold event of 8,2000 years ago by catastrophic drainage of Laurentide lakes. *Nature* 400: 344–348. https://doi.org/10.1038/22504.

Batbaatar J and Gillespie AR (2015) Outburst floods of the Maly Yenisei. Part I. *International Geology Review* 58: 1723–1752. https://doi.org/10.1080/00206814.2015.1114908.

Baynes ERC, Attal M, Dugmore AJ, Kirstein LA, and Whaler KA (2015a) Catastrophic impact of extreme flood events on the morphology and evolution of the lower Jökulsá á Fjöllum (northeast Iceland) during the Holocene. *Geomorphology* 250: 422–436. https://doi.org/10.1016/j.geomorph.2015.05.009.

Baynes ERC, Attal M, Niedermann S, Kirstein LA, Dugmore AJ, and Naylor M (2015b) Erosion during extreme flood events dominates Holocene canyon evolution in northeast Iceland. *Proceedings of the National Academy of Sciences* 112: 2355–2360. https://doi.org/10.1073/pnas.1415443112.

Beebee RA (2003) *Snowmelt Hydrology, Paleohydrology, and Landslide Dams in the Deschutes River Basin, Oregon*. Unpublished Ph.D. Dissertation Eugene, Oregon: University of Oregon.

Beeson JW, Goldfinger C, and Fortin WF (2017) Large-scale modification of submarine geomorphic features on the Cascadia accretionary wedge caused by catastrophic flooding events. *Geosphere* 13: 1713–1728. https://doi.org/10.1130/GES01388.1.

Begam S, Sen D, and Dey S (2018) Moraine dam breach and glacial lake outburst flood generation by physical and numerical models. *Journal of Hydrology* 563: 694–710. https://doi.org/10.1016/j.jhydrol.2018.06.038.

Begét JE, Larsen JF, Neal CA, Nye CJ, and Schaefer JR (2005) *Preliminary Volcano-Hazard Assessment for Okmok Volcano, Umnak Island Alaska*. Alaska Department of Natural Resources, Division of Geological and Geophysical Surveys Report of Investigations 2004-3, 39.

Behrens DK, Bonbardelli FA, Largier JL, and Twohy E (2013) Episodic closure of the tidal inlet at the mouth of the Russian River—A small bar-built estuary in California. *Geomorphology* 189: 66–80. https://doi.org/10.1016/j.geomorph.2013.01.017.

Benito G (1997) Energy expenditure and geomorphic work of the cataclysmic Missoula flooding in the Columbia River Gorge, USA. *Earth Surface Processes and Landforms* 22: 457–472.

Benito G and O'Connor JE (2003) Number and size of last-glacial Missoula floods in the Columbia River valley between the Pasco Basin, Washington, and Portland, Oregon. *Geological Society of America Bulletin* 115: 624–638.

Benito G and Thorndycraft VR (2020) Catastrophic glacial-lake outburst flooding of the Patagonian Ice Sheet. *Earth-Science Reviews* 200: 102996. https://doi.org/10.1016/j.earscirev.2019.102996.

Benn DI, Owen LA, Finkel RC, and Clemmens S (2006) Pleistocene lake outburst floods and fan formation along the eastern Sierra Nevada, California: Implications for the interpretation of intermontane lacustrine records. *Quaternary Science Reviews* 25: 2729–2748.

Berger MJ, George DL, LeVeque RJ, and Mandli KT (2011) The GeoClaw software for depth-averaged flows with adaptive refinement. *Advances in Water Resources* 34: 1195–1206. https://doi.org/10.1016/j.advwatres.2011.02.016.

Björnsson H (1974) Explanation of jökulhlaups from Grımsvotn, Vatnajokull, Iceland. *Jökull* 24: 1–26.

Björnsson H (1976) Marginal and supraglacial lakes in Iceland. *Jökull* 26: 40–51.

Björnsson H (1977) The cause of jökulhlaups in the Skaftá river, Vatnajökull. *Jökull* 27: 71–78.

Björnsson H (1992) Jökulhlaups in Iceland: Prediction, characteristics and simulation. *Annals of Glaciology* 16: 95–106.

Björnsson H (2009) Jökulhlaups in Iceland: Sources, release and drainage. In: Burr DM, Carling PA, and Baker VR (eds.) *Megaflooding on Earth and Mars*, pp. 50–64. Cambridge: Cambridge University Press.

Björnsson H (2010) Understanding jökulhlaups: From tale to theory. *Journal of Glaciology* 56: 1002–1010.

Björnsson H, Rott H, Gudmundsson S, Fischer A, Siegel A, and Gudmundsson MT (2001) Glacier-volcano interactions deduced by SAR interferometry. *Journal of Glaciology* 47: 58–70.

Blair TC (1987) Sedimentary processes, vertical stratification sequences, and geomorphology of the Roaring River alluvial fan, Rocky Mountain National Park, Colorado. *Journal of Sedimentary Research* 57: 1–18.

Blair TC (2001) Outburst flood sedimentation on the proglacial Tuttle Canyon alluvial fan, Owens Valley, California, U.S.A. *Journal of Sedimentary Research* 71: 657–679.

Blown I and Church M (1985) Catastrophic lake drainage within the Homathko River basin, British Columbia. *Canadian Geotechnical Journal* 22: 551–563.

Bohorquez P, Cañada-Pereira P, Jimenez-Ruiz PJ, and del Moral-Erencia JD (2019a) The fascination of a shallow-water theory for the formation of megaflood-scale dunes and antidunes. *Earth-Science Reviews* 193: 91–108. https://doi.org/10.1016/j.earscirev.2019.03.021.

Bohorquez P, Jimenez-Ruiz PJ, and Carling PA (2019b) Revisiting the dynamics of catastrophic late Pleistocene glacial-lake drainage, Altai Mountains, central Asia. *Earth-Science Reviews* 200: 102892. https://doi.org/10.1016/j.earscirev.2019.102892.

Bolch T, Peters J, Yegorov A, Pradhan B, Buchroithner M, and Blagoveshchensky V (2011) Identification of potentially dangerous glacial lakes in the northern Tien Shan. *Natural Hazards* 59: 1691–1714. https://doi.org/10.1007/s11069-011-9860-2.

Boner FC and Stermitz F (1967) *Floods of June 1964 in Northwestern Montana*. U.S. Geological Survey Water-Supply Paper 1840-B, 242.

Bovis MJ and Jakob M (2000) The July 29, 1998 debris flow and landslide dam at Capricorn Creek, Mount Meager volcanic complex, southern Coast Mountains, British Columbia. *Canadian Journal of Earth Sciences* 27: 1321–1334.

Breien H, De Blasio FV, Elverhøi A, and Høeg K (2008) Erosion and morphology of a debris flow caused by a glacial lake outburst flood, Western Norway. *Landslides* 5: 271–280. https://doi.org/10.1007/s10346-008-0118-3.

Bretz JH (1923a) The Channeled Scabland of the Columbia Plateau. *Journal of Geology* 31: 617–649.

Bretz JH (1923b) Glacial drainage on the Columbia plateau. *Geological Society of America Bulletin* 34(573–608). https://doi.org/10.1130/GSAB-34-573.

Bretz JH (1924) The Dalles type of river channel. *Journal of Geology* 32: 139–149.

Bretz JH (1928) Bars of the Channeled Scabland [Washington]. *Geological Society of America Bulletin* 39: 643–701.

Bretz JH (1932) *The Grand Coulee*. American Geographical Society Special Publication No. 15: Washington, DC, 89.

Brückner H and Engel M (2020) Noah's Flood—Probing an ancient narrative using Geoscience. In: Herget J and Fontana A (eds.) *Palaeohydrology: Geography of the Physical Environment*. Cham: Springerhttps://doi.org/10.1007/978-3-030-23315-0_7.

Brunner GW (2014) *Using HEC-RAS for Dam Break Studies*. Davis, CA: U.S. Army Corps of Engineers Hydrologic Engineering Center.74. https://www.hec.usace.army.mil/publications/TrainingDocuments/TD-39.pdf.

Brunner GW (2016) *HEC-RAS River Analysis System 2D Modeling User's Manual*. Davis, CA: US Army Corps of Engineers Hydrologic Engineering Center.171. https://www.hec.usace.army.mil/software/hec-ras/documentation/HEC-RAS%205.0%202D%20Modeling%20Users%20Manual.pdf.

Burr DM (2010) Palaeoflood-generating mechanisms on Earth, Mars, and Titan. *Global and Planetary Change* 70: 5–13. https://doi.org/10.1016/j.gloplacha.2009.11.003.

Burr DM, Grier JA, McEwen AS, and Keszthelyi LP (2002a) Repeated aqueous flooding from the Cerberus Fossae: Evidence for very recently extant, deep groundwater on Mars. *Icarus* 159: 53–73. https://doi.org/10.1006/icar.2002.6921.

Burr DM, McEwen AS, and Sakimoto SEH (2002b) Recent aqueous floods from the Cerberus Fossae, Mars. *Geophysical Research Letters* 29: 13-1–13-4. https://doi.org/10.1029/2001GL013345.

Burr DM, Wilson L, and Bargery AS (2009) Floods from fossae: A review of Amazonian-aged extensional-tectonic megaflood channels on Mars. In: Burr DM, Carling PA, and Baker VR (eds.) *Megaflooding on Earth and Mars*, pp. 194–208. Cambridge: Cambridge University Press.

Butler DR and Malanson GP (2005) The geomorphic influences of beaver dams and failures of beaver dams. *Geomorphology* 71: 48–60.

Capart H (2013) Analytical solutions for gradual dam breaching and downstream river flooding. *Water Resources Research* 49: 1968–1987. https://doi.org/10.1002/wrcr.20167.

Capra L (2007) Volcanic natural dams: Identification, stability, and secondary effects. *Natural Hazards* 43: 45–61.

Capra L (2011) Volcanic natural dams associated with sector collapses: Textural and sedimentological constraints on their stability. In: Evans S, Hermanns R, Strom A, and Scarascia-Mugnozza G (eds.) *Natural and Artificial Rockslide Dams*. vol. 133, pp. 279–294. Springer Lecture Notes in Earth Sciences. https://doi.org/10.1007/978-3-642-04764-0_9.

Capra L and Macías JL (2002) The cohesive Naranjo debris-flow deposit (10 km^3): A dam breakout flow derived from the Pleistocene debris-avalanche deposit of Nevado de Colima Volcano (México). *Journal of Volcanology and Geothermal Research* 117: 213–235.

Carey M (2005) Living and dying with glaciers: People's historical vulnerability to avalanches and outburst floods in Peru. *Global and Planetary Change* 47: 122–134. https://doi.org/10.1016/j.gloplacha.2004.10.007.

Carling PA (1996) Morphology, sedimentology and palaeohydraulic significance of large gravel dunes, Altai Mountains, Siberia. *Sedimentology* 43: 647–664.

Carling PA (2013) Freshwater megaflood sedimentation: What can we learn about generic processes? *Earth-Science Reviews* 125: 87–113. https://doi.org/10.1016/j.earscirev.2013.06.002.

Carling PA and Fan X (2020) Particle comminution defines megaflood and superflood energetics. *Earth-Science Reviews* 204: 103087. https://doi.org/10.1016/j.earscirev.2020.103087.

Carling PA and Glaister MS (1987) Reconstruction of a flood resulting from a moraine-dam failure using geomorphological evidence and dam-break modeling. In: Mayer L and Nash D (eds.) *Catastrophic Flooding*, pp. 181–200. Boston, MA: Allen and Unwin.

Carling PA, Hoffmann M, and Blatter AS (2002) Initial motion of boulders in bedrock channels. In: House PK, Webb RH, Baker VR, and Levish DR (eds.) *Ancient Floods, Modern Hazards: Principles and Applications of Paleoflood Hydrology*. vol. 5, pp. 147–160. American Geophysical Union Water Science and Applications.

Carling PA, Kidson R, Cao Z, and Herget J (2003) Palaeohydraulics of extreme flood events; reality and myth. In: Gregory K and Benito G (eds.) *Palaeohydrology: Understanding Global Change*, pp. 325–336. Chichester: Wiley.

Carling PA, Burr DM, Johnsen TF, and Brennand TA (2009a) A review of open-channel megflood depositional landforms on Earth and Mars. In: Burr DM, Carling PA, and Baker VR (eds.) *Megaflooding on Earth and Mars*, pp. 33–49. Cambridge: Cambridge University Press.

Carling PA, Martini P, Herget J, Borodavko P, and Parnachov S (2009b) Megaflood sedimentary valley fill: Altai Mounatins, Siberia. In: Burr DM, Carling PA, and Baker VR (eds.) *Megaflooding on Earth and Mars*, pp. 243–264. Cambridge: Cambridge University Press.

Carling PA, Perillo M, Best J, and Garcia MH (2017) The bubble bursts for cavitation in natural rivers: Laboratory experiments reveal minor role in bedrock erosion. *Earth Surface Processes and Landforms* 42: 1308–1316. https://doi.org/10.1002/esp.4101.

Carr MH (1979) Formation of Martian flood features by release of water from confined aquifers. *Journal of Geophysical Research* 84: 2995–3007.

Carrivick JL (2006) Application of 2D hydrodynamic modelling to high-magnitude outburst floods: An example from Kverkfjöll, Iceland. *Journal of Hydrology* 321: 187–199. https://doi.org/10.1016/j.jhydrol.2005.07.042.

Carrivick JL (2007) Hydrodynamics and geomorphic work of jökulhlaups (glacial outburst floods) from Kverkfjöll volcano, Iceland. *Hydrological Processes* 21: 725–740. https://doi.org/10.1002/hyp.6248.

Carrivick JL (2009) Jökulhlaups from Kverkfjöll volcano, Iceland: Modelling transient hydraulic phenomena. In: Burr DM, Carling PA, and Baker VR (eds.) *Megaflooding on Earth and Mars*, pp. 273–289. United Kingdom: Cambridge University Press.

Carrivick JL (2010) Dam break—Outburst flood propagation and transient hydraulics: A geosciences perspective. *Journal of Hydrology* 380: 338–355. https://doi.org/10.1016/j.jhydrol.2009.11.009.

Carrivick JL and Rushmer EL (2006) Understanding high-magnitude outburst floods. *Geology Today* 22: 60–65.

Carrivick JL and Tweed FS (2013) Proglacial lakes: Character, behaviour and geological importance. *Quaternary Science Reviews* 78: 34–52. https://doi.org/10.1016/j.quascirev.2013.07.028.

Carrivick JL and Tweed FS (2016) A global assessment of the societal impacts of glacier outburst floods. *Global and Planetary Change* 144: 1–16. https://doi.org/10.1016/j.gloplacha.2016.07.001.

Carrivick JL and Tweed FS (2019) A review of glacier outburst floods in Iceland and Greenland with a megafloods perspective. *Earth-Science Reviews* 196: 102876. https://doi.org/10.1016/j.earscirev.2019.102876.

Carrivick JL, Russell AJ, Tweed FS, and Twigg D (2004) Palaeohydrology and sedimentary impacts of jökulhlaups from Kverkfjöll, Iceland. *Sedimentary Geology* 172: 19–40.

Carrivick JL, Manville V, Graettinger A, and Cronin SJ (2010) Coupled fluid dynamics-sediment transport modelling of a Crater Lake break-out lahar: Mt. Ruapehu, New Zealand. *Journal of Hydrology* 388: 399–413. https://doi.org/10.1016/j.jhydrol.2010.05.023.

Carrivick JL, Turner AGD, Russell AJ, Ingeman-Nielsen T, and Yde JC (2013) Outburst flood evolution at Russell Glacier, western Greenland: Effects of a bedrock channel cascade with intermediary lakes. *Quaternary Science Reviews* 67: 39–58. https://doi.org/10.1016/j.quascirev.2013.01.023.

Carrivick JL, Tweed FS, Ng F, Quincey DJ, Mallalieu J, Ingeman-Nielsen T, Mikkelsen AB, Palmer SJ, Yde JC, Homer R, Russell AJ, and Hubbard A (2017) Ice-dammed lake drainage evolution at Russell Glacier, West Greenland. *Frontiers in Earth Science* 5. https://doi.org/10.3389/feart.2017.00100.

Carter DT, Ely LL, O'Connor JE, and Fenton CR (2006) Late Pleistocene outburst flooding from pluvial Lake Alvord into the Owyhee River, Oregon. *Geomorphology* 75: 346–367.

Casagli N, Ermini L, and Rosati G (2003) Determining grain size distribution of the material composing landslide dams in the Northern Apennines: Sampling and processing methods. *Engineering Geology* 69: 83–97.

Cassanelli JP and Head JW (2018) Formation of outflow channels on Mars: Testing the origin of Reull Vallis in Hesperia Planum by large-scale lava-ice interactions and top-down melting. *Icarus* 305: 56–79. https://doi.org/10.1016/j.icarus.2018.01.001.

Cencetti C, Fredduzzi A, Marchesini I, Naccini M, and Tacconi P (2006) Some considerations about the simulation of breach channel erosion on landslide dams. *Computational Geosciences* 10(2): 201–219.

Cenderelli DA (2000) Floods from natural and artificial dam failures. In: Wohl EE (ed.) *Inland Flood Hazards: Human Riparian, and Aquatic Communities*, pp. 73–103. New York: Cambridge University Press.

Cenderelli DA and Wohl EE (1998) Sedimentology and clast orientation of deposits produced by glacial-lake outburst floods in the Mount Everest region, Nepal. In: Kalvoda J and Rosenfield CL (eds.) *Geomorphological Hazards in High Mountain Areas*, pp. 1–26. Dordrecht: Kluwer Academic Publishers.

Cenderelli DA and Wohl EE (2003) Flow hydraulics and geomorphic effects of glacial-lake outburst floods in the Mount Everest region, Nepal. *Earth Surface Processes and Landforms* 28: 385–407.

Chai HJ, Liu HC, Zhang ZY, and Wu ZW (2000) The distribution, causes and effects of damming landslides in China. *Journal of the Chengdu Institute of Technology* 27: 1–19.

Chapman MG, Gudmundsson MT, Russell AJ, and Hare TM (2003) Possible Juventae Chasma sub-ice volcanic eruptions and Maja Valles ice outburst floods on Mars: Implications of Mars Global Surveyor crater densities, geomorphology, and topography. *Journal of Geophysical Research, Planets* 108. https://doi.org/10.1029/2002JE002009. 5113.

Chesner CA and Rose WI (1991) Stratigraphy of the Toba Tuffs and the evolution of the Toba Caldera Complex, Sumatra, Indonesia. *Bulletin of Volcanology* 53: 343–356.

Chitwood LA and Jensen RA (2000) Large prehistoric flood along Paulina Creek, Newberry Volcano, Oregon. In: Jensen RA and Chitwood LA (eds.) *What's New at Newberry Volcano, Oregon*, pp. 31–40. Bend, Oregon: U.S. Department of Agriculture Forest Service.

Clague JJ and Evans SG (1992) *A Self-Arresting Moraine Dam Failure, St. Elias Mountains, British Columbia*. Current Research, Part A. Geological Survey of Canada Paper 92-1A 185–188.

Clague JJ and Evans SG (1994) Formation and failure of natural dams in the Canadian Cordillera. *Geological Survey of Canada Bulletin* 464: 35.

Clague JJ and Evans SG (1997) The 1994 jökulhlaup at Farrow Creek, British Columbia, Canada. *Geomorphology* 19: 77–87.

Clague JJ and Evans SG (2000) A review of catastrophic drainage of moraine-dammed lakes in British Columbia. *Quaternary Science Reviews* 19: 1763–1783.

Clague JJ and Mathews WH (1973) The magnitude of jökulhlaups. *Journal of Glaciology* 12: 501–504.

Clague JJ and O'Connor JE (2020) Glacier-related outburst floods. In: Haeberli W and Whiteman C (eds.) *Snow and Ice-related Hazards, Risks, and Disasters*. Amsterdam: Elsevier.

Clague JJ, Evans SG, and Blown IG (1985) A debris flow triggered by the breaching of a moraine-dammed lake, Klattasine Creek, British Columbia. *Canadian Journal of Earth Sciences* 22: 1492–1502.

Clarke GKC (1982) Glacier outburst floods from "Hazard Lake", Yukon Territory, and the problem of flood magnitude prediction. *Journal of Glaciology* 28: 3–21.

Clarke GKC (2003) Hydraulics of subglacial outburst floods: New insights from the Spring–Hutter formulation. *Journal of Glaciology* 49: 299–313.

Clarke GKC, Leverington DW, Teller JT, and Dyke AS (2004) Paleohydraulics of the last outburst flood from glacial Lake Agassiz and the 8200 BP cold event. *Quaternary Science Reviews* 23: 389–407.

Clarke GKC, Leverington DW, Teller JT, Dyke AS, and Marshall SJ (2005) Fresh arguments against the Shaw megaflood hypothesis. A reply to comments by David Sharpe on 'Paleohydraulics of the last outburst flood from glacial Lake Agassiz and the 8200 BP cold event'. *Quaternary Science Reviews* 24: 1533–1541.

Coleman NM (2013) Hydrographs of a Martian flood from a breached crater lake, with insights about flow calculations, channel erosion rates, and chasma growth. *Journal of Geophysical Research, Planets* 118: 263–277. https://doi.org/10.1029/2012JE004193.

Coleman NM (2015) Hydrographs of a Martian flood from the breach of Galilaei crater. *Geomorphology* 236: 90–108. https://doi.org/10.1016/j.geomorph.2015.01.034.

Coleman NM (2019) *Johnstown's Flood of 1889, Power Over Truth and the Science Behind the Disaster*. Springer. https://doi.org/10.1007/978-3-319-95216-1.

Coleman NM and Baker VR (2009) Surface morphology and origin of outflow channels in the Valles Marineris region. In: Burr DM, Carling PA, and Baker VR (eds.) *Megaflooding on Earth and Mars*, pp. 172–193. United Kingdom: Cambridge University Press.

Coleman SE, Andrews DP, and Webby MG (2002) Overtopping breaching of noncohesive homogeneous embankments. *Journal of Hydraulic Engineering* 128: 829–838.

Colhoun EA, Commonr R, and Cruickshank MM (1965) Recent bog flows and debris slides in the north of Ireland. *Scientific Proceedings of Royal Dublin Society, Series* A2(1): 163–174.

Conaway JS (1999) *Hydrogeology and Paleohydrology of the Williamson River Basin, Klamath County, Oregon*. Unpublished M.S. thesis Portland, Oregon: Portland State University.

Condron A and Winsor P (2012) Meltwater routing and the Younger Dryas. *Proceedings of the National Academy of Sciences* 109: 19928–19933. https://doi.org/10.1073/pnas.1207381109.

Cook KL, Andermann C, Gimbert F, Adhikari BR, and Hovius N (2018) Glacial lake outburst floods as drivers of fluvial erosion in the Himalaya. *Science* 362: 53–57. https://doi.org/10.1126/science.aat4981.

Costa JE (1983) Paleohydraulic reconstruction of flash-flood peaks from boulder deposits in the Colorado Front Range. *Geological Society of America Bulletin* 94: 986–1004.

Costa JE (1984) Physical geomorphology of debris flows. In: Costa JE and Fleisher PJ (eds.) *Developments and Applications of Geomorphology*, pp. 268–317. Berlin: Springer-Verlag.

Costa JE (1988) Floods from dam failures. In: Baker VR, Kochel RC, and Patton PC (eds.) *Flood Geomorphology*, pp. 439–469. New York: John Wiley and Sons.

Costa JE (1991) Nature, mechanics, and mitigation of the Val Pola Landslide, Valtellina, Italy, 1987–1988. *Zeitschrift für Geomorphologie* 35: 15–38.

Costa JE and O'Connor JE (1995) Geomorphically effective floods. In: Costa JE, Miller AJ, Potter DW, and Wilcock PR (eds.) *Natural and Anthropogenic Influences in Fluvial Geomorphology*, *American Geophysical Union Monograph*, vol. 89, 45–56.

Costa JE and Schuster RL (1988) The formation and failure of natural dams. *Geological Society of America Bulletin* 100: 1054–1068.

Costa JE and Schuster RL (1991) *Documented Historical Landslide Dams from Around the World*. U.S. Geological Survey Open-File Report 91-239, 490.

Costard F and Gautier E (2007) The Lena River: Hydromorphodynamic features in a deep permafrost zone. In: Gupta A (ed.) *Geomorphology and Management*, pp. 225–233. New York: John Wiley.

Cotton CA (1965) Antarctic scablands. *New Zealand Journal of Geology and Geophysics* 9: 130–132. https://doi.org/10.1080/00288306.1966.10420202.

Craddock W, Kirby E, Harkins N, Zhang H, Shi X, and Liu J (2010) Rapid fluvial incision along the Yellow River during headward basin integration. *Nature Geoscience* 3: 209–213. https://doi.org/10.1038/ngeo777.

Crow R, Karlstrom KE, Mcintosh W, Peters L, and Dunbar N (2008) History of Quaternary volcanism and lava dams in western Grand Canyon based on lidar analysis, 40Ar/39Ar dating, and field studies: Implications for flow stratigraphy, timing of volcanic events, and lava dams. *Geosphere* 4: 183–206.

Cummings ML and Conaway JS (2009) Landscape and hydrologic response in the Williamson River basin following the Holocene eruption of Mount Mazama, Cascade volcanic arc. In: O'Connor JE, Dorsey RJ, and Madin I (eds.) *Volcanoes to Vineyards: Geologic Field Trips Through the Dynamic Landscapes of the Pacific Northwest*, pp. 271–294. Boulder, CO: Geological Society of America.

Currey DR (1990) Quaternary palaeolakes in the evolution of semidesert basins, with special emphasis on Lake Bonneville and the Great Basin, U.S.A. *Palaeogeography, Palaeoclimatology, Palaeoecology* 76: 189–214.

Dai FC, Lee CF, Deng JH, and Tham LG (2005) The 1786 earthquake-triggered landslide dam and subsequent dam-break flood on the Dadu River, southwestern China. *Geomorphology* 65: 205–221.

Davies TR, Manville V, Kunz M, and Donadidni L (2007) Modeling landslide dambreak flood magnitudes: Case study. *Journal of Hydraulic Engineering* 133: 713–720.

Davis SN and Karzulovíc J (1963) Landslides at Lago Riñihue. *Bulletin of the Seismological Society of America* 53: 1403–1414.

De Lorenzo G and Macchione F (2014) Formulas for the peak discharge from breached earthfill dams. *Journal of Hydraulic Engineering* 140: 56–57. https://doi.org/10.1061/(ASCE)HY.1943-7900.0000796.

Delaney KB and Evans SG (2011) Rockslide dams in the northwest Himalayas (Pakistan, India) and the adjacent Pamir Mountains (Afghanistan, Tajikistan), Central Asia. In: Evans S, Hermanns R, Strom A, and Scarascia-Mugnozza G (eds.) *Natural and Artificial Rockslide Dams*, *Springer Lecture Notes in Earth Sciences*, vol. 133, 205–242. https://doi.org/10.1007/978-3-642-04764-0_7.

Delaney KB and Evans SG (2015) The 2000 Yigong landslide (Tibetan Plateau), rockslide-dammed lake and outburst flood: Review, remote sensing analysis, and process modelling. *Geomorphology* 246: 377–393. https://doi.org/10.1016/j.geomorph.2015.06.020.

Delcamp A, Roberti G, and van Wyk de Vries B (2016) Water in volcanoes: Evolution, storage and rapid release during landslides. *Bulletin of Volcanology* 78: 87. https://doi.org/10.1007/s00445-016-1082-8.

Denlinger RP and O'Connell DRH (2010) Simulations of cataclysmic outburst floods from Pleistocene Glacial Lake Missoula. *Geological Society of America Bulletin* 122: 678–689.

Denlinger RP, George DL, Cannon C, O'Connor J, and Waitt RB (2020) *Diverse Cataclysmic Floods From Pleistocene Glacial Lake Missoula*. Geological Society of America Special Paper 548.

Depetris PJ and Pasquini AI (2000) The hydrological signal of the Perito Moreno Glacier damming of Lake Argentino (southern Andean Patagonia): The connection to climate anomalies. *Global and Planetary Change* 26: 367–374.

Ding Y and Liu J (1992) Glacier lake outburst flood disasters in China. *Annals of Glaciology* 16: 180–184.

Dixit A (2003) Floods and vulnerability: Need to rethink flood management. *Natural Hazards* 28: 155–179. https://doi.org/10.1023/A:1021134218121.

Dohm JM, Anderson RC, Baker VR, Ferris JC, Hare TM, Strom RG, Rudd LP, Rice JW, Casavant RR, and Scott DH (2000) System of gigantic valleys northwest of Tharsis Montes, Mars: Latent catastrophic flooding, northwest watershed, and implications for northern plains ocean. *Geophysical Research Letters* 27: 3559–3562.

Donnelly-Nolan JM and Nolan KM (1986) Catastrophic flooding and eruption of ash-flow tuff at Medicine Lake volcano, California. *Geology* 14: 875–878.

Driedger CL and Fountain AG (1989) Glacier outburst floods at Mount Rainier, Washington State, U.S.A. *Annals of Glaciology* 13: 51–55.

Duffield W, Riggs N, Kaufman D, Champion D, Fenton C, Forman S, Mcintosh W, Hereford R, Plescia J, and Ort M (2006) Multiple constraints on the age of a Pleistocene lava dam across the Little Colorado River at Grand Falls, Arizona. *Geological Society of America Bulletin* 118: 421–429.

Dunning SA, Petley DN, and Strom AL (2005) The morphologies and sedimentology of valley confined rock-avalanche deposits and their effect on potential dam hazard. In: Hungr O, Fell R, Couture R, and Eberhardt E (eds.) *Proceedings of the International Conference on Landslide Risk Management*, pp. 691–704. London: Balkema.

Dunning SA, Large ARG, Russell AJ, Roberts MJ, Duller R, Woodward J, Mériaux A-S, Tweed FS, and Lim M (2013) The role of multiple glacier outburst floods in proglacial landscape evolution: The 2010 Eyjafjallajökull eruption, Iceland. *Geology* 41: 1123–1126. https://doi.org/10.1130/G34665.1.

Dussaillant A, Benito G, Buytaert W, Carling P, Meier C, and Espinoza F (2010) Repeated glacial-lake outburst floods in Patagonia: An increasing hazard? *Natural Hazards* 54: 469–481.

Dwivedi SK, Archarya MD, and Simard D (2000) The Tam Pokhari Glacier Lake outburst flood of 3 September 1998. *Journal of Nepal Geological Society* 22: 539–546.

Dyer W (1886) Peat floods in the Falklands. *Nature* 34: 440–441. https://doi.org/10.1038/034440a0.

Eghbali AH, Behzadian K, Hooshyaripor F, Farmani R, and Duncan AP (2017) Improving prediction of dam failure peak outflow using neuroevolution combined with K-means clustering. *Journal of Hydrologic Engineering* 22. https://doi.org/10.1061/(ASCE)HE.1943-5584.0001505.

Eisbacher GH and Clague JJ (1984) *Destructive Mass Movements in High Mountains—Hazard and Management*. Canada: Geological Survey of Canada Paper 84-16 230.

Ely LL, Brossy CC, House PK, Safran EB, O'Connor JE, Champion DE, Fenton CR, Bondre NR, Orem CA, Grant GE, Henry CD, and Turrin BD (2012) Owyhee River intracanyon lava flows: Does the river give a dam? *Geological Society of America Bulletin* 124: 1667–1687. https://doi.org/10.1130/B30574.1.

Emmer A (2017) Geomorphologically effective floods from moraine-dammed lakes in the Cordillera Blanca, Peru. *Quaternary Science Reviews* 177: 220–234. https://doi.org/10.1016/j.quascirev.2017.10.028.

Emmer A (2018) GLOFs in the WOS: Bibliometrics, geographies and global trends of research on glacial lake outburst floods (Web of Science, 1979–2016). *Natural Hazards and Earth System Sciences* 18: 813–827. https://doi.org/10.5194/nhess-18-813-2018.

Emmer A and Vilimek V (2014) New method for assessing the potential hazardousness of glacial lakes in the Cordillera Blanca, Peru. *Hydrology and Earth System Sciences* 11: 3461–3479. https://doi.org/10.5194/hess-18-3461-2014.

Emmer A, Merkl S, and Mergili M (2015) Spatio-temporal patterns of high-mountain lakes and related hazards in western Austria. *Geomorphology* 246: 602–616. https://doi.org/10.1016/j.geomorph.2015.06.032.

Emmer A, Klimeš J, Mergili M, Vilímek V, and Cochachin A (2016a) 882 lakes of the Cordillera Blanca: An inventory, classification, evolution and assessment of susceptibility to outburst floods. *Catena* 147: 269–279. https://doi.org/10.1016/j.catena.2016.07.032.

Emmer A, Vilímek V, Huggel C, Klimeš J, and Schaub Y (2016b) Limits and challenges to compiling and developing a database of glacial lake outburst floods. *Landslides* 13: 1579–1584. https://doi.org/10.1007/s10346-016-0686-6.

Emmer A, Harrison S, Mergili M, Allen S, Frey H, and Huggel C (2020) 70 years of lake evolution and glacial lake outburst floods in the Cordillera Blanca (Peru) and implications for the future. *Geomorphology*. , 107178. https://doi.org/10.1016/j.geomorph.2020.107178.

Ermini L and Casagli N (2003) Prediction of the behaviour of landslide dams using a geomorphological dimensionless index. *Earth Surface Processes and Landforms* 28: 31–47. https://doi.org/10.1002/esp.424.

Erokhin SA, Zaginaev VV, Meleshko AA, Ruiz-Villanueva V, Petrakov DA, Chernomorets SS, Viskhadzhieva KS, Tutubalina OV, and Stoffel M (2018) Debris flows triggered from non-stationary glacier lake outbursts: The case of the Teztor Lake complex (northern Tian Shan, Kyrgyzstan). *Landslides* 15: 83–98. https://doi.org/10.1007/s10346-017-0862-3.

Evans SG (1986) The maximum discharge of outburst floods caused by the breaching of man-made and natural dams. *Canadian Geotechnical Journal* 23: 385–387.

Evans SG and Clague JJ (1994) Recent climatic change and catastrophic geomorphic processes in mountain environments. *Geomorphology* 10: 107–128.

Evans SG, Delaney KB, Hermanns RL, Strom A, and Scarascia-Mugnozza G (2011) The formation and behaviour of natural and artificial rockslide Dams: Implications for engineering performance and hazard management. In: Evans S, Hermanns R, Strom A, and Scarascia-Mugnozza G (eds.) *Natural and Artificial Rockslide Dams*, *Springer Lecture Notes in Earth Sciences*, vol. 133, 1–75. https://doi.org/10.1007/978-3-642-04764-0_1.

Falatkova K, Šobr M, Neureiter A, Schöner W, Jansky B, Häusler H, Engel Z, and Beneš V (2019) Development of proglacial lakes and evaluation of related out-burst susceptibility at the Adygine ice-debris complex, northern Tien Shan. *Earth Surface Dynamics Discussions* 7: 301–320. https://doi.org/10.5194/esurf-7-301-2019.

Fan X, Van Westen CJ, Korup O, Gorum T, Xu Q, Dai F, Huang R, and Wang G (2012) Transient water and sediment storage of the decaying landslide dams induced by the 2008 Wenchuan earthquake, China. *Geomorphology* 171–172: 58–68. https://doi.org/10.1016/j.geomorph.2012.05.003.

Fan X, Xu Q, van Westen CJ, Huang R, and Tang R (2017) Characteristics and classification of landslide dams associated with the 2008 Wenchuan earthquake. *Geoenvironmental Disasters* 4: 12. https://doi.org/10.1186/s40677-017-0079-8.

Fan X, Scaringi G, Korup O, West AJ, Van Westen CJ, Tanyas H, Hovius N, Hales TC, Jibson RW, Allstadt KE, Zhang L, Evans SG, Xu C, Li G, Pei X, Xu Q, and Huang R (2019) Earthquake-induced chains of geologic hazards: Patterns, mechanisms, and impacts. *Reviews of Geophysics* 57: 421–503. https://doi.org/10.1029/2018RG000626.

Fan X, Dufresne A, Subramanian SS, Storm A, Hermanns R, Tacconi-Stefanelli C, Hewitt K, Yunus AP, Dunning S, Capra L, Geertsema M, Miller B, Casagli N, Jansen JD, and Xu Q (2020) The formation and impact of landslide dams—State of the art. *Earth-Science Reviews* 203: 103116. https://doi.org/10.1016/j.earscirev.2020.103116.

Fenton CR, Webb RH, Cerling TE, Poreda RJ, and Nash BP (2002) Cosmogenic 3He ages and geochemical discrimination of lava-dam outburst-flood deposits in western Grand Canyon, Arizona. In: House PK, Webb RH, and Levish DR (eds.) *Ancient Floods, Modern Hazards, Principles and Applications of Paleoflood Hydrology*, *American Geophysical Union Water Science and Application Series*, vol. 4, 191–215.

Fenton CR, Poreda RJ, Nash BP, Webb RH, and Cerling TE (2004) Geochemical discrimination of five Pleistocene lava-dam outburst-flood deposits, Grand Canyon. *Journal of Geology* 112: 91–110.

Fenton CR, Webb RH, and Cerling TE (2006) Peak discharge of a Pleistocene lava-dam outburst flood in Grand Canyon, Arizona, USA. *Quaternary Research* 65: 324–335.

Flowers GE, Björnsson H, Pálsson F, and Clarke GKC (2004) A coupled sheet-conduit mechanism for jökulhlaup propagation. *Geophysical Research Letters* 31: L05401.

Foley MM, Bellmore JR, O'Connor JE, Duda JJ, East AE, Grant GE, Anderson CW, Bountry JA, Collins MJ, Connolly PJ, Craig LS, Evans JE, Greene SL, Magilligan FJ, Magirl CS, Major JJ, Pess GR, Randle TJ, Shafroth PB, Torgersen CE, Tullos D, and Wilcox AC (2017) Dam removal: Listening in. *Water Resources Research* 53: 5229–5246. https://doi.org/10.1002/2017WR020457.

Fowler AC (1999) Breaking the seal at Grı´msvötn. *Journal of Glaciology* 45: 506–516.

Fread DL (1988) *The NWS DAMBRK model: Theoretical Background and User Documentation*. U.S. National Oceanic and Atmospheric Administration, Hydrologic Research Laboratory HRL-258 325.

Fread DL (1991) *BREACH: An Erosion Model for Earthen Dam Failures*. Maryland: U.S. National Weather Service, U.S. National Oceanic and Atmospheric Administration, Hydrologic Research Laboratory, Silver Springs35.

Fread DL (1993) NWS FLDWAV Model: The Replacement of DAMBRK for Dam-Break Flood Prediction. In: *Proceedings 10th Annual Conference of the Association of State Dam Safety Officials, Kansas City, Missouri* 177–184.

Fricker HA, Scambos T, Bindschadler R, and Padman L (2007) An active subglacial water system in West Antarctica mapped from space. *Science* 315: 1544–1548.

Froehlich DC (1987) Embankment-dam breach parameters. In: *Proceedings 1987 National Conference on Hydraulic Engineering. American Society of Civil Engineers, New York* 570–575.

Froehlich DC (1995) Peak outflow from breached embankment dam. *Journal of Water Resources Planning and Management* 121: 90–97.

Froehlich DC (2008) Embankment dam breach parameters and their uncertainties. *Journal of Hydraulic Engineering* 134: 1708–1721.

Froehlich DC (2016) Predicting peak discharge from gradually breached embankment dam. *Journal of Hydrologic Engineering* 21, 04016041. https://doi.org/10.1061/(ASCE)HE.1943-5584.0001424.

Fujita K, Sakai A, Takenaka S, Nuimura T, Surazakov AB, Sawagaki T, and Yamanokuchi T (2013) Potential flood volume of Himalayan glacial lakes. *Natural Hazards and Earth System Sciences* 13: 1827–1839. https://doi.org/10.5194/nhess-13-1827-2013.

Gallino GL and Pierson TC (1985) *Polallie Creek debris flow and subsequent dam-break flood of 1980, East Fork Hood River basin, Oregon*. U.S. Geological Survey Water Supply Paper 2273 22.

Garcia-Castellanos D and O'Connor JE (2018) Outburst floods provide erodability estimates consitent with long-term landscape evolution. *Scientific Reports* 8: 10573. https://doi.org/10.1038/s41598-018-28981-y.

Garcia-Castellanos D, Estrada F, Jiménez-Munt I, Gorini C, Fernàndez M, Vergés J, and De Vicente R (2009) Catastrophic flood of the Mediterranean after the Messinian salinity crisis. *Nature* 462(7274): 778–781.

Garcia-Castellanos D, Micallef A, Estrada F, Camerlenghi A, Ercilla G, Periáñez R, and Abril-Hernández JM (2020) The Zanclean megaflood of the Mediterranean—Searching for additional evidence. *Earth-Science Reviews* 201: 103061. https://doi.org/10.1016/j.earscirev.2019.103061.

George DL (2011) Adaptive finite volume methods with well-balanced Riemann solvers for modeling floods in rugged terrain: Application to the Malpasset dam-break flood (France, 1959). *International Journal for Numerical Methods in Fluids* 66: 1000–1018. https://doi.org/10.1002/fld.2298.

Gerasimov VA (1965) *Issykskaia katastrofa 1963 g. i otrazhenie ee in geomorfoogii doliny r. Issyk [The Issyk catastrophe in 1963 and its effect on geomorphology of the Issyk River valley]*. Akademiia Nauk SSSR, Izvestiia Vsesoiuznogo, Geograficheskogo Obshchestva, 97-6 541–547. [In Russian; senior author in possession of translation].

Ghirotti M (2012) The 1963 Vaiont landslide, Italy. In: Clague JJ and Stead D (eds.) *Landslides: Types, Mechanisms and Modeling*, pp. 359–372. Cambridge: Cambridge University Press.

Gilbert GK (1890) *Lake Bonneville*. U.S. Geological Survey Monograph 1438.
Glancy PA and Bell JW (2000) *Landslide-Induced Flooding at Ophir Creek, Washoe County, Western Nevada, May 30, 1983*. U.S. Geological Survey Professional Paper 1617 94.
Glen JW (1954) The stability of ice-dammed lakes and other waterfilled holes in glaciers. *Journal of Glaciology* 2: 316–318.
Gordon AD (1990) Coastal lagoon entrance dynamics. In: *22nd International Conference on Coastal Engineering, July 2–6,* 1990, Delft, Netherlands. https://doi.org/10.1061/9780872627765.220.
Goudge TA and Fassett CI (2018) Incision of Licus Vallis, Mars from multiple Lake overflow floods. *Journal of Geophysical Research, Planets* 123: 405–420. https://doi.org/10.1002/2017JE005438.
Goudge TA, Fassett CI, Head JW, Mustard JF, and Aureli KL (2016) Insights into surface runoff on early Mars from paleolake basin morphology and stratigraphy. *Geology* 44: 419–422. https://doi.org/10.1130/G37734.1.
Goudge TA, Fassett CI, and Mohrig D (2018) Incision of paleolake outlet canyons on Mars from overflow flooding. *Geology* 47: 1–4. https://doi.org/10.1130/G45397.1.
Graettinger AH, Manville V, and Briggs RM (2010) Depositional record of historic lahars in the upper Whangaehu Valley, Mt. Ruapehu, New Zealand: Implications for trigger mechanisms, flow dynamics and lahar hazards. *Bulletin of Volcanology* 72: 279–296. https://doi/org/10.1007/s00445-009-0318-2.
Grinsted A, Hvidberg CS, Campos N, and Dahl-Jense D (2017) Periodic outburst floods from an ice-dammed lake in East Greenland. *Scientific Reports* 7: 9966. https://doi.org/10.1038/s41598-017-07960-9.
Grosswald MG (1980) Late Weichselian ice sheet of northern Eurasia. *Quaternary Research* 13: 1–32.
Gupta S, Collier JS, Palmer-Felgate A, and Potter G (2007) Catastrophic flooding origin of shelf valley systems in the English Channel. *Nature* 448: 342–345. https://doi.org/10.1038/nature06018.
Gupta S, Collier JS, Garcia-Moreno D, Oggioni F, Trentesaux A, Vanneste K, DeBatst M, Camelbeeck T, Potter G, van Vliet-Lanoe B, and Arthur JCR (2017) Two-stage opening of the Dover Strait and the origin of island Britain. *Nature Communications* 8: 15101. https://doi.org/10.1038/ncomms15101.
Gurnell AM (1998) The hydrogeomorphic effects of beaver dam-building activity. *Progress in Physical Geography* 22: 167–189.
Gurung DR, Khanal NR, Bajracharya SR, Tsering K, Joshi S, Tshering P, Chhetri LK, Lotay Y, and Penjor T (2017) Lemthang Tsho glacial Lake outburst flood (GLOF) in Bhutan: Cause and impact. *Geoenvironmental Disasters* 4: 17. https://doi.org/10.1186/s40677-017-0080-2.
Guthrie RH, Friele P, Allstadt K, Roberts N, Evans SG, Delaney KB, Roche D, Clague JJ, and Jakob M (2012) The 6 August 2010 Mount Meager rock slide-debris flow, Coast Mountains, British Columbia: Characteristics, dynamics, and implications for hazard and risk assessment. *Natural Hazards and Earth System Sciences* 12: 1277–1294.
Haeberli W (1983) Frequency and characteristics of glacier floods in the Swiss Alps. *Annals of Glaciology* 4: 85–90.
Haeberli W, Kääb A, Vonder D, and Teysseire P (2001) Prevention of outburst floods from periglacial lakes at Grubengletscher, Valais, Swiss Alps. *Journal of Glaciology* 47: 111–122.
Hamblin WK (1994) Late Cenozoic Lava Dams in the Western Grand Canyon. *Geological Society of America Memoirs* 183: 139.
Hancox GT, McSaveney MJ, Manville VR, and Davies TR (2005) The October 1999 Mt. Adams rock avalanche and subsequent landslide dam-break flood and effects in Poerua River, Westland, New Zealand. *New Zealand Journal of Geology and Geophysics* 48: 683–705.
Hanisch J and Söder CO (2000) Geotechnical assessment of the Usoi landslide dam and the right bank of Lake Sarez. In: Alford D and Schuster RL (eds.) *Usoi Landslide Dam and Lake Sarez, An Assessment of Hazard and Risk in the Pamir Mountains, Tajikistan. United Nations International Strategy for Disaster Reduction Prevention Series*, vol. 1, 23–42.
Hanna JC and Phillips RJ (2005) Hydrological modeling of the Martian crust with application to the pressurization of aquifers. *Journal of Geophysical Research, Planets* 110: E01004. https://doi.org/10.1029/2004JE002330.
Hanna JC and Phillips RJ (2006) Tectonic pressurization of aquifers in the formation of Mangala and Athabasca Valles, Mars. *Journal of Geophysical Research, Planets* 111: E03003. https://doi.org/10.1029/2005JE002546.
Hanson GJ, Cook KR, and Hunt SL (2005) Physical modeling of overtopping erosion and breach formation of cohesive embankments. *Transactions of the American Society of Agricultural Engineers* 48: 1783–1794. https://doi.org/10.13031/2013.20012.
Harrison LM, Dunning SA, Woodward J, and Davies TRH (2015) Post-rock-avalanche dam outburst flood sedimentation in Ram Creek, Southern Alps, New Zealand. *Geomorphology* 241: 125–144. https://doi.org/10.1016/j.geomorph.2015.03.038.
Harrison S, Kargel JS, Huggel C, Reynolds J, Shugar DH, Betts RA, Emmer A, Glasser N, Haritashya UK, Klimeš J, Reinhardt L, Schaub Y, Wilyshire A, Regmi D, and Vilímek V (2018) Climate change and the global pattern of moraine-dammed glacial lake outburst floods. *The Cryosphere* 12: 1195–1209. https://doi.org/10.5194/tc-12-1195-2018.
Hartley JA (1981) Stories of our times; Boston's great molasses flood. *Modern Maturity* 24(4): 16–18.
Head JW, Mustard JF, Kreslavsky MA, Milliken RE, and Marchant DR (2003) Recent ice ages on Mars. *Nature* 426(6968): 797–802.
Hejun C, Hanchao L, and Zhuoyuan A (1998) Study on the categories of landslide-damming of rivers and their characteristics. *Journal of the Chengdu Institute of Technology* 25: 411–416.
Hemphill-Haley MA, Lindberg DA, and Reheis MC (1999) Lake Alvord and Lake Coyote: A hypothesized flood. In: Narwold C (ed.) *Quaternary Geology of the Northern Quinn River and Alvord Valleys, Southeastern Oregon*, pp. A21–A27. Arcata, CA: Friends of the Pleistocene Pacific Cell Field Trip Guidebook, Humboldt State University.
Herget J (2005) *Reconstruction of Pleistocene Ice-dammed Lake Outburst Floods in the Altai Mountains, Siberia*. Geological Society of America Special Paper 386, 118.
Herget J and Carling PA (2004) Review on large scale gravel dunes caused by Pleistocene ice-dammed lake outburst floods. In: *Proceedings of Marine Sandwave and River Dune Dynamics, 1 & 2 April 2004, Enschede, The Netherlands* 96–101.
Herget J and Gregori L (2020) Outburst flood from Möhne Reservoir in May 1943 after aerial bombing. In: Herget J and Fontana A (eds.) *Palaeohydrology: Geography of the Physical Environment*. Cham: Springer. https://doi.org/10.1007/978-3-030-23315-0_3.
Herget J, Schűtte F, and Klosterhalfen A (2015) Empirical modelling of outburst flood hydrographs. *Zeitschrift für Geomorphologie* 59: 177–198. https://doi.org/10.1127/zfg_suppl/2015/S-59224.
Herget J, Agatova AR, Carling PA, and Nepop RK (2020) Altai megafloods—The temporal context. *Earth-Science Reviews* 200: 102995. https://doi.org/10.1016/j.earscirev.2019.102995.
Hermanns RL, Niedermann S, Ivy-Ochs S, and Kubick PW (2004) Rock avalanching into a landslide-dammed lake causing multiple dam failure in Las Conchas valley (NW Argentina)–Evidence from surface exposure dating and stratigraphic analyses. *Landslides* 1: 113–122. https://doi.org/10.1007/s10346-004-0013-5.
Hermanns RL, Folguera A, Penna I, Fauqué L, and Niedermann S (2011a) Landslide dams in the Central Andes of Argentina (northern Patagonia and the Argentine northwest). In: Evans SG, Hermanns RL, Strom AL, and Scarascia Mugnozza G (eds.) *Natural and Artificial Rockslide Dams*, *Springer Lecture Notes in Earth Sciences*, vol. 133, 147–176. https://doi.org/10.1007/978-3-642-04764-0_5.
Hermanns RL, Hewitt K, Strom A, Evans SG, Dunning SA, and Scarascia-Mugnozza G (2011b) The classification of rockslide dams. In: Evans S, Hermanns R, Strom A, and Scarascia-Mugnozza G (eds.) *Natural and Artificial Rockslide Dams*, *Springer Lecture Notes in Earth Sciences*, vol. 133, 581–593. https://doi.org/10.1007/978-3-642-04764-0_24.
Hermanns RL, Dalhle H, Bjerke PL, Crosta GB, Anda E, Blikra LH, Saintot A, and Longva O (2013) Rockslide dams in Møre og Romsdal County, Norway. In: Margottini C, Canuti P, and Sassa K (eds.) *Landslide Science and Practice*, pp. 3–12. Berlin, Heidelberg: Springer. https://doi.org/10.1007/978-3-642-31319-6_1.
Hewitt K (1968) Record of natural damming and related floods in the Upper Indus Basin. *Indus* 10(3): 11–19.
Hewitt K (1982) Natural dams and outburst floods of the Karakoram Himalaya. In: Glen JW (ed.) *Hydrological Aspects of Alpine and High-Mountain Areas*. vol. 138, pp. 259–269. International Association of Hydrological Sciences Publication.
Hewitt K (1998) Catastrophic landslides and their effects on the Upper Indus streams, Karakoram Himalaya, northern Pakistan. *Geomorphology* 26: 47–80.
Hewitt K (2002) Styles of rock-avalanche depositional complexes conditioned by very rugged terrain, Karakoram Himalaya, Pakistan. In: Evans SG and Graff JV (eds.) *Catastrophic Landslides: Effects, Occurence, and Mechanisms*, *Geological Society of America Reviews in Engineering Geology*, vol. 15, 345–378.
Hewitt K (2006) Disturbance regime landscapes: Mountain drainage systems interrupted by large rockslides. *Progress in Physical Geography* 30: 365–393.

Hewitt K (2009) Catastrophic rock slope failures and late Quaternary developments in the Nanga Parbat–Haramosh Massif, Upper Indus basin, northern Pakistan. *Quaternary Science Reviews* 28: 1055–1099.

Hewitt K (2011) Rock avalanche dams on the Trans Himalayan Upper Indus streams: A survey of late Quaternary events and hazard-related characteristics. In: Evans S, Hermanns R, Strom A, and Scarascia-Mugnozza G (eds.) *Natural and Artificial Rockslide Dams*, *Springer Lecture Notes in Earth Sciences*, vol. 133, 177–204. https://doi.org/10.1007/978-3-642-04764-0_6.

Hewitt K and Liu J (2010) Ice-dammed lakes and outburst floods, Karakoram Himalaya: Historical perspectives on emerging threats. *Physical Geography* 31: 528–551. https://doi.org/10.2747/0272-3646.31.6.528.

Hewitt K, Clague JJ, and Orwin JF (2008) Legacies of catastrophic rock slope failures in mountain landscapes. *Earth-Science Reviews* 87: 1–38.

Hewitt K, Gosse J, and Clague JJ (2011) Rock avalanches and the pace of late Quaternary development of river valleys in the Karakoram Himalaya. *Geological Society of America Bulletin* 123: 1836–1850.

Hickson CJ, Russell JK, and Stasiuk MV (1999) Volcanology of the 2350 B.P. eruption of Mount Meager Volcanic Complex, British Columbia, Canada: Implications for hazards from eruptions in topographically complex terrain. *Bulletin of Volcanology* 60: 489–507.

Hilgendorf Z, Wells G, Larson PH, Millet J, and Kohout M (2020) From basins to rivers: Understanding the revitalization and significance of top-down drainage integration mechanisms in drainage basin evolution. *Geomorphology* 352: 107020. https://doi.org/10.1016/j.geomorph.2019.107020.

Hillman G (1998) Flood wave attenuation by a wetland following a beaver dam failure on a second order boreal stream. *Wetlands* 18(1): 21–34.

Hodgson KA and Nairn IA (2005) The c. AD 1315 syn-eruption and AD 1904 post-eruption breakout floods from Lake Tarawera, Haroharo caldera, North Island, New Zealand. *New Zealand Journal of Geology and Geophysics* 48: 491–506.

House PK, Pearthree PA, and Perkins MD (2009) Stratigraphic evidence for the role of lake-spillover in the birth of the lower Colorado River in southern Nevada and western Arizona. In: Reheis MC, Hershler R, and Miller DM (eds.) *Geologic and Biologic Evolution of the Southwest*, 333–351. Geological Society of America Special Paper 439.

Howard KA, Shervais JW, and Mckee EH (1982) Canyon-filling lavas and lava dams on the Boise River, Idaho, and their significance for evaluating downcutting during the last two million years. In: Bonnichsen B and Breckenridge RM (eds.) *Cenozoic Geology of Idaho*, pp. 629–644. Moscow, Idaho: Idaho Bureau of Mines and Geology.

Hsü KJ (1983) *Mediterranean Was a Desert: A Voyage of the Glomar Challenger*. Princeton, New Jersey: Princeton University Press216.

Hu HP, Feng JL, and Chen F (2018) Sedimentary records of a palaeo-lake in the middle Yarlung Tsangpo: Implications for terrace genesis and outburst flooding. *Quaternary Science Reviews* 192: 135–148. https://doi.org/10.1016/j.quascirev.2018.05.037.

Huggel C, Kääb A, Haeberli W, Teysseire P, and Paul F (2002) Remote sensing based assessment of hazards from glacier lake outbursts: A case study in the Swiss Alps. *Canadian Geotechnical Journal* 39: 316–330.

Huggel C, Kääb A, and Haeberli W (2003a) Regional-scale models of debris flows triggered by lake outbursts: The June 25, 2001 debris flow at Täsch (Switzerland) as a test study. In: Rickenmann D and Chen L (eds.) *Debris-Flow Hazards Mitigation: Mechanics, Prediction, and Assessment*, pp. 1151–1162. Rotterdam: Millpress.

Huggel C, Kääb A, Haeberli W, and Krummenacher B (2003b) Regional-scale GIS-models for assessment of hazards from glacier lake outbursts: Evaluation and application in the Swiss Alps. *Natural Hazards and Earth System Sciences* 3: 647–662.

Huggel C, Haeberli W, Kääb A, Bieri D, and Richardson S (2004) An assessment procedure for glacial hazards in the Swiss Alps. *Canadian Geotechnical Journal* 41: 1068–1083.

Hulsing H (1981) *The Breakout of Alaska's Lake George*. Washington, DC: U.S. Geological Survey, U.S. Government Printing Office, 15.

Irwin RP and Grant JA (2009) Large basin overflow floods on Mars. In: Burr DM, Carling PA, and Baker VR (eds.) *Megaflooding on Earth and Mars*, pp. 209–224. Cambridge: Cambridge University Press. https://doi.org/10.1017/CBO9780511635632.011.

Ischuk AR (2011) Usoi rockslide dam and Lake Sarez, Pamir Mountains, Tajikistan. In: Evans S, Hermanns R, Strom A, and Scarascia-Mugnozza G (eds.) *Natural and Artificial Rockslide Dams*, *Springer Lecture Notes in Earth Sciences*, vol. 133, 423–440. https://doi.org/10.1007/978-3-642-04764-0_16.

Iverson RM (1997) The physics of debris flows. *Reviews of Geophysics* 35: 245–296. https://doi.org/10.1029/97RG00426.

Iverson RM (2006) Langbein Lecture: Shallow Flows That Shape Earth's Surface. *Eos, Transactions of the American Geophysical Union* 87(52). Abstract H22A-01.

Ives JD (1986) *Glacier Lake Outburst Floods and Risk Engineering in the Himalaya—A Review of the Langmoche Disaster, Khumbu Himal, 4 August 1985*. International Centre for Integrated Mountain Development Occasional Paper 5 42.

Jackson LE Jr. (1979) A catastrophic glacial outburst flood (jökulhlaup) mechanism for debris flow generation at the Spiral Tunnels, Kicking Horse River basin, British Columbia. *Canadian Geotechnical Journal* 16: 806–813. https://doi.org/10.1139/t79-087.

Jacobson RB, O'Connor JE, and Oguchi T (2016) Surficial geologic tools in fluvial geomorphology. In: Kondolf GM and Piegay H (eds.) *Tools in Fluvial Geomorphology*, 2nd edn, pp. 15–40. Chichester: John Wiley and Sons. ISBN: 978-0-470-68405-4.

Jakob M and Jordan P (2001) Design flood estimates in mountain streams—The need for a geomorphic approach. *Canadian Journal of Civil Engineering* 28: 425–439.

Janda RJ, Scott KM, Nolan KM, and Martinson HA (1981) Lahar movement, effects and deposits. In: Lipman PW and Mullineaux DR (eds.) *The 1980 Eruptions of Mount St. Helens*, 461–478. Washington: U.S Geological Survey Professional Paper, 1250.

Jansen RB (1980) *Dams and Public Safety*. Washington, DC: U.S. Department of the Interior, 332.

Janský B, Šobr M, and Engel Z (2010) Outburst flood hazard: Case studies from the Tien-Shan Mountains, Kyrgyzstan. *Limnologica* 40: 358–364. https://doi.org/10.1016/j.limno.2009.11.013.

Johannesson T (2002) Propagation of a subglacial flood wave during the initiation of a jökulhlaup. *Journal of Hydrological Sciences* 47: 417–434.

Johnson DM, Petersen RR, Lycan DR, Sweet JW, Neuhaus ME, and Schaedel AL (1985) *Atlas of Oregon Lakes*. Corvallis, Oregon: Oregon State University Press, 317.

Johnson PJ, Valentine GA, Stauffer PH, Lowry CS, Sonder I, Pulgarín BA, Santacoloma CC, and Agudelo A (2018) Groundwater drainage from fissures as a source for lahars. *Bulletin of Volcanology* 80: 39. https://doi.org/10.1007/s00445-018-1214-4.

Kääb A, Huggel C, Barbero S, Chiarle M, Cordola M, Epifani F, Haeberli W, Mortara G, Semino P, Tamburini A, and Viazzo G (2004) Glacier hazards at Belvedere Glacier and the Monte Rosa east face, Italian Alps: Processes and mitigation. In: *Internationales Symposion Interpraevent 2004—Riva/Trient* 1-67–1-78.

Karátson D, Thouret J-C, Moriya I, and Lomoschitz A (1999) Erosion calderas: Origins, processes, structural and climatic control. *Bulletin of Volcanology* 61: 174–193. https://doi.org/10.1007/s004450050270.

Kataoka KS (2011) Geomorphic and sedimentary evidence of a gigantic outburst flood from Towada caldera after the 15 ka Towada–Hachinohe ignimbrite eruption, northeast Japan. *Geomorphology* 125: 11–26. https://doi.org/10.1016/j.geomorph.2010.08.006.

Kataoka KS, Urabe A, Manville V, and Kajiyama A (2008) Breakout flood from an ignimbrite-dammed valley after the 5 ka Numazawako eruption, northeast Japan. *Geological Society of America Bulletin* 120: 1233–1247.

Kattelmann R (2003) Glacial lake outburst floods in the Nepal Himalaya: A manageable hazard? *Natural Hazards* 28: 145–154.

Kehew AE, Esch JM, Ewald SK, and Kozlowski AL (2009) Constraints on aquifer occurence in tunnel channels, Saginaw, Michigan. *Geological Society of America Abstracts with Programs* 41(7): 213.

Keisling BA, Nielsen LT, Hvidberg CS, Nuterman R, and DeCoto RM (2020) Pliocene-Pleistocene megafloods as a mechanism for Greenlandic megacanyon formation. *Geology*. https://doi.org/10.1130/G47253.1.

Kershaw JA, Clague JJ, and Evans SG (2005) Geomorphic and sedimentological signature of a two-phase outburst flood from moraine-dammed Queen Bess Lake, British Columbia, Canada. *Earth Surface Processes and Landforms* 30: 1–25.

Keszthelyi LP, Denlinger RP, O'Connell DRH, and Burr DM (2007) Initial insights from 2.5D hydraulic modeling of floods in Athabasca Valles, Mars. *Geophysical Research Letters* 34: L21206. https://doi.org/10.1029/2007GL031776.

Kilburn CRJ and Petley DN (2003) Forecasting giant, catastrophic slope collapse: Lessons from Vajont, northern Italy. *Geomorphology* 54: 21–32.

King J, Loveday I, and Schuster RL (1989) The 1985 Bairaman landslide dam and resulting debris flow, Papua New Guinea. *Quarterly Journal of Engineering Geology, London* 22: 257–270.
Kingslake J, Ng F, and Sole A (2015) Modelling channelized surface drainage of supraglacial lakes. *Journal of Glaciology* 61: 185–199. https://doi.org/10.3189/2015JoG14J158.
Kochel RC, Nickelsen RP, and Eaton LS (2009) Catastrophic middle Pleistocene jökulhlaups in the upper Susquehanna River: Distinctive landforms from breakout floods in the central Appalachians. *Geomorphology* 110: 80–95.
Komar PD (1980) Modes of sediment transport in channelized water flows with ramifications to the erosion of the Martian outflow channels. *Icarus* 42: 317–319. https://doi.org/10.1016/0019-1035(80)90097-4.
Komar PD (1983) Shape of streamlined islands on Earth and Mars: Experiments and analyses of the minimum drag form. *Geology* 11: 651–654. https://doi.org/10.1130/0091-7613(1983)11<651:SOSIOE>2.0.CO;2.
Komar PD (1984) The lemniscate loop-comparisons with the shapes of streamlined landforms. *Journal of Geology* 92: 133–145. https://doi.org/10.1086/628844.
Komar PD (1987) Selective gravel entrainment and the empirical evaluation of flow competence. *Sedimentology* 34: 1165–1176.
Komar PD (1988) Sediment transport by floods. In: Baker VR, Kochel RC, and Patton PC (eds.) *Flood Geomorphology*, pp. 97–111. New York: John Wiley and Sons.
Komatsu G and Baker VR (1997) Paleohydrology and flood geomorphology of Ares Vallis. *Journal of Geophysical Research* 102(E2): 4151–4160.
Komatsu G, Baker VR, Arzhannikov SG, Gallagher R, Arzhannikova A, Murana A, and Oguchi T (2015) Catastrophic flooding, palaeolakes, and late Quaternary drainage reorganization in northern Eurasia. *International Geology Review* 58: 1693–1722. https://doi.org/10.1080/00206814.2015.1048314.
Korup O (2002) Recent research on landslide dams—A literature review with special attention to New Zealand. *Progress in Physical Geography* 26: 206–235.
Korup O (2004) Geomorphometric characteristics of New Zealand landslide dams. *Engineering Geology* 73: 13–35.
Korup O (2006) Rock-slope failure and the river long profile. *Geology* 34: 45–48.
Korup O and Tweed FS (2007) Ice, moraine, and landslide dams in mountainous terrain. *Quaternary Science Reviews* 26: 3406–3422.
Korup O, Strom AL, and Weidinger JT (2006) Fluvial response to large rock-slope failures: Examples from the Himalayas, the Tien Shan, and the Southern Alps in New Zealand. *Geomorphology* 78: 3–21.
Korup O, Clague JJ, Hermanns RL, Hewitt K, Strom AL, and Wedinger JT (2007) Giant landslides, topography, and erosion. *Earth and Planetary Science Letters* 261: 578–579.
Korup O, Denmore AL, and Schlunegger F (2010) The role of landslides in mountain range evolution. *Geomorphology* 120: 77–90. https://doi.org/10.1016/j.geomorph.2009.09.017.
Kougkoulos I, Cook SJ, Edwards LA, Clarke LJ, Symeonakis E, Dortch JM, and Nesbitt K (2018) Modelling glacial lake outburst flood impacts in the Bolivian Andes. *Natural Hazards* 94: 1415–1438. https://doi.org/10.1007/s11069-018-3486-6.
Kraus NC, Militello A, and Todoroff G (2002) Barrier breaching processes and barrier spit breach, Stone Lagoon, California. *Shore and Beach* 70(4): 21–28.
Kropáček J, Neckel N, Tyrna B, Holzer N, Hovden A, Gourmelen N, Schneider C, Buchroithner M, and Hoschschild V (2015) Repeated glacial lake outburst flood threatening the oldest Buddhistmonastery in north-western Nepal. *Natural Hazards Earth System Science* 15: 2425–2437. https://doi.org/10.5194/nhess-15-2425-2015.
Laenan A, Scott KM, Costa JE, and Orzol LL (1987) *Hydrologic Hazards Along Squaw Creek From a Hypothetical Failure of the Glacial Moraine Impounding Carver Lake Near Sisters, Oregon*. U.S. Geological Survey Open-File Report 87–41 48. https://doi.org/10.3133/ofr8741.
Lagmay AMF, Rodolfo KS, Siringan FP, Uy H, Remotigue C, Zamora P, Lapus M, Rodolfo R, and Ong J (2007) Geology and hazard implications of the Maraunot notch in the Pinatubo Calera, Philippines. *Bulletin of Volcanology* 69: 797–809.
Lala JM, Rounce DR, and McKinney DC (2018) Modeling the glacial lake outburst flood process chain in the Nepal Himalaya: Reassessing Imja Tsho's hazard. *Hydrology and Earth System Sciences* 22: 3721–3737. https://doi.org/10.5194/hess-22-3721-2018.
Lamb M and Fonstad M (2010) Rapid formation of a modern bedrock canyon by a single flood event. *Nature Geoscience* 3: 477–481. https://doi.org/10.1038/ngeo894.
Lamb MP, Dietrich WE, Aciego SM, DePaolo DJ, and Manga M (2008) Formation of Box Canyon, Idaho, by megaflood: Implications for seepage erosion on Earth and Mars. *Science* 320: 1067–1070. https://doi.org/10.1126/science.1156630.
Lamb MP, Mackey BH, and Farley KA (2014) Amphitheater-headed canyons formed by megaflooding at Malad Gorge, Idaho. *Proceedings of the National Academy of Science* 111: 57–62. https://doi.org/10.1073/pnas.1312251111.
Lamb MP, Finnegan NJ, Scheingross JS, and Sklar LS (2015) New insights into the mechanics of fluvial bedrock erosion through flume experiments and theory. *Geomorphology* 244: 33–55. https://doi.org/10.1016/j.geomorph.2015.03.003.
Lancaster ST and Grant GE (2006) Debris dams and the relief of headwater streams. *Geomorphology* 82: 84–97.
Lang KA, Huntington KW, and Montgomery DR (2013) Erosion of the Tsangpo Gorge by megafloods, eastern Himalaya. *Geology* 41: 1003–1006. https://doi.org/10.1130/G34693.1.
Lang J, Alho P, Kasvi E, Goseberg N, and Winsemann J (2019) Impact of Middle Pleistocene (Saalian) glacial lake-outburst floods on the meltwater-drainage pathways in northern central Europe: Insights from 2D numerical flood simulation. *Quaternary Science Reviews* 209: 82–99. https://doi.org/10.1016/j.quascirev.2019.02.018.
Lapotre MGA, Lamb MP, and Williams RME (2016) Canyon formation constraints on the discharge of catastrophic outburst floods of Earth and Mars. *Journal of Geophysical Research, Planets* 121: 1232–1263. https://doi.org/10.1002/2016JE005061.
Larsen IJ and Lamb MP (2016) Progressive incision of the Channeled Scablands by outburst floods. *Nature* 538: 229–232. https://doi.org/10.1038/nature19817.
Larson GL (1989) Geographical distribution, morphology and water quality of caldera lakes: A review. *Hydrobiologia* 171: 23–32.
Latrubesse EM, Park E, Sieh K, Dang T, Lin YN, and Yun S (2020) Dam failure and a catastrophic flood in the Mekong basin (Bolaven Plateau), southern Laos, 2018. *Geomorphology* 362: 107221. https://doi.org/10.1016/j.geomorph.2020.107221.
Lee J (2018) Modeling the connections between internally and externally drained basins using GIS, Google Earth©, and remote sensing. *Progress in Physical Geography: Earth and Environment* 42: 274–304. https://doi.org/10.1177/0309133318776462.
Lee KL and Duncan JM (1975) *Landslide of April 25, 1974, on the Mantaro River, Peru*. Natural Research Council, Committee on Natural Disasters, Commission on Sociotechnical Systems72.
Lesemann J-E and Brennand TA (2009) Regional reconstruction of subglacial hydrology and glaciodynamic behaviour along the southern margin of the Cordilleran Ice Sheet in British Columbia, Canada and northern Washington State, USA. *Quaternary Science Reviews* 28: 2420–2444.
Li T, Schuster RL, and Wu J (1986) Landslide dams in southcentral China. In: Schuster RL (ed.) *Landslide Dams: Process, Risk, and Mitigation*. vol. 3, pp. 146–162. American Civil Engineers Special Publication.
Liestøl O (1956) Glacier dammed lakes in Norway. *Norsk Geografisk Tidsskrift* 15: 122–149.
Lind P (2009) *Holocene Floodplain Development of the Lower Sycan River, Oregon*. Unpublished Master's thesis Eugene, Oregon: University of Oregon203.
Lind P, O'Connor JE, and McDowell P (2007) Post-Mazama break-out flood on the Sycan River, southern Oregon. *Eos, Transactions of the American Geophysical Union* 88(52). Abstract H51E-0807.
Lipscomb SW (1989) Branch flow model of the Knik and Matanuska rivers, Alaska. In: *Proceedings of the Advanced Seminar on One-Dimensional Open-Channel Flow and Transport Modeling, National Space Technology Laboratory* 62–64.
Liu C and Sharma CK (1988) *Report on First Expedition to Glaciers and Glacier Lakes in the Pumqu (Arun) and Poiqu (Bhote-Sun Kosi) River Basins, Xizang (Tibet), China: Sino-Nepalese Investigation of Glacier Lake Outburst Floods in the Himalayas*. Beijing, China: Science Press192.
Liu W, Carling PA, Hu K, Wang H, Zhou Z, Zhou L, Liu D, Lai Z, and Zhang X (2019) Outburst floods in China: A review. *Earth-Science Reviews* 197: 102895. https://doi.org/10.1016/j.earscirev.2019.102895.
Lliboutry L, Arnao VM, Pautre A, and Schneider B (1977) Glaciological problems set by the control of dangerous lakes in Cordillera Blanca, Peru: I. Historical failures of morainic dams, their causes and prevention. *Journal of Glaciology* 18: 239–254.
Lockwood JP, Costa JE, Tuttle ML, Nni J, and Tebor SG (1988) The potential for catastrophic dam failure at Lake Nyos Maar, Cameroon. *Bulletin of Volcanology* 50: 340–349.

Lord ML and Kehew AE (1987) Sedimentology and paleohydrology of glacial-lake outburst deposits in southeastern Saskatchewan and northwestern North Dakota. *Geological Society of America Bulletin* 99: 663–673.

Lubbock G (1894) The Gohna Lake. *Geographical Journal* 4: 457.

Lyell C (1830) *Principles of Geology*. vol. 1, London: John Murray511.

Macchione F (2008) Model for predicting floods due to earthen dam breaching; I: Formation and evaluation. *Journal of Hydraulic Engineering* 134: 1688–1696.

Macchione F and Rino A (2008) Model for predicting floods due to earthen dam breaching. II: Comparison with other methods and predictive use. *Journal of Hydraulic Engineering* 134: 1697–1707. https://doi.org/10.1061/(ASCE)0733-9429(2008)134:12(1697).

Macchione F and Sirangelo B (1990) Floods resulting from progressively breached dams. Proceedings of Lausanne Symposia, August 1990, Hydrology in Mountainous Regions, vol. 194, pp. 325–332. International Association of Hydrological Sciences Publication.

Macdonald TC and Langridge-Monopolis J (1984) Breaching characteristics of dam failures. *Journal of Hydraulic Engineering* 110: 567–586.

Macías JL, Capra L, Scott KM, Espíndola JM, García-Palomo A, and Costa JE (2004) 26 May 1982 breakout flows derived from failure of a volcanic dam at El Chichón, Chiapas, Mexico. *Geological Society of America Bulletin* 116: 233–246.

Magirl CS, Gartner JW, Smart GM, and Webb RH (2009) Water velocity and the nature of critical flow in large rapids on the Colorado River, Utah. *Water Resources Research* 45: W05427. https://doi.org/10.1038/ngeo894.

Magnin F, Haeberli W, Linsbauer A, Dline P, and Ravenel L (2020) Estimating glacier-bed overdeepenings as possible sites of future lakes in the de-glaciating Mont Blanc massif (western European Alps). *Geomorphology* 350: 106913. https://doi.org/10.1016/j.geomorph.2019.106913.

Major JJ, O'Connor JE, Podolak CJ, Keith MK, Grant GE, Spicer KR, Pittman S, Bragg HM, Wallick JR, Tanner DQ, Rhode A, and Wilcock PR (2012) *Geomorphic Response of the Sandy River, Oregon, to Removal of Marmot Dam*. U.S. Geological Survey Professional Paper 1792 64. https://pubs.usgs.gov/pp/1792/.

Malde HE (1968) *The Catastrophic Late Pleistocene Bonneville Flood in the Snake River Plain, Idaho*. U.S. Geological Survey Professional Paper 596 52.

Malde HE (1982) Yahoo Clay, a lacustrine unit impounded by the McKinney Basalt in the Snake River canyon near Bliss, Idaho. In: Bonnichsen B and Breckenridge RM (eds.) *Cenozoic Geology of Idaho*, pp. 617–628. Moscow, Idaho: Idaho Bureau of Mines and Geology.

Manga M (2004) Martian floods at Cerberus Fossae can be produced by groundwater discharge. *Geophysical Research Letters* 31(2), L02702.

Mangerud J, Jakobsson M, Alexanderson H, Astakhov V, Clarke GKC, Henriksen M, Hjort C, Krinner G, Lunkka J-P, Möller P, Murray A, Nikolskaya O, Saarnisto M, and Svendsen JIJI (2004) Ice-dammed lakes and rerouting of the drainage of northern Eurasia during the Last Glaciation. *Quaternary Science Reviews* 23: 1313–1332.

Manville V (2001) *Techniques for Evaluating the Size of Potential Dam-break Floods from Natural Dams*. New Zeala nd Institute of Geological and Nuclear Sciences, Science Report 2001/28 72.

Manville V (2004) Paleohydraulic analysis of the 1953 Tangwai lahar: New Zealand's worst volcanic disaster. *Acta Vulcanologica* 16(1–2): 137–152.

Manville V (2010a) An overview of break-out floods from intracaldera lakes. *Global and Planetary Change* 70: 14–23. https://doi.org/10.1016/j.gloplacha.2009.11.004.

Manville V (2010b) *Anatomy of a Sudden Onset Flood: The 18 March 2007 Crater Lake Break-Out Lahar, Mt. Ruapehu, New Zealand*. EGU General Assembly 2010 Abstracts 4143.

Manville V (2015) Volcano-hydrologic hazards from volcanic lakes. In: Rouwet D, Christenson B, Tassi F, and Vandemeulebrouck J (eds.) *Volcanic Lakes*, pp. 21–71. Berlin, Germany: Springer-Verlag. https://doi.org/10.1007/978-3-642-36833-2_2.

Manville V and Cronin SJ (2007) Breakout lahar from New Zealand's Crater Lake. *Eos, Transactions of the American Geophysical Union* 88: 442–443.

Manville V, White JDL, Houghton BF, and Wilson CJN (1999) Paleohydrology and sedimentology of a post-1.8 ka breakout flood from intracaldera Lake Taupo, North Island, New Zealand. *Geological Society of America Bulletin* 111: 1435–1447. https://doi.org/10.1130/0016-7606(1999)111<1435:PASOAP>2.3.CO;2.

Manville V, Hodgson KA, and Nairn IA (2007) A review of break-out floods from volcanogenic lakes in New Zealand. *New Zealand Journal of Geology and Geophysics* 50: 131–150.

Marchant DR, Jamieson SSR, and Sugden DE (2011) The geomorphic signature of massive subglacial floods in Victoria Land, Antarctica. *American Geophysical Union, Geophysical Monograph* 192: 111–126. https://doi.org/10.1029/2010GM000943.

Marche C, Mahdi T, and Quach T (2006) Erode: Une methode fiable pour etablir l'hydrogramme de rupture potentielle par surverse de chaque digue en terre. *Transactions of the International Congress on Large Dams* 22(3): 337–360.

Margold M and Jansson KN (2011) Glacial geomorphology and glacial lakes of central Transbaikalia, Siberia, Russia. *Journal of Maps* 2011: 18–30.

Margold M, Jansen JD, Codilean AT, Preusser F, Gurinov AL, Fujioka R, and Fink D (2018) Repeated megafloods from glacial Lake Vitim, Siberia, to the Arctic Ocean over the past 60,000 years. *Quaternary Science Reviews* 187: 41–61. https://doi.org/10.1016/j.quascirev.2018.03.005.

Massey C, Manville V, Hancox G, Keys H, Lawrence C, and McSaveney M (2010) Outburst flood (lahar) triggered by retrogressive landsliding, 18 March 2007 at Mt Ruapehu, New Zealand—A successful early warning. *Landslides* 7: 303–315.

Mathews WH (1973) *Record of Two Jökulhlaups*. vol. 95, International Association of Hydrological Sciences Publication99–110.

Mathews WH and Clague JJ (1993) The record of jökulhlaups from Summit Lake, northwestern British Columbia. *Canadian Journal of Earth Sciences* 30: 499–508.

Mayo LR (1989) Advance of Hubbard Glacier and 1986 outburst of Russell Fiord, Alaska, U.S.A. *Journal of Glaciology* 13: 189–194.

McCullough DG (1968) *The Johnstown Flood*. New York: Simon and Schuster304.

McGimsey RG, Waythomas CF, and Neal CA (1994) High stand and catastrophic draining of intracaldera Surprise Lake, Aniakchak Volcano, Alaska. In: Till AB and Moore TE (eds.) *Geologic Studies in Alaska by the U.S. Geological Survey*, 59–71. U.S. Geological Survey Bulletin 2107.

McKillop R and Clague J (2007a) A procedure for making objective preliminary assessments of outburst flood hazard from moraine-dammed lakes in southwestern British Columbia. *Natural Hazards* 41: 131–157.

McKillop RJ and Clague JJ (2007b) Statistical, remote sensing-based approach for estimating the probability of catastrophic drainage from moraine-dammed lakes in southwestern British Columbia. *Global and Planetary Change* 56: 153–171.

McSweeney SL, Kennedy DM, Rutherfurd ID, and Stout JC (2017) Intermittently closed/open lakes and lagoons: Their global distribution and boundary conditions. *Geomorphology* 292: 142–152. https://doi.org/10.1016/j.geomorph.2017.04.022.

Meek N (2019) Episodic forward prolongation of trunk channels in the western United States. *Geomorphology* 340: 172–183. https://doi.org/10.1016/j.geomorph.2019.05.002.

Melnick D, Charlet F, Echtler HP, and DeBatist M (2006) Incipient axial collapse of the Main Cordillera and strain partitioning gradient between the central and Patagonian Andes, Lago Laja, Chile. *Tectonics* 25: TC5004. https://doi.org/10.1029/2005TC001918.

Mergili M and Schneider F (2011) Regional-scale analysis of lake outburst hazards in the southwestern Pamir, Tajikistan, based on remote sensing and GIS. *Natural Hazards and Earth System Sciences* 11: 1447–1462. https://doi.org/10.5194/nhess-11-1447-2011.

Mergili M, Emmer A, Juřicová A, Cochachin A, Fischer JT, Huggel C, and Pudasaini SP (2018) How well can we simulate complex hydro-geomorphic process chains? The 2012 multi-lake outburst flood in the Santa Cruz Valley (Cordillera Blanca, Perú). *Earth Surface Processes and Landforms* 43: 1373–1389. https://doi.org/10.1002/esp.4318.

Meyer W, Sabol MA, Glicken HX, and Voight B (1985) *The Effects of Ground Water, Slope Stability and Seismic Hazards on the Stability of the South Fork Castle Creek Blockage in the Mount St. Helens area, Washington*. U.S. Geological Survey Professional Paper 1345 42.

Meyer W, Sabol MA, and Schuster RL (1986) Landslide dammed lakes at Mount St. Helens, Washington. In: Schuster RL (ed.) *Landslide Dams: Process, Risk, and Mitigation*. vol. 3, pp. 21–41. American Society of Civil Engineers Special Publication.

Montgomery DR, Hallet B, Liu Y, Finnegan N, Anders A, Gillespie A, and Greenberg HM (2004) Evidence for Holocene megafloods down the Tsangpo River gorge, southeastern Tibet. *Quaternary Research* 62: 201–207.

Montgomery DR, Som SM, Jackson MPA, Schreiber BC, Gillespie AR, and Adams JB (2009) Continental-scale salt tectonics on Mars and the origin of Valles Marineris and associated outflow channels. *Geological Society of America Bulletin* 121: 117–133. https://doi.org/10.1130/B26307.1.

Mool PK (1995) Glacier lake outburst floods in Nepal. *Journal of Nepal Geological Society* 11: 273–280.

Morris MW, Hassan MAAM, and Vaskinn KA (2007) Breach formation: Field test and laboratory experiments. *Journal of Hydraulic Research* 45(supplement 1): 9–17. https://doi.org/10.1080/00221686.2007.9521828.

Morris M, West M, and Hassan M (2018) A guide to breach prediction. *Dams and Reservoirs* 28: 150–152. https://doi.org/10.1680/jdare.18.00031.

Munro-Stasiuk MJ, Shaw J, Sjogren DB, Brennand TA, Fisher TG, Sharpe DR, Kor PSG, Beaney CL, and Rains BB (2009) The morphology and sedimentology of landforms created by subglacial megafloods. In: Burr DM, Carling PA, and Baker VR (eds.) *Megaflooding on Earth and Mars*, pp. 78–103. United Kingdom: Cambridge University Press.

Murton JB, Bateman MD, Dallimore SR, Teller JT, and Yang Z (2010) Identification of Younger Dryas outburst flood path from Lake Agassiz to the Arctic Ocean. *Nature* 464(7289): 740–743. https://doi.org/10.1038/nature08954.

Nash T, Bell D, Davies T, and Nathan S (2010) Analysis of the formation and failure of Ram Creek landslide dam, South Island, New Zealand. *New Zealand Journal of Geology and Geophysics* 51: 187–193. https://doi.org/10.1080/00288300809509859.

Neupane R, Chen H, and Cao C (2019) Review of moraine dam failure mechanism. *Geomatics, Natural Hazards and Risk* 10: 1948–1966. https://doi.org/10.1080/19475705.2019.1652210.

Newhall CG, Paull CK, Bradbury JP, Higuera-Gundy A, Poppe LJ, Self S, Bonar-Sharpless N, and Ziagos J (1987) Recent geologic history of Lake Atitlán, a caldera lake in western Guatemala. *Journal of Volcanology and Geothermal Research* 33: 88–107.

Ng F and Björnsson H (2003) On the Clague-Mathews relation for jökulhlaups. *Journal of Glaciology* 49: 161–172. https://doi.org/10.3189/172756503781830836.

Ng F and Liu S (2009) Temporal dynamics of a jökulhlaup system. *Journal of Glaciology* 55(192): 651–665.

Nicoletti PG and Parise M (2002) Seven landslide dams of old seismic origin in southeastern Sicily (Italy). *Geomorphology* 46: 203–222.

Nie Y, Sheng Y, Liu Q, Liu L, Liu S, Zhang Y, and Song C (2017) A regional-scale assessment of Himalayan glacial lake changes using satellite observations from 1990 to 2015. *Remote Sensing of Environment* 189: 1–13. https://doi.org/10.1016/j.rse.2016.11.008.

Nye JF (1976) Water flow in glaciers: Jökulhlaups, tunnels and veins. *Journal of Glaciology* 17: 181–207.

O'Connor JE (2016) The Bonneville Flood—A veritable débâcle. *Developments in Earth Surface Processes* 20: 105–126. https://doi.org/10.1016/B978-0-444-63590-7.00006-8.

O'Connor JE and Costa JE (1993) Geologic and hydrologic hazards in glacierized basins in North America resulting from 19th and 20th century global warming. *Natural Hazards* 8: 121–140.

O'Connor JE, Curran JH, Beebee RA, Grant GE, and Sarna-Wojcicki A (2003) Quaternary geology and geomorphology of the lower Deschutes River canyon, Oregon. In: O'Connor JE and Grant GE (eds.) *A Peculiar River—Geology, Geomorphology, and Hydrology of the Deschutes River, Oregon*, *American Geophysical Union Water Science and Application Series*, vol. 7, 73–94.

O'Connor JE, Baker VR, Waitt RB, Smith LN, Cannon CM, George DL, and Denlinger RP (2020) The Missoula and Bonneville floods—A review of ice-age Megafloods in the Columbia River Basin. *Earth-Science Reviews*. https://doi.org/10.1016/j.earscirev.2020.103181.

O'Connor JE (1993) *Hydrology, Hydraulics, and Geomorphology of the Bonneville Flood*. Geological Society of America Special Paper 274, 83.

O'Connor JE (2004) The evolving landscape of the Columbia River Gorge—Lewis and Clark and cataclysms on the Columbia. *Oregon Historical Quaterly* 105: 390–421.

O'Connor JE and Baker VR (1992) Magnitudes and implications of peak discharges from glacial Lake Missoula. *Geological Society of America Bulletin* 104: 267–279.

O'Connor JE and Beebee RA (2009) Floods from natural rock-material dams. In: Burr DM, Carling PA, and Baker VR (eds.) *Megaflooding on Earth and Mars*, pp. 128–171. United Kingdom: Cambridge University Press. http://refhub.elsevier.com/S0012-8252(20)30223-3/rf9017.

O'Connor JE and Burns SF (2009) Cataclysms and controversy—Aspects of the geomorphology of the Columbia River Gorge. In: O'connor JE, Dorsey RJ, and Madin I (eds.) *Volcanoes to Vineyards: Geologic Field Trips Through Dynamic Landscapes*, pp. 237–252. Boulder, CO: Geological Society of America.

O'Connor JE and Costa JE (2004) *The World's Largest Floods, Past and Present—Their Causes and Magnitudes*. U.S. Geological Survey Circular 1254 19.

O'Connor JE and Waitt RB (1995) Beyond the Channeled Scabland—A field trip guide to Missoula flood features in the Columbia, Yakima, and Walla Walla Valleys of Washington and Oregon. *Oregon Geology* 57(I): 51–60. (II) 75–86; (III), 99–115.

O'Connor JE, Pierson TC, Turner D, Atwater BF, and Pringle PT (1996) An exceptionally large Columbia River flood between 500 and 600 years ago—Breaching of the Bridge-of-the-Gods landslide? *Geological Society of America Program with Abstracts* 28(7): 97.

O'Connor JE, Hardison JH III, and Costa JE (2001) *Debris Flows From Failures of Neoglacial Moraine Dams in the Three Sisters and Mt. Jefferson Wilderness Areas, Oregon*. U.S. Geological Survey Professional Paper 1608 93.

O'Connor JE, Grant GE, and Costa JE (2002) The geology and geography of floods. In: House PK, Webb RH, and Levish DR (eds.) *Ancient Floods, Modern Hazards, Principles and Applications of Paleoflood Hydrology*, *American Geophysical Union Water Science and Application Series*, vol. 4, 191–215.

Othberg KL (1994) Geology and Geomorphology of the Boise Valley and Adjoining Areas, Western Snake River Plain, Idaho. *Idaho Geological Survey Bulletin* 29: 54.

Outland CF (1963) *Man-Made Disaster: The Story of St. Francis Dam*. Glendale, CA: Arthur H. Clarak Co., 249.

Palmer L (1977) Large landslides of the Columbia River Gorge, Oregon and Washington. In: Coates DR (ed.) *Geological Society of America Reviews in Engineering Geology*. vol. III, pp. 69–84. Boulder, CO: Geological Society of America.

Park C and Schmincke H (2020a) Multistage damming of the Rhine River by tephra fallout during the 12,900 BP plinian Laacher See eruption (Germany). Syn-eruptive Rhine damming I. *Journal of Volcanology and Geothermal Research* 390, 106688. https://doi.org/10.1016/j.jvolgeores.2019.106688.

Park C and Schmincke H (2020b) Boundary Conditions for Damming of a Large River by Fallout During the 12,900 BP Plinian Laacher See Eruption (Germany). Syn-Eruptive Rhine Damming II. *Journal of Volcanology and Geothermal Research* 390, 106791. https://doi.org/10.1016/j.jvolgeores.2020.106791.

Parkinson M and Stretch D (2007) Breaching timescales and peak outflows for perched, temporary open estuaries. *Coastal Engineering Journal* 49: 267–290.

Peng M and Zhang LM (2012) Breaching paramters of landslide dams. *Landslides* 9: 13–31. https://doi.org/10.1007/s10346-011-0271-y.

Perrin ND and Hancox GT (1992) Landslide dammed lakes in New Zealand: Preliminary studies on the distributions, causes, and effects. In: Bell DH (ed.) *Landslides—Vol. 2, Proceedings of the 6th International Symposium on Landslides, Christchurch, New Zealand* 1457–1466.

Peters JL and Brennand TA (2020) Palaeogeographical reconstruction and hydrology of glacial Lake Purcell during MIS 2 and its potential impact on the Channeled Scabland, USA. *Boreas*. https://doi.org/10.1111/bor.12434.

Pickert G, Weitbrecht V, and Bieberstein A (2011) Breaching of overtopped river embankments controlled by apparent cohesion. *Journal of Hydraulic Research* 49: 143–156.

Pierson TC, Janda RJ, Thouret J-C, and Borrero CA (1990) Perturbation and melting of snow and ice by the 13 November 1985 eruption of Nevado del Ruiz, Colombia, and consequent mobilization, flow, and deposition of lahars. *Journal of Volcanology and Geothermal Research* 41: 17–66.

Plaza-Nieto G and Zevallos O (1994) The 1993 La Josefina rockslide and Rio Paute landslide dam, Ecuador. *Landslide News* 8: 4–6.

Ponce VM and Tsivoglou AM (1981) Modeling gradual dam breaches. *Proceedings of the American Society of Civil Engineers* 107: 829–838.

Porter SC and Denton GH (1967) Chronology of neoglaciation in the North American Cordillera. *American Journal of Science* 265: 177–210.

Post A and Mayo LR (1971) *Glacial-dammed Lakes and Outburst Floods in Alaska*. U.S. Geological Survey Hydrological Atlas HA-455, pp. 10, 3 plates.

Praetorius SK, Condron A, Mix AC, Walczak MH, McKay JL, and Du J (2020) The role of northeast Pacific meltwater events in deglacial climate change. *Science Advances* 6: https://doi.org/10.1126/sciadv.aay2915.

Procter JN, Cronin SJ, Fuller IC, Sheridan M, Neall VE, and Keys H (2010) Lahar hazard assessment using Titan2D for an alluvial fan with rapidly changing geomorphology: Whangaehu River, Mt. Ruapehu. *Geomorphology* 116: 162–174.

Pulgarín B, Cardona C, Calvache M, Lockhart A, and White R (2007) Huila lahars caused by rapid, voluminous water expulsion. In: *Abstract Volume, Cities on Volcanoes 5, Shimabara, Japan*, 113.

Ranasinghe R and Pattiaratchi C (2003) The seasonal closure of tidal inlets: Causes and effects. *Coastal Engineering Journal* 45: 601–627.

Ray HA and Kjelström LC (1978) *The Flood in Southeastern Idaho From the Teton Dam Failure of June 5, 1976*. U.S. Geological Survey Open-file Report 77–765, 48.

Reheis MC, Sarna-Wojcicki AM, Reynolds RL, Repenning CA, and Mifflin MD (2002) Pliocene to Middle Pleistocene lakes in the western Great Basin: Ages and connections. In: Hershler R, Madsen DB, and Currey DR (eds.) *Great Basin Aquatic Systems History*, pp. 53–108. Washington, DC: Smithsonian Institution Press.
Reynolds JJ (1992) The identification and mitigation of glacier-related hazards: Examples from the Cordillera Blanca, Peru. In: McCall GJH, Laming DJC, and Scott SC (eds.) *Geohazards—Natural and Man-Made*, pp. 143–157. London: Chapman and Hall.
Richardson D (1968) *Glacier Outburst Floods in the Pacific Northwest*. U.S. Geological Survey Professional Paper 600-D D79–D86.
Richardson K and Carling PA (2005) *A Typology of Sculpted Forms in Open Bedrock Channels*. Geological Society of America Special Paper 392, 108.
Richardson SD and Reynolds JM (2000) An overview of glacial hazards in the Himalayas. *Quaternary International* 65–66: 31–47. https://doi.org/10.1016/S1040-6182(99)00035-X.
Richer M, Mann CP, and Stix J (2004) Mafic magma injection triggers eruption at Ilopango Caldera, El Salvador, Central America. In: Rose WI Jr., Bommer JJ, López DL, Carr MJ, and Major JJ (eds.) *Natural Hazards in El Salvador*, 175–189. Geological Society of America Special Paper 375.
Rico M, Benito G, and Díez-Herrero A (2008) Floods from tailings dam failures. *Journal of Hazardous Materials* 154(1-3): 79–87.
Risley JC, Walder JS, and Denlinger RP (2006) Usoi Dam wave overtopping and flood routing in the Bartang and Panj Rivers, Tajikistan. *Natural Hazards* 38: 375–390.
Roberts MJ (2005) Jökulhlaups: A reassessment of floodwater flow through glaciers. *Reviews of Geophysics* 43(1), RG1002.
Roda M, Kleinhans MG, Zegers TE, and Oosthoek JHP (2014) Catastrophic ice lake collapse in Aram Chaos, Mars. *Icarus* 236: 104–121. https://doi.org/10.1016/j.icarus.2014.03.023.
Rodier JA and Roche M (1984) *World Catalogue of Maximum Observed Floods*. International Association of Hydrologic Sciences Publication No. 143354.
Rogers JD (1992) Reassessment of the St. Francis Dam failure. In: Pipken BW and Proctor RJ (eds.) *Engineering Geology Practice in Southern California. Association of Engineering Geologists*. vol. 4, pp. 639–665. Southern California Section Special Publication.
Rosenwinkel S, Landgraf A, Schwanghart W, Volkmer F, Dzhumabaeva A, Merchel S, Rugel G, Preusser F, and Korup O (2017) Late Pleistocene outburst floods from Issyk Kul, Kyrgyzstan? *Earth Surface Processes and Landforms* 42: 1535–1548. https://doi.org/10.1002/esp.4109.
Rounce DR, McKinney DC, Lala JM, Byers AC, and Watson CS (2016) A new remote hazard and risk assessment framework for glacial lakes in the Nepal Himalaya. *Hydrological Earth System Sciences* 20: 3455–3475. https://doi.org/10.5194/hess-20-3455-2016.
Rounce DR, Byers AC, Byers EA, and McKinney DC (2017) Brief communication: Observations of a glacier outburst flood from Lhotse Glacier, Everest area, Nepal. *The Cryosphere* 11: 443–449. https://doi.org/10.5194/tc-11-443-2017.
Ruedemann R and Schoonmaker WJ (1938) Beaver dams as geologic agents. *Science* 88(2292): 523–525.
Ruiz-Villanueva V, Allen S, Arora M, Goel MK, and Stoffel M (2017) Recent catastrophic landslide lake outburst floods in the Himalayan mountain range. *Progress in Physical Geography: Earth and Environment* 41: 3–28. https://doi.org/10.1177/0309133316658614.
Russell AJ, Tweed FS, Roberts MJ, Harris TD, Gudmundsson MT, Knudsen Ó, and Marren PM (2010) An unusual jökulhlaup resulting from subglacial volcanism, Sólheimajökull, Iceland. *Quaternary Science Reviews* 29: 1363–1381.
Ryan WBF (2007) Status of the Black Sea flood hypothesis. In: Yanko-Hombach V, Gilbert AS, and Dolukhanov PM (eds.) *The Black Sea Flood Question*, pp. 63–88. The Netherlands: Springer.
Ryan WBF and Pitman W (1999) *Noah's Flood: The New Scientific Discoveries about the Event That Changed History*. New York: Simon and Schuster319.
Ryan WBF, Pitman WC III, Major CO, Shimkus K, Moskalenko V, Jones GA, Dimitrov P, Gorür N, Sakinç M, and Yüce H (1997) An abrupt drowning of the Black Sea shelf. *Marine Geology* 138: 119–126.
Ryan WBF, Major CO, Lericolais G, and Goldstein SL (2003) Catastrophic flooding of the Black Sea. *Annual Review of Earth and Planetary Sciences* 31: 525–554.
Rydlund PH Jr. (2006) *Estimated Flood Inundation Extent Along Taum Sauk Creek Representing a Hypothetical Embankment Failure on the East Side*. U.S. Geological Survey Scientific Investigations Report 2006-5284 43.
Safran EB, Anderson SW, Mills-Novoa M, House PK, and Ely L (2011) Controls on large landslide distribution and implications for the geomorphic evolution of the southern interior Columbia River basin. *Geological Society of America Bulletin* 123: 1851–1862. https://doi.org/10.1016/j.geomorph.2015.06.040.
Safran EB, O'Connor JE, Ely LL, House PK, Grant G, Harrity K, Croall K, and Jones E (2015) Plugs or flood-makers? The unstable landslide dams of eastern Oregon. *Geomorphology* 248: 237–251.
Salese F, Pondrelli M, Neeseman A, Schmidt G, and Ori GG (2019) Geological evidence of planet-wide groundwater system on Mars. *Journal of Geophysical Research, Planets* 124: 374–395. https://doi.org/10.1029/2018JE005802.
Sattar A, Goswami A, Kulkarni AV, and Emmer A (2020) Lake evolution, hydrodynamic outburst flood modeling and sensitivity analysis in the central Himalaya: A case study. *Watermark* 12: 237. https://doi.org/10.3390/w12010237.
Schaefer JR, Scott WE, Evans WC, Jorgenson J, Mcgimsey RG, and Wang B (2008) The 2005 catastrophic acid crater lake drainage, lahar, and acidic aerosol formation at Mount Chiginagak volcano, Alaska, USA: Field observations and preliminary water and vegetation chemistry results. *Geochemistry, Geophysics, Geosystems* 9(7), Q07018.
Schuster RL (2000) Outburst debris flows from failure of natural dams. In: Wieczorek GF and Naeser ND (eds.) *Debris Flow Hazards Mitigaton: Mechanics, Prediction and Assessment, Proceedings, 2nd International Conference on Debris Flow Hazard Mitigation, Taipei, Taiwan,* 29–42.
Schuster RL and Costa JE (1986) A perspective on landslide dams. In: Schuster RL (ed.) *Landslide Dams: Process, Risk, and Mitigation*. vol. 3, pp. 1–20. American Society of Civil Engineers Special Publication.
Schuster RL and Highland LM (2001) *Socioeconomic and Environmental Impacts of Landslides in the Western Hemisphere*. U.S. Geological Survey Open-file Report 01-0276 47.
Schuster RL, Salcedo DA, and Valenzuela L (2002) Overview of catastrophic landslides of South America in the twentieth century. In: Evans SG and Degraff JV (eds.) *Catastrophic Landslides: Effects, Occurrence, and Mechanisms*, *Geological Society of America Reviews in Engineering Geology*, vol. 15, 1–34.
Scott KM (1988) *Origin, Behavior, and Sedimentology of Lahars and Lahar-runout Flows in the Toutle-Cowlitz River System*. U.S. Geological Survey Professional Paper 1447-A A1–A74.
Scott KM (1989) *Magnitude and Frequency of Lahars and Lahar-runout Flows in the Toutle-Cowlitz River System*. U.S. Geological Survey Professional Paper 1447-B B1–B33.
Scott KM and Gravlee GC (1968) *Flood Surge on the Rubicon River, California—Hydrology, Hydraulics and Boulder Transport*. U.S. Geological Survey Professional Paper 422-M M1–M40.
Selting AJ and Keller EA (2001) The Mission debris flow: An example of a prehistoric landslide dam failure, Santa Barbara, California. *Geological Society of America Abstracts with Programs* 33(6). Paper No. 29-20.
Shang Y, Yang Z, Li L, Liu D, Liao Q, and Yangchun W (2003) A super-large landslide in Tibet in 2000: Background, occurrence, disaster, and origin. *Geomorphology* 54: 225–243.
Shaw J (1983) Drumlin formation related to inverted meltwater erosional marks. *Journal of Glaciology* 29: 461–479.
Shaw J (2002) The meltwater hypothesis for subglacial landforms. *Quaternary Science Reviews* 90: 5–22.
Shaw J, Munro-Stasiuk MJ, Sawyer B, Beaney CL, Lesemann J-E, Musacchio A, Rains BB, and Young RR (1999) The Channeled Scabland: Back to Bretz? *Geology* 27: 605–608.
Shen D, Shi Z, Peng M, Zhang L, and Jiang M (2020) Longevity analysis of landslide dams. *Landslides*. https://doi.org/10.1007/s10346-020-01386-7.
Sherrod DR and Wills BB (2014) *Debris Flow From 2012 Failure of Moraine-dammed Lake, Three Fingered Jack Volcano, Mount Jefferson Wilderness, Oregon*. U.S. Geological Survey Scientific Investigations Report 2014–5208 13. https://doi.org/10.3133/sir20145208.
Shroder JF Jr. (1998) Slope failure and denudation in the western Himalaya. *Geomorphology* 26: 81–105.
Si Y (1998) The world's most catastrophic dam failures. In: Qing D, Thibodeau JG, Williams MR, Dai Q, Yi M, and Ronning Topping A (eds.) *The River Dragon Has Come! Three Gorges Dam and the Fate of China's Yangtze River and its People*, pp. 25–38. Armonk, NY: M.E. Sharpe.
Singer BS, Le Mével H, Licciardi JM, Córdova L, Tikoff B, Garibaldi N, Andersen NL, Diefenbach AK, and Feigl KL (2018) Geomorphic expression of rapid Holocene silicic magma rseservoir growth beneath Laguna del Maule, Chile. *Science Advances* 4: eaat1513. https://doi.org/10.1126/sciadv.aat1513.
Singh VP, Scarlatos PD, Collins JG, and Jourdan MR (1988) Breach erosion of earthfill dams (BEED) model. *Natural Hazards* 1: 161–180.

Smith DG and Fisher TG (1993) Glacial Lake Agassiz: The northwestern outlet and paleoflood. *Geology* 21: 9–12.
Somos-Valenzuela MA, Chisolm RE, Rivas DS, Portocarrero C, and McKinney DC (2016) Modeling a glacial lake outburst flood process chain: The case of Lake Palcacocha and Huaraz, Peru. *Hydrology and Earth System Sciences* 20: 2519–2543. https://doi.org/10.5194/hess-20-2519-2016.
Spring U and Hutter K (1981) Numerical studies of jökulhlaups. *Cold Regions Science and Technology* 4: 227–244.
Spring U and Hutter K (1982) Conduit flow of a fluid through its solid phase and its application to intraglacial channel flow. *International Journal of Engineering Science* 20: 327–363.
Stearns HT (1931) *Geology and Water Resources of the Middle Deschutes River basin, Oregon*. U.S. Geological Survey Water Supply Paper 637-D 125–220.
Stelling P, Gardner JE, and Begét J (2005) Eruptive history of Fisher Caldera, Alaska, USA. *Journal of Volcanology and Geothermal Research* 139: 163–183.
Stimac JA, Goff F, Counce D, Laracque ACL, Hilton DR, and Moregenstern W (2004) The crater lake and hydrothermal system of Mount Pinatubo, Philippines: Evolution in the decade after eruption. *Bulletin of Volcanology* 66: 149–167. https://doi.org/10.1007/s00445-003-0300-3.
Strachey R (1894) The landslip at Gohna, in British Garwhal [Garhwal]. *Geographical Journal* 4: 162–170.
Strasser M, Schindler C, and Anselmetti FS (2008) Late Pleistocene earthquake-triggered moraine dam failure and outburst of Lake Zurich, Switzerland. *Journal of Geophysical Research* 113(F2), F02003.
Stretch D and Parkinson M (2006) The breaching of sand barriers at perched, temporary open/closed estuaries—A model study. *Coastal Engineering Journal* 48: 13–30.
Sturm M and Benson CS (1985) A history of jökulhlaups from Strandline Lake, Alaska. *Journal of Glaciology* 31: 272–280.
Sturm M, Beget JE, and Benson C (1987) Observations of jökulhlaups from ice-dammed Strandline Lake, Alaska: Implications for paleohydrology. In: Mayer L and Nash BP (eds.) *Catastrophic Flooding*, pp. 79–94. London: Allen and Unwin.
Swanson FJ, Oyagi N, and Tominaga M (1986) Landslide dams in Japan. In: Schuster RL (ed.) *Landslide Dams: Process, Risk, and Mitigation*. vol. 3, pp. 131–145. American Society of Civil Engineers Special Publication.
Tacconi Stefanelli C, Segoni S, Casagl N, and Catani F (2016) Geomorphic indexing of landslide dams evolution. *Engineering Geology* 208: 1–10. https://doi.org/10.1016/j.enggeo.2016.04.024.
Tacconi Stefanelli C, Vilímek V, Emmer A, and Catani F (2018) Morphological analysis and features of the landslide dams in the Cordillera Blanca, Peru. *Landslides* 15: 507–521. https://doi.org/10.1007/s10346-017-0888-6.
Teller JT (2003) Controls, history, outbursts, and impact of large late-Quaternary proglacial lakes in North America. In: Gillespie AR, Porter SC, and Atwater BF (eds.) *Developments in Quaternary Sciences*. vol. 1, pp. 45–61. Elsevier.
Teller JT (2012) Importance of freshwater injections into the Arctic Ocean in triggering the Younger Dryas cooling. *Proceedings of the National Academy of Sciences* 109: 19880–19881. https://doi.org/10.1073/pnas.1218344109.
Teller JT and Leverington DW (2004) Glacial Lake Agassiz: A 5000 yr history of change and its relationship to the d18O record of Greenland. *Geological Society of America Bulletin* 116: 729–742.
Teller JT, Leverington DW, and Mann JD (2002) Freshwater outbursts to the oceans from glacial Lake Agassiz and their role in climate change during the last deglaciation. *Quaternary Science Reviews* 21: 879–887.
Temple DM, Hanson GJ, and Hunt SL (2010) Observations on dam overtopping breach processes and prediction. *Journal of Dam Safety* 8(2): 28–33.
Teng J, Jakeman AJ, Vaze J, Croke BFW, Dutta D, and Kim S (2017) Flood inundation modelling: A review of methods, recent advances and uncertainty analysis. *Environmental Modelling and Software* 90: 201–216. https://doi.org/10.1016/j.envsoft.2017.01.006.
Thiel GA (1932) Giant current ripples in coarse fluvial gravel. *Journal of Geology* 40: 452–458. https://doi.org/10.1086/623965.
Thiele R, Moreno H, and Petit-Breuilh ME (1998) Quaternary geological-geomorphological evolution of the uppermost course of the Rio Laja valley. *Revista Geologica de Chile* 25: 229–253.
Thórarinsson S (1939) The ice dammed lakes of Iceland with particular reference to their values as indicators of glacier oscillations. *Geografiska Annaler* 21: 216–242.
Thornton CI, Pierce MW, and Abt SR (2011) Enhanced predictions for peak outflow from breached embankment dams. *Journal of Hydrologic Engineering* 16: 81–88. https://doi.org/10.1061/(ASCE)HE.1943-5584.0000288.
Tómasson H (1996) The jökulhlaup from Katla in 1918. *Annals of Glaciology* 22: 249–254.
Tómasson H (2002) Catastrophic floods in Iceland. *Proceedings of Extremes of the Extremes: Extraordinary Floods Symposium, International Association of Hydrological Sciences Publication* vol. 271, 121–126.
Trabant DC, March RS, and Thomas DS (2003) *Hubbard Glacier, Alaska: Growing and Advancing in Spite of Global Climate Change and the 1986 and 2002 Russell Lake Outburst Floods*. U.S.Geological Survey Fact Sheet 001-03 4.
Turzewski MD, Huntington KW, and LeVeque RJ (2019) The geomorphic impact of outburst floods: Integrating observations and numerical simulations of the 2000 Yigong flood, eastern Himalaya. *Journal of Geophysical Research - Earth Surface* 124: 1056–2079. https://doi.org/10.1029/2018JF004778.
Tweed FS and Russell AJ (1999) Controls on the formation and sudden drainage of glacier-impounded lakes: Implications for jökulhlaup characteristics. *Progress in Physical Geography* 23: 79–110.
Umbal JV and Rodolfo KS (1996) The 1991 lahars of southwestern Mount Pinatubo and evolution of the lahar-dammed Mapanuepe Lake. In: Newhall CG and Punongbayan RS (eds.) *Fire and Mud: Eruptions and Lahars of Mount Pinatubo*, pp. 951–970. Seattle, Washington: University of Washington Press.
Valiani A, Caleffi V, and Zanni A (2002) Case study: Malpasset dam-break simulation using a two-dimensional finite volume method. *Journal of Hydraulic Engineering* 128: 460–472.
Vallance JW and Iverson RM (2015) Chapter 37: Lahars and their deposits. In: Sigurdsson H, Houghton B, McNutt S, Rymer H, and Stix J (eds.) *The Encyclopedia of Volcanoes*, 2nd edn, pp. 649–664. Academic Press. https://doi.org/10.1016/B978-0-12-385938-9.00037-7.
Van Niekerk L, Van Der Merwe JH, and Huizinga P (2005) Hydrodynamics of the Bot river estuary revisited. *Water SA* 31: 73–85.
Vanaman KM, O'Connor JE, and Riggs N (2006) Pleistocene history of Lake Millican, central Oregon. *Geological Society of America Abstracts with Programs* 38(7): 71.
Veh G, Korup O, von Specht S, Roessner S, and Walz A (2019) Unchanged frequency of moraine-dammed glacial lake outburst floods in the Himalaya. *Nature Climate Change* 9: 379–383. https://doi.org/10.1038/s41558-019-0437-5.
Veh G, Korup O, and Walz A (2020) Hazard from Himalayan glacier lake outburst floods. *Proceedings of the National Academy of Sciences* 117: 907–912. https://doi.org/10.1073/pnas.1914898117.
Voight B, Glicken H, Janda RJ, and Douglass PM (1981) Catastrophic rockslide avalanche of May 18. In: Lipman PW and Mullineaux DR (eds.) *The 1980 Eruptions of Mount St. Helens Washington*, 821–828. U.S. Geological Survey Professional Paper, 1250.
von Poschinger A (2011) The Flims rockslide dam. In: Evans SG, Hermanns RL, Strom A, and Scarascia-Mugnozza G (eds.) *Rockslide Dams*, *Springer-Verlag Lecture Notes in Earth Sciences*, vol. 133, 407–421.
Vuichard D and Zimmermann M (1987) The 1985 catastrophic drainage of a moraine-eammed lake, Khumbu Himal, Nepal: Cause and consequences. *Mountain Research and Development* 7: 91–110.
Wahl TL (1998) *Prediction of Embankment Dam Breach Parameters: A Literature Review and Needs Assessment*. U.S. Department of the Interior, Bureau of Reclamation, Dam Safety Office, Dam Safety Research Report DSO-98-004 67.
Wahl TL (2004) Uncertainty of predictions of embankment dam breach parameters. *Journal of Hydraulic Engineering* 130: 389–397.
Waitt RB (1980) About forty last-glacial Lake Missoula jökulhlaups through southern Washington. *Journal of Geology* 88: 653–679.
Waitt RB (2002) Great Holocene floods along Jökulsá á Fjöllum, north Iceland. In: Martini PI, Baker VR, and Garzon G (eds.) *Flood and Megaflood Processes and Deposits: Recent and Ancient Examples*, pp. 37–51. Oxford: Blackwell Science.
Waitt RB Jr. (1985) Case for periodic, colossal jökulhlaups from Pleistocene glacial Lake Missoula. *Geological Society of America Bulletin* 96: 1271–1286.
Waitt RB (2016) Megafloods and Clovis cache at Wenatchee, Washington. *Quaternary Research* 85: 430–444. https://doi.org/10.1016/j.yqres.2016.02.007.

Walder JS (1994) Channelized subglacial drainage over a deformable bed. *Journal of Glaciology* 40: 3–15.

Walder JS and Costa JE (1996) Outburst floods from glacier-dammed lakes: The effect of mode of lake drainages on flood magnitude. *Earth Surface Processes and Landforms* 21: 701–723.

Walder JS and Driedger CL (1994) Rapid geomorphic change caused by glacial outburst floods and debris flows along Tahoma Creek, Mount Rainier, Washington, U.S.A. *Arctic and Alpine Research* 26: 319–327.

Walder JS and Driedger CL (1995) Frequent outburst floods from south Tahoma Glacier, Mount Rainier, U.S.A.: Relation to debris flows, meteorological origin and implications for subglacial hydrology. *Journal of Glaciology* 41: 1–10.

Walder JS and Fountain AG (1997) Glacier generated floods. In: Leavesley GH, Lins HF, and Nobilis F (eds.) *Destructive Water: Water-Caused Natural Disasters—Their Abatement and Control*. vol. 239, pp. 107–113. International Association of Hydrological Sciences Publication.

Walder JS and O'Connor JE (1997) Methods for predicting peak discharge of floods caused by failure of natural and constructed earthen dams. *Water Resources Research* 33: 2337–2348.

Walder JS, Trabant DC, Cunico M, Fountain AG, Anderson SP, Anderson RS, and Malm A (2006) Local response of a glacier to annual filling and drainage of an ice-marginal lake. *Journal of Glaciology* 52: 440–450.

Walder JS, Iverson RM, Godt JW, Logan M, and Solovitz SA (2015) Controls on the breach geometry and flood hydrograph during overtopping of noncohesive earthen dams. *Water Resources Research* 51: 6701–6724. https://doi.org/10.1002/2014WR016620.

Walsh B, Jolly AD, and Procter JN (2016) Seismic analysis of the 13 October 2012 Te Maari, New Zealand, lake breakout lahar: Insights into flow dynamics and the implications on mass flow monitoring. *Journal of Volcanology and Geothermal Research* 324: 144–155. https://doi.org/10.1016/j.volgeores.2016.06.004.

Wang SJ and Jiao ST (2015) Evolution and outburst risk analysis of moraine-dammed lakes in the central Chinese Himalaya. *Journal of Earth System Science* 124: 567–576. https://doi.org/10.1007/s12040-015-0559-8.

Wang X, Liu S, Ding Y, Guo W, Jiang Z, Lin J, and Han Q (2012) An approach for estimating the breach probabilities of moraine-dammed lakes in the Chinese Himalayas using remote-sensing data. *Natural Hazards and Earth System Sciences* 12: 3109–3122. https://doi.org/10.5194/nhess-12-3109-2012.

Wang W, Xiang Y, Gao Y, Lu A, and Yao T (2014) Rapid expansion of glacial lakes caused by climate and glacier retreat in the Central Himalayas. *Hydrological Processes* 29: 859–874. https://doi.org/10.1002/hyp.10199.

Wang S, Qin D, and Xiao C (2015) Moraine-dammed lake distribution and outburst flood risk in the Chinese Himalaya. *Journal of Glaciology* 61: 115–126. https://doi.org/10.3189/2015JoG14J097.

Wang B, Chen Y, Wu C, Peng Y, Song J, Liu W, and Liu X (2018) Empirical and semi-analytical models for predicting peak outflows caused by embankment dam failures. *Journal of Hydrology* 562: 692–702. https://doi.org/10.1016/j.jhydrol.2018.05.049.

Wassmer P, Schneider JL, Pollet N, and Schmitter-Voirin C (2004) Effects of the internal structure of a rock-avalanche dam on the drainage mechanism of its impoundment, Flims sturzstrom and Ilanz paleo-lake, Swiss Alps. *Geomorphology* 61: 3–17.

Waythomas CF (2001) Formation and failure of volcanic debris dams in the Chakachatna River valley associated with eruptions of the Spurr volcanic complex, Alaska. *Geomorphology* 39: 111–129.

Waythomas CF, Walder JS, Mcgimsey RG, and Neal CA (1996) A catastrophic flood caused by drainage of a caldera lake at Aniakchak Volcano, Alaska, and implications for volcanic hazards assessment. *Geological Society of America Bulletin* 108: 861–871.

Webby MG (1996) Discussion [of Froehlich (1995)]. *Journal of Water Resources Planning and Management* 122: 316–317.

Webby MG and Jennings DN (1994) Analysis of dam-break flood caused by failure of Tunawaea landslide dam. In: *Proceedings of International Conference on Hydraulics in Civil Engineering 1994*. University of Brisbane, Queensland, Australia, 163–168.

Westoby MJ, Glasser NF, Brasington J, Hambrey MJ, Quincey DJ, and Reynolds JM (2014) Modelling outburst floods from moraine-dammed glacial lakes. *Earth-Science Reviews* 134: 137–159. https://doi.org/10.1016/j.earscirev.2014.03.009.

Whipple KX and Tucker GE (1999) Dynamics of the stream-power river incision model: Implications for height limits of mountain ranges, landscape response timescales, and research needs. *Journal of Geophysical Research - Solid Earth* 104: 17661–17674. https://doi.org/10.1029/1999JB900120.

Whipple KX, Hancock GS, and Anderson RS (2000) River incision into bedrock: Mechanics and relative efficacy of plucking, abrasion, and cavitation. *Geological Society of America Bulletin* 112: 490–503.

White KD and Zufelt JE (1994) *Ice Jam Data Collection*. U.S. Army Corps of Engineers Cold Regions Research and Engineering Laboratory Special Report 94-7, 37.

White KD, Tuthill AM, and Furman L (2006) Studies of ice jam flooding in the United States. In: Vasiliev O, van Gelder P, Plate E, and Bolgov M (eds.) *Extreme Hydrological Events: New Concepts for Security, Springer NATO Science Series*, vol. 78, 255–268. https://doi.org/10.1007/978-1-4020-5741-0_16.

Whitehouse IE and Griffiths GA (1983) Frequency and hazard of large rock avalanches in the central Southern Alps, New Zealand. *Geology* 11: 331–334.

Wiedmer M, Montgomery DR, Gillespie AR, and Greenberg H (2010) Late Quaternary megafloods from Glacial Lake Atna, southcentral Alaska, U.S.A. *Quaternary Research* 73: 413–424.

Wilcox AC, O'Connor JE, and Major JM (2014a) Rapid reservoir erosion, hyperconcentrated flow, and downstream deposition triggered by breaching of 38-m-tall Condit Dam, White Salmon River, Washington. *Journal of Geophysical Research - Earth Surface* 119: 1376–1394. https://doi.org/10.1002/2013JF003073.

Wilcox AC, Wade AA, and Evans EG (2014b) Drainage events from a glacier-dammed lake, Bear Glacier, Alaska: Remote sensing and field observations. *Geomorphology* 220: 41–49. https://doi.org/10.1016/j.geomorph.2014.05.025.

Williams H (1941) Calderas and their origins. *University of California Bulletin of Geological Sciences* 25: 239–346.

Williams GP (1983) Paleohydrological methods and some examples from Swedish fluvial environments, I—Cobble and boulder deposits. *Geografiska Annaler* 65A: 227–243.

Wilson L, Bargery AS, and Burr DM (2009) Dynamics of fluid flow in Martian outflow channels. In: Burr DM, Carling PA, and Baker VR (eds.) *Megaflooding on Earth and Mars*, pp. 290–311. United Kingdom: Cambridge University Press.

Wingham DJ, Siegert MJ, Shepherd AP, and Muir AS (2006) Rapid discharge connects Antarctic subglacial lakes. *Nature* 440: 1033–1036.

Winsemann J and Lang J (2020) Flooding northern Germany: Impacts and magnitudes of Middle Pleistocene glacial lake-outburst floods. In: Herget J and Fontana A (eds.) *Palaeohydrology*. Cham: Springer Geography of the Physical Environmenthttps://doi.org/10.1007/978-3-030-23315-0_2.

Winsemann J, Alho P, Laamanen L, Goseberg N, Lang J, and Klostermann J (2016) Flow dynamics, sedimentation and erosion of glacial lake outburst floods along the Middle Pleistocene Scandinavian Ice Sheet (northern central Europe). *Boreas* 45: 260–283. https://doi.org/10.1111/bor.12146.

Wolfe BA and Begét JE (2002) Destruction of an Aleut village by a catastrophic flood release from Okmok Caldera, Umnak Island, Alaska. *Geological Society of America Abstracts with Programs* 34(6): 126.

Wood SH and Clemens DM (2002) Geologic and tectonic history of the western Snake River Plain, Idaho and Oregon. In: Bonnichsen B, White CM, and Mccurry M (eds.) *Tectonic and Magmatic Evolution of the Snake River Plain Volcanic Province, Idaho Geological Survey Bulletin*, vol. 30, 69–103.

Worni R, Huggel C, Stoffel M, and Pulgarín B (2012a) Challenges of modeling current very large lahars at Nevado del Huila Volcano, Colombia. *Bulletin of Volcanology* 74: 309–324. https://doi.org/10.1007/s00445-011-0522-8.

Worni R, Stoffel M, Huggel C, Volz C, Casteller A, and Luckman BH (2012b) Analysis and dynamic modeling of a moraine failure and glacier lake outburst flood at Ventisquero Negro, Patagonian Andes (Argentina). *Journal of Hydrology* 444–445: 134–145. https://doi.org/10.1016/j.jhydrol.2012.04.013.

Worni R, Huggel C, and Stoffel M (2013) Glacial lakes in the Indian Himalayas—From an area-wide glacial lake inventory to on-site and modeling based risk assessment of critical glacial lakes. *Science of the Total Environment* 456–469: S71–S84.

Worni R, Huggel C, Clague JJ, Schaub Y, and Stoffel M (2014) Coupling glacial lake impact, dam breach, and flood processes: A modeling perspective. *Geomorphology* 224: 161–176. https://doi.org/10.1016/j.geomorph.2014.06.031.

Wu W (2013) Simplified physically based model of earthen embankment breaching. *Journal of Hydraulic Engineering* 139: 837–851. https://doi.org/10.1061/(ASCE)HY.1943-7900.0000741.

Wu Q, Zhao Z, Liu L, Granger DE, Want H, Cohen DJ, Wu X, Ye M, Bar-Josef O, Lu B, Zhang J, Zhang P, Yuan D, Qi W, Cai L, and Bai S (2016) Outburst flood at 1920 BCE supports historicity of China's Great Flood and the Xia dynasty. *Science* 353: 579–582. https://doi.org/10.1126/science.aaf0842.

Xin W, Shiyin L, Wanqin G, and Junli X (2008) Assessment and simulation of glacier lake outburst floods for Longbasaba and Pida lakes, China. *Mountain Research and Development* 28: 310–317. https://doi.org/10.1659/mrd.0894.

Xu D (1988) Characteristics of debris flow caused by outburst of glacial lake in Boqu River, Xizang, China, 1981. *GeoJournal* 17: 569–580.

Xu D and Feng Q (1994) Dangerous glacier lakes and their outburst features in the Tibetan Himalayas. *Bulletin of Glacier Research* 12: 1–8.

Xu Q, Fan X, Huang R, and Van Westen C (2009) Landslide dams triggered by the Wenchuan Earthquake, Sichuan Province, south west China. *Bulletin of Engineering Geology and the Environment* 68: 373–386. https://doi.org/10.1007/s10064-009-0214-1.

Xu M, Bogen J, Wang Z, Bønses TE, and Gytri S (2014) Pro-glacial lake sedimentation from jökulhlaups (GLOF), Blåmannsisen, northern Norway. *Earth Surface Processes and Landforms* 40: 654–665. https://doi.org/10.1002/esp.3664.

Xu Y and Zhang LM (2009) Breaching parameters for earth and rockfill dams. *Journal of Geotechnical and Geoenvironmental Engineering* 135: 1957–1970. https://doi.org/10.1061/(ASCE)GT.1943-5606.0000162.

Yager EM, Venditti JG, Smith HJ, and Schmeeckle MW (2018) The trouble with shear stress. *Geomorphology* 323: 41–50. https://doi.org/10.1016/j.geomorph.2018.09.008.

Yamada T and Sharma CK (1993) Glacier lakes and outburst floods in the Nepal Himalaya. In: Young GJ (ed.) *Snow and Glacier Hydrology*. vol. 218, pp. 319–330. International Association of Hydrological Sciences.

Yanchilina AG, Ryan WBF, McManus JF, Dimitrov P, Dimitrov D, Slavova K, and Filipova-Marinova M (2017) Compilation of geophysical, geochronological, andgeochemical evidence indicates a rapid Mediterranean-derived submergence ofthe Black Sea's shelf and subsequent substantial salinification in the early Holocene. *Marine Geology* 383: 14–34. https://doi.org/10.1016/j.margeo.2016.11.001.

Yanchilina AG, Ryan WBF, Kenna TC, and McManus JF (2019) Meltwater floods into the Black and Caspian Seas during Heinrich Stadial 1. *Earth-Science Reviews*. , 102931. https://doi.org/10.1016/j.earscirev.2019.102931.

Yi J, Wang P-J, Shan X-L, Wang H-F, Sun S, and Chen H (2019) Lahar deposits generated after the Millenium eruption of the Changbaishan Tianchi volcano in the Erdabaihe River system, China. *Journal of Volcanology and Geothermal Research* 380: 1–18. https://doi.org/10.1016/j.volcgeores.2019.05.003.

Youd TL, Wilson RC, and Schuster RL (1981) Stability of blockage in North Fork Toutle River. In: Lipman PW and Mullineaux DR (eds.) *The 1980 Eruptions of Mount St. Helens Washington*, 821–828. U.S. Geological Survey Professional Paper 1250.

Zhang JY, Li Y, Xuan GX, Wang XG, and Li J (2009) Overtopping breaching of cohesive homogeneous earth dam with different cohesive strength. *Science in China, Series E Technological Sciences* 52: 3024–3029.

Zhang G, Bolch T, Allen S, Linsbauer A, Chen W, and Wang W (2019) Glacial lake evolution and glacier-lake interactions in the Poiqu River basin, central Himalaya, 1964-2017. *Journal of Glaciology* 65: 347–365. https://doi.org/10.1017/jog.2019.13.

Zhong Q, Chen S, Fu Z, and Shan Y (2020) New empirical model for breaching of earth-rock dams. *Natural Hazards Review* 21(2). https://doi.org/10.1061/(ASCE)NH.1527-6996.0000374.

Zhou GGD, Zhou M, Shrestha MS, Song D, Choi C, Cui KFE, Peng M, Shi Z, Zhu X, and Chen H (2019) Experimental investigation on the longitudinal evolution of landslide dam breaching and outburst floods. *Geomorphology* 334: 29–43. https://doi.org/10.1016/j.geomorph.2019.02.035.

Zuffa GG, Normark WR, Serra F, and Brunner CA (2000) Turbidite megabeds in an oceanic rift valley recording jökulhlaups of late Pleistocene glacial lakes of the western United States. *Journal of Geology* 108: 253–274. https://doi.org/10.1086/314404.